DISSERTATION

PHENOMENOLOGICAL MODELS OF MAGNETIZATION DAMPING

Submitted by

Michael Andreas Kraemer

Department of Physics

In partial fulfillment of the requirements

For the Degree of Doctor of Philosophy

Colorado State University

Fort Collins, Colorado

Spring 2006

COLORADO STATE UNIVERSITY

July 20, 2005

WE HEREBY RECOMMEND THAT THE DISSERTATION PREPARED UNDER OUR SUPERVISION BY MICHAEL ANDREAS KRAEMER ENTITLED 'PHENOMENOLOGICAL MODELS OF MAGNETIZATION DAMPING' BE ACCEPTED AS FULFILLING IN PART REQUIREMENTS FOR THE DEGREE OF DOCTOR OF PHILOSOPHY.

Committee on Graduate Work

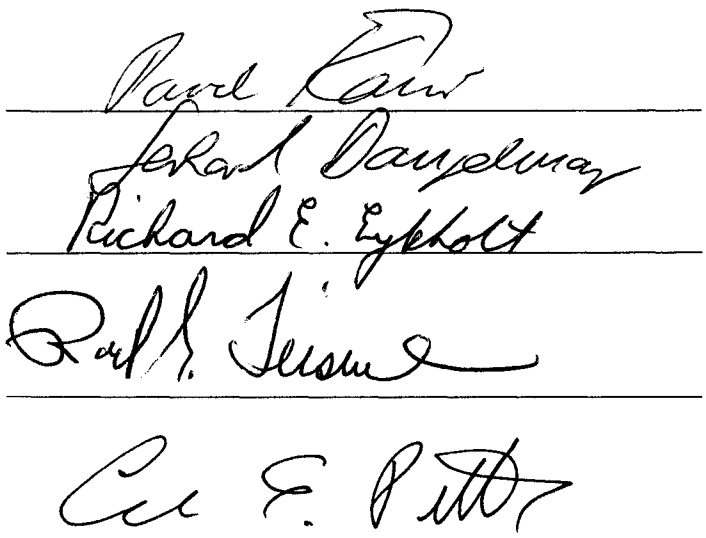

Adviser

Department Head

Abstract of Dissertation

Phenomenological Models of Magnetization Damping

In the last 70 years many models have been published for the relaxation of magnetization precession in ferromagnetic materials. Such models are important to predict energy loss for three phenomena: the free precession decay, the precession driven by an applied microwave field, and the noise of a system in equilibrium. Five models of magnetization damping are typical and were selected for this thesis: Landau-Lifshitz (LL) damping, Bloch-Bloembergen (BB) damping, Codrington-Olds-Torrey (COT) damping, Gilbert (G) damping and Modified Bloch-Bloembergen (MBB) damping. Traditionally, these models have been characterized in the small-signal limit by their susceptibility tensors, which relate the complex amplitudes of driving field and the magnetization response in a linear manner.

This work categorizes the five damping models according to which field or magnetization components drive the damping. The models are compared with regard to their relaxation rate of the free decay, the geometrical shape of their trajectory, their susceptibility tensor, their energy loss for the precession driven by an external microwave field, and their thermal noise in equilibrium. The energy loss of the driven precession is determined both as time-averaged loss and as instantaneous loss.

The analyses in this work take advantage of the Smith matrix form of the equations of motion for the magnetization precession in the small-signal limit. The Smith matrix form is the general form of a linearized system of coupled harmonic oscillators, solved for the external driving force. Traditionally, energy loss and noise power spectra have been calculated with the

components of the susceptibility tensor involving bulky ratios of complex expressions. In this work, all calculations are carried out with the real-valued matrices that multiply the magnetization and its derivative in the Smith form of the equations of motion. The three main advantages are the following: a) The calculations are simpler. b) Many results about energy loss and thermal noise are expressed in simple form in terms of a single matrix, the symmetric part of the damping matrix. c) The Smith matrix form allows calculation of instantaneous, time-dependent loss, where traditionally only time-averaged loss was considered.

The power spectra of field noise as well as magnetization noise are analyzed with the fluctuation-dissipation theorem and the Wiener-Khinchine theorem. In this work a classical proof of the fluctuation-dissipation theorem is given, which is more elementary than most found in the literature and uses Boltzmann statistics and ordinary differential equations.

Michael Andreas Kraemer
Department of Physics
Colorado State University
Fort Collins, CO 80523
Spring 2006

Table of Contents

Chapter 1

Introduction

Table of contents:

1.1 Issues in models of magnetization relaxation

1.1.a Contrast of phenomenological models of magnetization damping

Microscopic damping mechanisms relax the magnetization vector in a ferromagnetic sample to its equilibrium in the direction of the internal magnetic field. In this way the angle between magnetization and field tends to decrease, as magnetic energy is converted into the mechanical energy of lattice vibrations and of the electronic system. In the presence of a microwave driving field ferromagnetic resonance occurs near the natural frequency of the free magnetization precession. In contrast to a system of coupled harmonic oscillators, such as masses connected with springs, a

ferromagnetic sample is a gyroscopic system. That means that the magnetization response to an applied magnetic field always has a precessional component, that is one that rotates about the direction of the instantaneous field. For small precession angles, the shape of the precession orbit is elliptical. The eccentricity of the precession ellipse depends on demagnetizing fields and on the polarization of the microwave driving field.

The first mathematical model of magnetic damping was published by Landau and Lifshitz [1935], eleven years before the first ferromagnetic resonance experiment by Griffiths [1946]. A modification of this model, due to Gilbert [1955], is a direct analog of the viscous damping in the simple harmonic oscillator. Both the Landau-Lifshitz model and the Gilbert model conserve the magnitude of the magnetization vector. Other, non-viscous, magnetic damping models do not constrain the magnitude of the magnetization to be constant, and correspond to a more general class of microscopic damping mechanisms than the Landau-Lifshitz and Gilbert models. The first model of this kind was proposed by Bloembergen [1950] and is called the Bloch-Bloembergen model, because it applies some of Bloch's [1946] nuclear magnetic resonance results to ferromagnetic resonance. The equations of the Bloch-Bloembergen model lead to negative loss in a spherical sample for an anti-Larmor polarized driving field. This weakness was addressed by several authors and led to multiple modifications of the Bloch-Bloembergen model between 1950 and today.

This thesis presents a selection of five magnetic damping models, explains underlying ideas, points out differences and checks the compatibility with fundamental laws of physics such as energy conservation and the fluctuation-dissipation theorem.

1.1.b Instantaneous versus time-averaged energy loss

The linearization of the equations of motion for the magnetization in a uniformly magnetized sample yields a linear system of ordinary differential equations for the transverse magnetization components as a function of time. The linearization is allowed in the small-signal limit, when the

magnetization components transverse to the static applied field are small compared with the saturation magnetization. By linearization, the dimension of the system is reduced from three to two.

In this thesis sufficient and necessary conditions are derived so that the loss is positive in the small-signal limit for all possible polarizations of the driving field. Some damping models yield negative loss for certain sample geometries and certain driving fields. This is a violation of the law of energy conservation, and such models must be rejected as unphysical.

An important issue in the derivation of criteria for positive loss is whether the time-averaged loss or the instantaneous loss should be considered. Of course, if the loss is positive at every instant of time, then the time-averaged loss is positive as well. The converse is not true, however: There are examples when the time-averaged loss is positive, but the instantaneous loss is negative during some portions of the precession cycle. The criteria for positive instantaneous loss are consequently more stringent than those for positive time-averaged loss. Conservation of energy requires positive loss at every instant of time.

1.1.c Isotropy of magnetization damping and of thermal magnetic noise

The fluctuation-dissipation theorem quantitatively describes the relation between the measured noise power and the susceptibility in a system of coupled harmonic oscillators. The type of noise considered here is due to thermally generated random driving forces, such as the Johnson noise in resistors. The random driving forces in the case of Johnson noise are voltages arising from the random, thermal motion of the conduction electrons in the resistors. These random voltages are uncorrelated between different resistors in the circuit relative to a length scale larger than the mean free path of the conduction electrons. The magnetic analog of the electric Johnson noise are thermally generated, fluctuating magnetic fields. These random magnetic fields can be considered uncorrelated relative to a physical length scale larger than 5-10 lattice spacings. This length defines the micromagnetic length scale over which the magnetization is a well-defined vector quantity.

By the fluctuation-dissipation theorem, random fluctuation fields are uncorrelated in space as well as between Cartesian components if and only if the damping matrix in the linearized equations of motion is a multiple of the unit matrix. Hence only damping models that possess a damping matrix with this property are consistent with damping mechanisms that are homogeneous and isotropic on the micromagnetic length scale. The five magnetic damping models analyzed in this thesis are evaluated by this criterion.

1.1.d Power loss due to magnetic noise

The application of the fluctuation-dissipation theorem to magnetic noise yields expressions for the spectral density of the noise power. One must carefully distinguish between the signal power of a certain physical quantity, which is simply its squared magnitude, and the physical power loss in watts that is dissipated in the sample. Therefore one has three powers involved: the signal power of the internal magnetic field, the signal power of the magnetization, and the physical power dissipated in the sample. For all five magnetic damping models the signal power of the internal magnetic field is white, that means its spectral density is independent of the frequency. In contrast, the spectral densities of the signal power of the magnetization response and of the physical power loss resemble ferromagnetic resonance curves. Both attain a maximum near the Kittel resonance frequency. But while the signal power of the magnetization response converges to zero with increasing frequency, the physical power loss converges to a small, but positive value that is proportional to the damping parameter. As a consequence the total noise power, obtained by integrating the spectral power density over all frequencies, is infinite for four of the five damping models examined in this thesis.

An infinite noise power is, of course, unphysical. To avoid this divergence of the noise integral, one might assume a cutoff frequency for the spectral power density of the magnetic noise. Another way to remove the divergence is to add a small mass term in the equations of motion. This mass term forces the spectral power density to converge to zero for increasing frequency.

1.2 Outline of thesis

Chapter 1 of this thesis is the present introduction. It introduces the main issues and outlines each of the following chapters.

Chapter 2 derives and solves the torque equation of motion for the magnetization precession, first for bulk material and then for a uniformly magnetized ellipsoidal sample, where demagnetizing fields are present. The equations of motion are solved in the small-signal-limit, that is for small precession angles. In the small signal limit the three full nonlinear equations of motion for the three magnetization components reduce to a system of two linear equations for the two transverse magnetization components. Transverse here means perpendicular to the static applied field. The linear system for the transverse magnetization response is presented

a) explicitly solved for the time derivatives of the magnetization vector,

b) explicitly solved for the driving field, with certain constant matrices multiplying the magnetization and its time derivative. This form is called the Smith matrix form in this thesis, after Neil Smith, who first wrote the linearized equations of damped magnetic precession in this form. The Smith matrix form of the equations of motion is the analog to the equation for the simple harmonic oscillator with a viscous damping term. It is useful in the loss calculations in Chapter 4 and the analysis of magnetic noise with the fluctuation-dissipation theorem in Chapter 5.

Chapter 3 introduces five phenomenological damping models in chronological order: Landau-Lifshitz damping, Bloch-Bloembergen damping, Codrington-Olds-Torrey damping, Gilbert damping and modified Bloch-Bloembergen damping. For each model the equations of motion are derived in the small signal limit by what drives the relaxation. The geometric shape of the trajectory is analyzed, relaxation rates of the free precession decay and the susceptibility tensor of the driven precession is calculated. It is found that all damping models except the Bloch-Bloembergen model strive to align the magnetization vector with its instantaneous equilibrium. In contrast, the Bloch-Bloembergen model strives to align the magnetization with the static component of the internal field. As a

consequence, Bloch-Bloembergen damping can lead to negative loss, which is proven in Chapter 4. For ellipsoidal samples, the trajectories of the free precession decay are compressed logarithmic spirals. The axes along which these spirals are compressed coincide with the transverse principal axes of the sample ellipsoid only for the Bloch-Bloembergen and modified Bloch-Bloembergen damping models. For the other three models, the compression axes are tilted away from the transverse principal axes by a small angle that is a function of the dimensionless damping parameter of the respective damping model.

Chapter 4 shows that in the Smith matrix form of the equations of motion all information about both instantaneous and time averaged loss is contained in the symmetric part of the damping matrix and the antisymmetric part of the stiffness matrix. The conditions for positive loss, both instantaneous and time-averaged, for all driving frequencies and all polarizations of the driving field are found to be the following:

a) The symmetric part of the damping matrix must be positive definite.

b) The antisymmetric part of the stiffness matrix must be zero, that is the stiffness matrix must be symmetric.

Chapter 5 examines the phenomenological damping models in the light of the fluctuation-dissipation theorem. The fluctuation-dissipation theorem relates the correlations of fluctuating physical quantities to their dissipative properties. By the Wiener-Khinchine theorem, the correlation matrix of a set of fluctuating physical quantities is the Fourier transform of the power spectral density matrix. Therefore, by application of both the fluctuation-dissipation and the Wiener-Khinchine theorem, the spectral densities of the noise components can be expressed in terms of the damping parameters of the system. The fluctuation-dissipation theorem is developed using the basic mathematical theory for the means, variances and covariances of a set of physical quantities with a multivariate Gaussian probability distribution. Then the fluctuation-dissipation theorem is used to determine the signal power spectral densities of both the noise fields and the magnetization response. It is shown that the field noise is white, that means its power spectral density is independent of

frequency. In contrast, the magnetization noise, as the system response to the field noise, is frequency-dependent, and reveals a maximum at the Kittel resonance frequency. These results are applied to the five damping models that were investigated in Chapter 3. Gilbert damping, Landau-Lifshitz damping and Codrington-Olds-Torrey damping are consistent with isotropic field noise. In contrast, modified Bloch-Bloembergen damping yields power densities of the field noise components that depend on the direction in the sample. Therefore, the modified Bloch-Bloembergen damping is not consistent with isotropic field noise.

Chapter 6 summarizes the main results of the thesis.

1.3 Units

The Gaussian cgs system of units is used exclusively in this thesis. The magnetic field **H** is expressed in Oersteds (Oe). The magnetization **M** is expressed in emu/cm^3. The corresponding magnetic induction **B** is expressed in Gauss (G). The saturation induction $4\pi M_s$ is expressed in Gauss, though the saturation magnetization M_s is in emu/cm^3.

1.4 Abbreviations

The names of the five damping models are abbreviated:

LL	Landau-Lifshitz
BB	Bloch-Bloembergen
COT	Codrington-Olds-Torrey
G	Gilbert
MBB	Modified Bloch-Bloembergen

Chapter 2

The undamped magnetic torque equation

Table of contents:

2.1 Introduction

The magnetic torque equation of motion describes the dynamics of the magnetization vector as a function of time in a uniformly magnetized, and saturated sample, which may be subjected to both a static and a microwave applied field. This chapter provides an overview of the techniques to solve the magnetic torque equation in the ideal case for which no dissipative mechanisms are present, so that the magnetic energy loss is zero at every instant of time. This chapter is tutorial in character. It develops step-by-step the techniques that will be used in the following chapters to calculate the undriven and the driven response of the damped magnetic precession.

The first authors to formulate a magnetic torque equation appear to be Landau and Lifshitz in their famous paper Landau-Lifshitz [1935] about domain wall motion and magnetization damping. Their Landau-Lifshitz equation is a nonlinear equation that contains a damping term. If this damping term is omitted, the undamped magnetic torque equation is obtained, which is the subject of this chapter.

Section 2.2 derives the undamped magnetic torque equation of motion from basic physical principles. Amazingly, the magnetic torque equation states no more and no less that the magnetization vector always precesses about the direction of the internal magnetic field, with an instantaneous angular velocity vector that is proportional to the instantaneous internal field vector. The precession has Larmor orientation, which means that the precession trajectory is traversed counter-clockwise as the reader is facing the total field vector. In an infinite medium, that is, in the absence of demagnetizing fields, the precession about a static applied field is circular and oriented in the Larmor sense.

Section 2.3 describes the driven precession in an infinite medium. The driving field is an external applied microwave field in the plane perpendicular to the static applied field. This plane is called the transverse plane. The transverse driving field may have an arbitrary elliptical polarization. The analysis of the equations of motion is performed in the small signal limit, where the driving field is

small compared to the static applied field and the magnetization response is small compared with the saturation magnetization. In the small signal limit, the system of three nonlinear differential equations reduces to a system of two linear differential equations for the transverse magnetization components. These equations can conveniently be written in a matrix form that is solved not for the time derivative of the magnetization components, but for the components of the external applied microwave field. This matrix form of the equations of motion for a system of coupled harmonic oscillators is commonly used by mechanical engineers, but has only recently been introduced in Smith [2002] to model the magnetic precession response in a ferromagnetic sample. It is called Smith matrix form in this thesis and is very useful in loss calculations, as will be shown in Chapter 4.

Section 2.4 treats the driven precession for a sample of ellipsoidal shape. Such a sample has a uniform demagnetizing field. The total field consists of the external applied field and the demagnetizing field. The equations of motion are formulated in the small signal limit, both explicitly solved for the time derivatives of the magnetization and in Smith matrix form. The Smith matrix form for an ellipsoidal sample resembles very much the Smith matrix form in an infinite medium. The difference is that the external applied field in the infinite medium is replaced by the so-called stiffness fields, which are determined by the geometry of the sample.

Section 2.5 describes the internal magnetic energy as a sum of a demagnetizing energy and a Zeeman energy. As an application, the specific form of the internal energy is derived in the small signal limit for an ellipsoidal sample. In this case, the internal energy is a quadratic form, whose matrix is the stiffness matrix of the equations of motion.

Section 2.6 determines the static equilibrium of the magnetization response when the external applied field is purely static. When, in contrast, the applied field contains a transverse microwave component, then the equilibrium is no longer static, but instantaneous (that is, time-dependent). The instantaneous equilibrium plays a central role in formulating the equations of motion for the damped magnetic precession in Chapter 3.

Section 2.7 summarizes the key results of Chapter 2.

2.2 The undamped magnetic torque equation

The undamped magnetic torque equation, or in short torque equation, is the equation of motion for the magnetization response in a ferromagnetic sample, when all fields are considered as *spatially uniform*. Any spatially inhomogeneous fields, which lead to spatially nonhomogenous (or spin wave) modes of the magnetization response, are not taken into account in the treatment in this thesis. Only the uniform mode response is considered. Therefore the magnetization vector is a function of time only, and not of the space coordinates. One obtains a system of three *ordinary* differential equations of first order for the three spatial components of the magnetization vector. In Section 2.2.a, this system is derived from two experimental facts:

(i) A magnetic dipole in a magnetic field experiences a torque.

(ii) The angular momentum of an electron is proportional to its magnetic dipole moment.

2.2.a Derivation of the torque equation

The precession of a magnetic moment $\boldsymbol{\mu}(t)$ in a magnetic field $\mathbf{H}(t)$ is determined by the torque $\boldsymbol{\mu}(t)\times\mathbf{H}(t)$ on the magnetic moment. The magnetic field comprises not only the external applied field, but also the demagnetizing fields, the effective anisotropy field, and other fields. For simplicity, only external applied fields and demagnetizing fields are considered in this thesis, so that the magnetic field coincides with the internal magnetic field $\mathbf{H}_{\text{int}}(t)$. The torque is equal to the rate of change of the angular momentum, $d\mathbf{J}(t)/dt$, so that

$$\frac{d\mathbf{J}(t)}{dt} = \boldsymbol{\mu}(t)\times\mathbf{H}_{\text{int}}(t). \tag{2.1}$$

In a given material the angular momentum and the magnetic dipole moment are proportional,

$$\boldsymbol{\mu}(t) = \gamma\mathbf{J}(t), \tag{2.2}$$

where the proportionality constant γ is called the gyromagnetic ratio. The magnetic moment in paramagnetic and ferromagnetic materials is associated primarily with the electron spin, with a negative gyromagnetic ratio of $\gamma \approx -1.76 \cdot 10^7 \text{rad}/(\text{Oe} \times \text{s}) \approx -2\pi \cdot 2.80 \text{ MHz/Oe}$. Note that the gyromagnetic ratio is negative due to the negative charge of the electron. To avoid ambiguities about the sign we will always write $-|\gamma|$ instead of γ. From Eqs. (2.1) and (2.2) an ordinary differential equation for the magnetic moment is obtained,

$$\frac{d\boldsymbol{\mu}(t)}{dt} = \gamma \frac{d\mathbf{J}(t)}{dt} = -|\gamma| \frac{d\mathbf{J}(t)}{dt} = -|\gamma| \boldsymbol{\mu}(t) \times \mathbf{H}_{\text{int}}(t). \tag{2.3}$$

A physical sample consists of many magnetic dipoles, so that the torque equation is usually expressed in terms of the magnetic moment $\boldsymbol{\mu}(t)$ per sample volume V. This quantity is called the magnetization,

$$\mathbf{M}(t) = \boldsymbol{\mu}(t)/V, \tag{2.4}$$

and allows to express the magnetic torque equation in the form

$$\frac{d\mathbf{M}(t)}{dt} = -|\gamma| \mathbf{M}(t) \times \mathbf{H}_{\text{int}}(t). \tag{2.5}$$

Note that the torque equation conserves the magnitude of the magnetization vector, because the time rate of change of the magnetization vector, $d\mathbf{M}(t)/dt$, is always perpendicular to the magnetization vector itself.

In the next section a particularly simple case of the torque equation is considered, where the internal field is constant in time. This is the case when the sample is an infinite medium, and when the external applied field is static.

2.2.b The torque equation in an infinite medium

In an infinite medium there are no demagnetizing fields, since no boundary surfaces exist where magnetic dipole fields could form. As the simplest case of magnetization precession consider the free precession in an infinite medium. "Free" means that only a static field H_{ext} is applied in $z-$direction, but no microwave driving field is applied. Then the internal field in the sample coincides with the static applied field,

$$\mathbf{H}_{\text{int}}(t)=\begin{pmatrix}0\\0\\H_{ext}\end{pmatrix}=const. \tag{2.6}$$

In components, the torque equation of motion becomes;

$$\frac{dM_x(t)}{dt}=-|\gamma|H_{ext}M_y(t), \tag{2.7}$$

$$\frac{dM_y(t)}{dt}=|\gamma|H_{ext}M_x(t), \tag{2.8}$$

and

$$\frac{dM_z(t)}{dt}=0. \tag{2.9}$$

The steady state periodic solution of this system is given by

$$M_x(t)=M_{trans}\cos\left(|\gamma|H_{ext}t+\psi\right), \tag{2.10}$$

$$M_y(t)=M_{trans}\sin\left(|\gamma|H_{ext}t+\psi\right), \tag{2.11}$$

and

$$M_z(t)=M_{long}=const. \tag{2.12}$$

Here M_{trans} and M_{long} are the constant magnitudes of the transverse and longitudinal magnetization components, respectively, relative to the static applied field. The magnetization response contains two arbitrary parameters: the amplitude M of the transverse magnetization response, and a phase angle ψ. The magnetization precesses in a circle parallel to the $x-y$ plane with constant angular velocity

$$\omega_H = |\gamma| H_{ext}. \tag{2.13}$$

This is the natural frequency of the undriven precession in an infinite medium. Figure 2-1 shows that the free precession is performed in the Larmor sense, that is, counter-clockwise as the observer looks into the static applied field vector.

In the general case of a time-dependent internal field $\mathbf{H}_{int}(t)$, the magnetization precesses with the instantaneous angular velocity vector $|\gamma|\mathbf{H}_{int}(t)$ about the internal field vector. Figure 2.2 illustrates that at every instant of time, the magnetization trajectory is tangential to an *instantaneous precession circle* in a plane perpendicular to the instantaneous internal field. Since $\mathbf{H}_{int}(t)$ is time-dependent, both the plane and the center of the instantaneous precession circle vary with time as well.

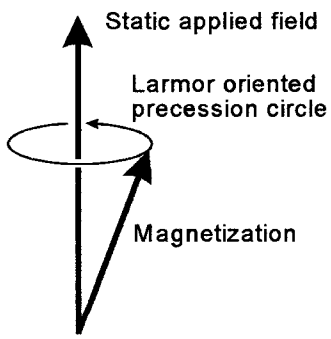

Figure 2-1: Free precession in an infinite medium, when the applied field is static. In this case the internal field coincides with the static applied field. The precession trajectory is a circle, traversed in the Larmor sense as the observer looks into the static applied field.

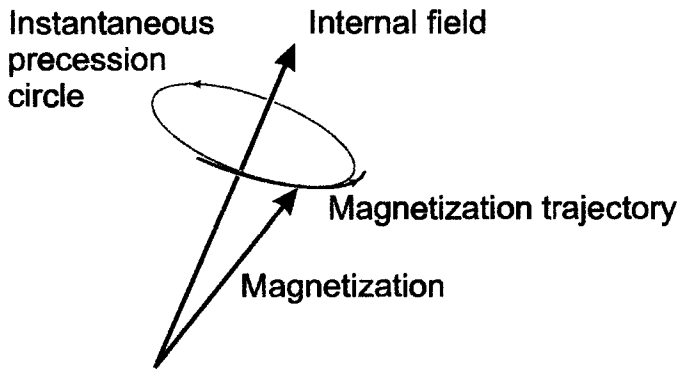

Figure 2-2: For a time-dependent internal field the magnetization response follows an instantaneous precession circle around the internal field in the Larmor sense. The plane, the center, and the radius of the instantaneous precession circle are time-dependent.

2.3 Driven precession in an infinite medium

2.3.a The small signal limit

The torque equation of motion developed in the last section describes the instantaneous precession of the magnetization about the direction of the instantaneous internal field. If the internal field is static, then the precession is called free precession. But if the internal field contains a microwave component, the precession is called driven precession, because the external applied microwave field acts as a driving field. The following analysis considers the microwave driving field as small compared with the static applied field, and the magnetization response as small compared with the saturation magnetization. This set of assumptions is called the small signal limit.

2.3.b Equations of motion in the Smith matrix form

As in the previous section, the magnetization precession is analyzed in an infinite medium. In such a medium, no demagnetizing fields are present, because there are no boundary surfaces to produce dipole fields. A static field of magnitude H_{ext} is applied in the z-direction, or longitudinal direction. In addition, in this section a small microwave field $\left(h_{ext-x}(t), h_{ext-y}(t)\right)^T$ is applied in the x-y plane, also called the transverse plane. Since there are no demagnetizing fields in an infinite medium, the internal field is the same as the external applied field in the sample,

$$\mathbf{H}_{\text{int}}(t) = \begin{pmatrix} h_{ext-x}(t) \\ h_{ext-y}(t) \\ H_{ext} \end{pmatrix}. \tag{2.14}$$

With this total internal field, the torque equation of motion in Eq. (2.5) becomes

$$\frac{dM_x(t)}{dt} = -|\gamma|\left[M_y(t)H_{ext} - M_s h_{ext-y}(t)\right], \tag{2.15}$$

$$\frac{dM_y(t)}{dt} = -|\gamma|\left[M_s h_{ext-x}(t) - M_x(t)H_{ext}\right], \tag{2.16}$$

and

$$\frac{dM_z(t)}{dt} = -|\gamma|\left[M_x(t)h_{ext-y}(t) - M_y(t)h_{ext-x}(t)\right]. \tag{2.17}$$

In the small signal limit, the transverse magnetization components $M_x(t)$ and $M_y(t)$ are much smaller than the saturation magnetization, and will, therefore, be denoted as $m_x(t)$ and $m_y(t)$, respectively. Due to the conservation of the magnitude of the total magnetization, the $z-$component of the magnetization vector is equal to the saturation magnetization, to first order in the $x-$ and $y-$components.

$$
\begin{aligned}
M_z(t) &= \sqrt{M_s^2 - m_x^2(t) - m_y^2(t)} \\
&= M_s\sqrt{1-\left[\frac{m_x(t)}{M_s}\right]^2 - \left[\frac{m_y(t)}{M_s}\right]^2} \\
&\approx M_s\left[1-\frac{1}{2}\frac{m_x^2(t)+m_y^2(t)}{M_s^2}\right] \\
&\approx M_s.
\end{aligned}
\tag{2.18}
$$

Therefore, in the small signal limit, the equations of motion for the transverse magnetization components $m_x(t)$ and $m_y(t)$ reduce to the system,

$$
\frac{dm_x(t)}{dt} = -|\gamma|\left[m_y(t)H_{ext} - M_s h_{ext-y}(t)\right] \tag{2.19}
$$

and

$$
\frac{dm_y(t)}{dt} = -|\gamma|\left[M_s h_{ext-x}(t) - m_x(t)H_{ext}\right]. \tag{2.20}
$$

With the natural frequency of the free precession, $\omega_H = |\gamma|H_{ext}$, from Eq. (2.13), this system is written in matrix form as

$$
\begin{pmatrix} \frac{dm_x(t)}{dt} \\ \frac{dm_y(t)}{dt} \end{pmatrix} = \begin{pmatrix} 0 & -\omega_H \\ \omega_H & 0 \end{pmatrix}\begin{pmatrix} m_x(t) \\ m_y(t) \end{pmatrix} + |\gamma|M_s\begin{pmatrix} 0 & 1 \\ -1 & 0 \end{pmatrix}\begin{pmatrix} h_{ext-x}(t) \\ h_{ext-y}(t) \end{pmatrix}. \tag{2.21}
$$

Solved for the driving field column vector $\left(h_{ext-x}(t), h_{ext-y}(t)\right)^T$, this equation becomes

$$
\frac{1}{|\gamma|M_s}\begin{pmatrix} 0 & -1 \\ 1 & 0 \end{pmatrix}\begin{pmatrix} \frac{dm_x(t)}{dt} \\ \frac{dm_y(t)}{dt} \end{pmatrix} + \frac{1}{|\gamma|M_s}\begin{pmatrix} \omega_H & 0 \\ 0 & \omega_H \end{pmatrix}\begin{pmatrix} m_x(t) \\ m_y(t) \end{pmatrix} = \begin{pmatrix} h_{ext-x}(t) \\ h_{ext-y}(t) \end{pmatrix}. \tag{2.22}
$$

This is the so-called Smith matrix form of the equations of motion in the small signal limit. The matrix

$$\vec{\mathbf{G}} = \frac{1}{|\gamma| M_s} \begin{pmatrix} 0 & -1 \\ 1 & 0 \end{pmatrix}, \tag{2.23}$$

which multiplies the time derivative term in the transverse magnetization response, is called the gyroscopic matrix. It is responsible for the precessional motion of the magnetization. The matrix

$$\vec{\mathbf{K}} = \frac{1}{|\gamma| M_s} \begin{pmatrix} \omega_H & 0 \\ 0 & \omega_H \end{pmatrix}, \tag{2.24}$$

which multiplies the magnetization term, is called the stiffness matrix. It measures the stiffness of the magnetization response to the external applied microwave field. The bigger the components of the stiffness matrix, the smaller the magnitude of the magnetization response to a given external applied microwave field. Later it is shown that the stiffness matrix determines the natural frequency of the undriven precession. With the gyroscopic matrix $\vec{\mathbf{G}}$ and the stiffness matrix $\vec{\mathbf{K}}$, the equations of motion in Eq. (2.22) can be written in matrix form as

$$\vec{\mathbf{G}} \frac{d\mathbf{m}(t)}{dt} + \vec{\mathbf{K}}\mathbf{m}(t) = \mathbf{h}_{ext}(t). \tag{2.25}$$

In Chapter 3 this equation will be supplemented by a damping term $\vec{\mathbf{D}} \frac{d\mathbf{m}(t)}{dt}$ on the left hand side to model the damped magnetization response. The constant matrix $\vec{\mathbf{D}}$ is called the damping matrix and depends on the particular damping model.

2.3.c Magnetization response in an infinite medium

The magnetization response to an external applied microwave field will now be determined by the so-called method of complex amplitudes. In this method each two-dimensional vector quantity $\mathbf{a}(t)$ with a harmonic time dependence at some frequency ω is characterized by its complex amplitude $\mathbf{a}_0$ through

$$\mathbf{a}(t) = \mathrm{Re}\left(\mathbf{a}_0 e^{i\omega t}\right). \tag{2.26}$$

By a suitable choice of the complex amplitude, every possible elliptical polarization of the sinusoidal vector quantity can be achieved. For example, to describe a circular polarization in the Larmor sense, relative to the direction of the z-axis, one may choose

$$\mathbf{a}_0 = \frac{a_0}{\sqrt{2}} e^{i\varphi} \begin{pmatrix} 1 \\ -i \end{pmatrix}, \tag{2.27}$$

where a_0 is the magnitude of $\mathbf{a}_0$, and φ is an arbitrary phase angle. Indeed, the components of the real vector quantity $\mathbf{a}(t)$ are

$$a_x(t) = \mathrm{Re}\left(\frac{a_0}{\sqrt{2}} e^{i\varphi} e^{i\omega t} \right) = \frac{a_0}{\sqrt{2}} \cos(\omega t + \varphi) \tag{2.28}$$

and

$$a_y(t) = \mathrm{Re}\left(-i \frac{a_0}{\sqrt{2}} e^{i\varphi} e^{i\omega t} \right) = \frac{a_0}{\sqrt{2}} \sin(\omega t + \varphi). \tag{2.29}$$

This is a circular precession in the Larmor sense. Table 2-1 gives the complex amplitude vectors corresponding to several special cases of elliptical polarization.

The complex amplitude method is now used to solve the system in Eq. (2.15) by means of matrix operations. Both the microwave driving field and the magnetization response are expressed in terms of their complex amplitudes. By this procedure, the time dependence is eliminated from the system, and a linear system is obtained for the complex amplitudes of the magnetization response. The matrix of this system is called the external susceptibility tensor. One starts with dynamic magnetization components of the form

$$m_x(t) = \mathrm{Re}\left(m_{x0} e^{i\omega t}\right) \tag{2.30}$$

and

$$m_y(t) = \mathrm{Re}\left(m_{y0}e^{i\omega t}\right), \tag{2.31}$$

and external applied microwave field components

$$h_{ext-x}(t) = \mathrm{Re}\left(h_{ext-x0}e^{i\omega t}\right) \tag{2.32}$$

and

$$h_{ext-y}(t) = \mathrm{Re}\left(h_{ext-y0}e^{i\omega t}\right). \tag{2.33}$$

The equations of motion reduce to a linear system for the complex amplitude components m_{x0} and m_{y0}:

Type of polarization	components of time dependent vector quantity	complex amplitude
Larmor	$a_x(t) = \frac{a_0}{\sqrt{2}}\cos(\omega t + \varphi),$ $a_y(t) = \frac{a_0}{\sqrt{2}}\sin(\omega t + \varphi)$	$\frac{a_0}{\sqrt{2}}e^{i\varphi}\begin{pmatrix}1\\-i\end{pmatrix}$
anti-Larmor	$a_x(t) = \frac{a_0}{\sqrt{2}}\cos(\omega t + \varphi),$ $a_y(t) = -\frac{a_0}{\sqrt{2}}\sin(\omega t + \varphi)$	$\frac{a_0}{\sqrt{2}}e^{i\varphi}\begin{pmatrix}1\\i\end{pmatrix}$
linear in x-direction	$a_x(t) = a_0\cos(\omega t + \varphi),$ $a_y(t) = 0.$	$a_0e^{i\varphi}\begin{pmatrix}1\\0\end{pmatrix}$
linear in y-direction	$a_x(t) = 0,$ $a_y(t) = a_0\cos(\omega t + \varphi).$	$a_0e^{i\varphi}\begin{pmatrix}0\\1\end{pmatrix}$

Table 2-1: Complex amplitudes corresponding to special cases of elliptical polarization of the microwave driving field.

$$\begin{pmatrix} 0 & -1 \\ 1 & 0 \end{pmatrix}\begin{pmatrix} i\omega m_{x0} \\ i\omega m_{y0} \end{pmatrix}+\begin{pmatrix} \omega_H & 0 \\ 0 & \omega_H \end{pmatrix}\begin{pmatrix} m_{x0} \\ m_{y0} \end{pmatrix}=|\gamma|M_s\begin{pmatrix} h_{ext-x0} \\ h_{ext-y0} \end{pmatrix}. \tag{2.34}$$

Combination of the two terms on the left hand side yields,

$$\begin{pmatrix} \omega_H & -i\omega \\ i\omega & \omega_H \end{pmatrix}\begin{pmatrix} m_{x0} \\ m_{y0} \end{pmatrix}=|\gamma|M_s\begin{pmatrix} h_{ext-x0} \\ h_{ext-y0} \end{pmatrix}. \tag{2.35}$$

The solution is obtained by inversion of the matrix on the left side,

$$\begin{pmatrix} m_{x0} \\ m_{y0} \end{pmatrix}=|\gamma|M_s\begin{pmatrix} \omega_H & -i\omega \\ i\omega & \omega_H \end{pmatrix}^{-1}\begin{pmatrix} h_{ext-x0} \\ h_{ext-y0} \end{pmatrix}=\frac{|\gamma|M_s}{\omega_H^2-\omega^2}\begin{pmatrix} \omega_H & i\omega \\ -i\omega & \omega_H \end{pmatrix}\begin{pmatrix} h_{ext-x0} \\ h_{ext-y0} \end{pmatrix}. \tag{2.36}$$

In short hand notation, one writes

$$\mathbf{m}_0=\ddot{\chi}(\omega)\mathbf{h}_{ext-0}, \tag{2.37}$$

with the susceptibility tensor in an infinite medium,

$$\ddot{\chi}(\omega)=\frac{|\gamma|M_s}{\omega_H^2-\omega^2}\begin{pmatrix} \omega_H & i\omega \\ -i\omega & \omega_H \end{pmatrix}. \tag{2.38}$$

The susceptibility tensor $\ddot{\chi}(\omega)$ contains complete information about the magnetization response, both about amplitude and phase. After Polder [1948], the susceptibility tensor of the undamped magnetic precession in an infinite medium is called the Polder susceptibility tensor. In Table 2-2 the complex amplitude of the magnetization response is shown for some special cases of the driving field. Notice the following:

- The response to a Larmor polarized driving field is Larmor polarized. The amplitude of the response becomes infinite at the resonance frequency $\omega_H=|\gamma|H_{ext}$, which is the natural frequency of the undriven precession. The Larmor response is in phase with the driving field if the driving frequency is below the resonance frequency, that is for $\omega<\omega_H$. The Larmor response is phase-shifted by 180^0 if the driving frequency is above the resonance frequency, that is for $\omega>\omega_H$.

Polarization of driving field	Components of driving field	Complex amplitude of driving field	Complex amplitude of magnetization response
Larmor	$h_{ext-x}(t)=\frac{h_0}{\sqrt{2}}\cos(\omega t),$ $h_{ext-y}(t)=\frac{h_0}{\sqrt{2}}\sin(\omega t)$	$\frac{h_0}{\sqrt{2}}\begin{pmatrix}1\\-i\end{pmatrix}$	$\frac{\lvert\gamma\rvert M_s}{\omega_H-\omega}\frac{h_0}{\sqrt{2}}\begin{pmatrix}1\\-i\end{pmatrix}$
anti-Larmor	$h_{ext-x}(t)=\frac{h_0}{\sqrt{2}}\cos(\omega t),$ $h_{ext-y}(t)=-\frac{h_0}{\sqrt{2}}\sin(\omega t)$	$\frac{h_0}{\sqrt{2}}\begin{pmatrix}1\\i\end{pmatrix}$	$\frac{\lvert\gamma\rvert M_s}{\omega_H+\omega}\frac{h_0}{\sqrt{2}}\begin{pmatrix}1\\i\end{pmatrix}$
linear in x direction	$h_{ext-x}(t)=h_0\cos(\omega t),$ $h_{ext-y}(t)=0.$	$\frac{h_0}{2}\begin{pmatrix}1\\-i\end{pmatrix}+\frac{h_0}{2}\begin{pmatrix}1\\i\end{pmatrix}$	$\frac{\lvert\gamma\rvert M_s}{\omega_H-\omega}\frac{h_0}{2}\begin{pmatrix}1\\-i\end{pmatrix}$ $+\frac{\lvert\gamma\rvert M_s}{\omega_H+\omega}\frac{h_0}{2}\begin{pmatrix}1\\i\end{pmatrix}$

Table 2-2: Magnetization response for special cases of the polarization of the driving field in an infinite medium.

- The response to an anti-Larmor polarized driving field is anti-Larmor polarized, and is always in phase with the driving field. The amplitude of the response is a decreasing function of the driving frequency.
- The response to a linearly polarized driving field is not linearly polarized, but elliptically polarized. The reason is that a linearly polarized field can be decomposed into a Larmor component and an anti-Larmor component of equal amplitudes. However the amplitudes of the corresponding Larmor and anti-Larmor components of the magnetization response are not equal. Therefore the magnetization response to a linearly polarized driving field is not linear.

In Fig. 2-3 the lossless susceptibility is shown as a function of the applied microwave field frequency

for a static applied field of 2000 Oe in an idealized bulk material with the same saturation magnetization as YIG, $4\pi M_s = 1750\ Oe$. The lossless susceptibility is shown for a Larmor oriented driving field, for an anti-Larmor polarized driving field, and for a linearly polarized driving field.

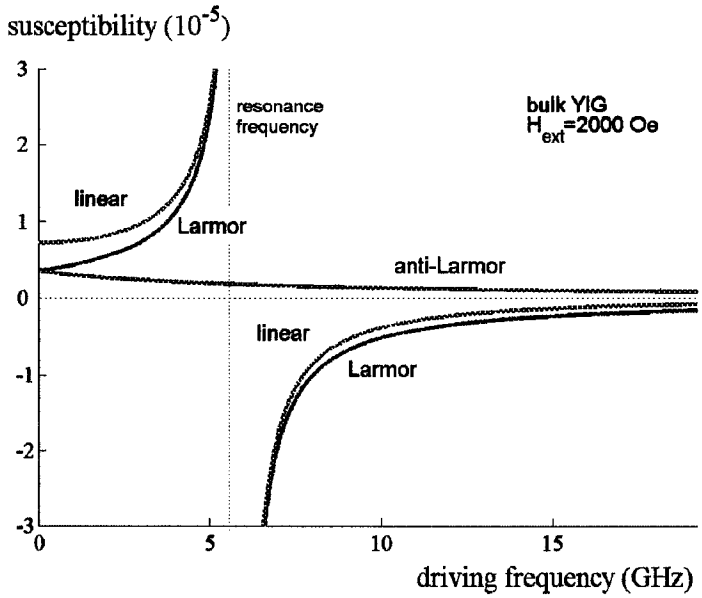

Figure 2-3: Susceptibility in an idealized lossless bulk material with the same saturation magnetization as YIG, that is with $4\pi M_s = 1750\ Oe$. The static applied field is $2000\ Oe$. The susceptibility is understood here to be the quotient of the complex amplitudes of the magnetization response and the microwave driving field. These complex amplitudes were shown in Table 2-2. For a Larmor driving field resonance occurs at the eigenfrequency of the free oscillation. For an anti-Larmor driving field, there is no resonance; instead the susceptibility is positive and decreases with the driving frequency. Resonance also occurs for a linear driving field, because it has a Larmor component. Positive susceptibility indicates that the magnetization response is in phase with the driving field, and negative susceptibility indicates that the magnetization response is 180^0 out of phase with the driving field.

2.4 Driven precession in an ellipsoidal sample

2.4.a Demagnetizing field in an ellipsoidal sample

In the previous section the magnetization precession was calculated for an infinite medium subjected to a static applied field. In the experimental practice, however, and in technological applications, one must deal with finite samples of a certain shape. To calculate the magnetic fields inside the sample it is necessary to solve the electromagnetic boundary value problem with Maxwell's equations. In general, this is a difficult task. However, simple closed-form solutions have been obtained in the case of special sample shapes, such as ellipsoids. Shapes such as thin films and rods can be considered as limiting cases of ellipsoids.

When a homogeneous sample is placed in an externally applied DC magnetic field, it becomes polarized. The magnetic poles induced at the surface lead to a demagnetizing field inside the sample that is opposed to the applied field. The magnetic field inside the sample, or internal field, is then the sum of the static applied field and the demagnetizing field. For an ellipsoidal sample, the demagnetizing field is determined by the demagnetizing factors N_x, N_y and N_z in the directions of the three principal symmetry axes of the ellipsoid. The sum of the demagnetizing factors is always 1. The demagnetizing field corresponding to the magnetization $\mathbf{M}(t)=\left[M_x(t),M_y(t),M_z(t)\right]^T$ is then given by

$$\mathbf{H}_{demag}(t)=-4\pi\begin{pmatrix}N_x & 0 & 0\\ 0 & N_y & 0\\ 0 & 0 & N_z\end{pmatrix}\begin{pmatrix}M_x(t)\\ M_y(t)\\ M_z(t)\end{pmatrix}. \tag{2.39}$$

The matrix

$$\vec{\mathbf{N}}=\begin{pmatrix}N_x & 0 & 0\\ 0 & N_y & 0\\ 0 & 0 & N_z\end{pmatrix} \tag{2.40}$$

is called the demagnetizing tensor.

Kittel [1949] has shown that the demagnetizing field of an applied time-dependent field can be written in a similar way as the demagnetizing field of an applied static field. In a ferromagnetic resonance experiment, if a static field is applied in the z – direction and a microwave field is applied perpendicularly to it with components $h_{ext-x}(t)$ and $h_{ext-y}(t)$, then the internal field in the sample is the sum of the external applied field and the demagnetizing field,

$$\mathbf{H}_{\text{int}}(t) = \mathbf{H}_{ext}(t) + \mathbf{H}_{demag}(t)$$

$$= \begin{pmatrix} h_{ext-x}(t) \\ h_{ext-y}(t) \\ H_{ext} \end{pmatrix} - 4\pi \begin{pmatrix} N_x & 0 & 0 \\ 0 & N_y & 0 \\ 0 & 0 & N_z \end{pmatrix} \cdot \begin{pmatrix} M_x(t) \\ M_y(t) \\ M_z(t) \end{pmatrix} \cdot \tag{2.41}$$

In the small signal limit, this reduces to

$$\mathbf{H}_{\text{int}}(t) = \begin{pmatrix} h_{ext-x}(t) \\ h_{ext-y}(t) \\ H_{ext} \end{pmatrix} - 4\pi \begin{pmatrix} N_x & 0 & 0 \\ 0 & N_y & 0 \\ 0 & 0 & N_z \end{pmatrix} \cdot \begin{pmatrix} m_x(t) \\ m_y(t) \\ M_s \end{pmatrix} = \begin{pmatrix} h_{ext-x}(t) - 4\pi N_x m_x(t) \\ h_{ext-y}(t) - 4\pi N_y m_y(t) \\ H_{ext} - 4\pi N_z M_s \end{pmatrix}. \tag{2.42}$$

In the next section the magnetization response to a microwave driving field is determined in an ellipsoidal sample, when the internal field is given by Eq. (2.42).

2.4.b Equations of motion in the Smith matrix form

The last section developed the uniform demagnetizing field in an ellipsoidal sample. The internal field is the sum of the static applied field, the transverse applied microwave field, and the demagnetizing field. The resulting equations of motion in the small signal limit have the same form for the ellipsoidal sample as for the infinite medium. However, the external applied field is replaced with the stiffness fields, and the natural frequency of the free precession is replaced with the geometric mean of the two stiffness frequencies. As for the infinite medium, the equations of motion

can be either

- solved explicitly for the time derivatives of the magnetization components, or
- written in Smith matrix form, solved for the components of the applied microwave field.

With the internal field in Eq. (2.42), the torque equation of motion becomes in the small signal limit:

$$\frac{dm_x(t)}{dt} = -|\gamma| m_y(t)[H_{ext} - 4\pi M_s N_z] - |\gamma| M_s(t)\left[-h_{ext-y}(t) + 4\pi N_y m_y(t)\right], \tag{2.43}$$

$$\frac{dm_y(t)}{dt} = |\gamma| m_x(t)[H_{ext} - 4\pi M_s N_z] - |\gamma| M_s(t)\left[h_{ext-x}(t) - 4\pi N_x m_x(t)\right], \tag{2.44}$$

With stiffness fields defined as

$$X_H = H_{ext} + (N_x - N_z)\cdot 4\pi M_s \tag{2.45}$$

and

$$Y_H = H_{ext} + (N_y - N_z)\cdot 4\pi M_s, \tag{2.46}$$

the equations of motion in the small signal limit can be written in compact form as

$$\frac{dm_x(t)}{dt} = |\gamma|\left[-Y_H m_y(t) + M_s h_{ext-y}(t)\right], \tag{2.47}$$

and

$$\frac{dm_y(t)}{dt} = |\gamma|\left[X_H m_x(t) - M_s h_{ext-x}(t)\right]. \tag{2.48}$$

These equations may be compared with the equations of motion in an infinite medium, given in Eqs. (2.19) and (2.20). The static applied field H_{ext} multiplying the magnetization components $m_x(t)$ and $m_y(t)$ has been replaced with the stiffness fields X_H and Y_H, respectively. Solved for the

components of the applied microwave field, the equations of motion take the Smith matrix form

$$\frac{1}{|\gamma|M_s}\begin{pmatrix}0 & -1\\ 1 & 0\end{pmatrix}\begin{pmatrix}dm_x(t)/dt\\ dm_y(t)/dt\end{pmatrix}+\frac{1}{|\gamma|M_s}\begin{pmatrix}\omega_x & 0\\ 0 & \omega_y\end{pmatrix}\begin{pmatrix}m_x(t)\\ m_y(t)\end{pmatrix}=\begin{pmatrix}h_{ext-x}(t)\\ h_{ext-y}(t)\end{pmatrix}. \tag{2.49}$$

Here

$$\omega_x=|\gamma|X_H \tag{2.50}$$

and

$$\omega_y=|\gamma|Y_H \tag{2.51}$$

are the stiffness *frequencies* corresponding to the stiffness *fields* X_H and Y_H, respectively. Notice the striking similarity to the Smith matrix form of the corresponding Eq. (2.22) in an infinite medium, given by

$$\frac{1}{|\gamma|M_s}\begin{pmatrix}0 & -1\\ 1 & 0\end{pmatrix}\begin{pmatrix}dm_x(t)/dt\\ dm_y(t)/dt\end{pmatrix}+\frac{1}{|\gamma|M_s}\begin{pmatrix}\omega_H & 0\\ 0 & \omega_H\end{pmatrix}\begin{pmatrix}m_x(t)\\ m_y(t)\end{pmatrix}=\begin{pmatrix}h_{ext-x}(t)\\ h_{ext-y}(t)\end{pmatrix}. \tag{2.52}$$

The anti-symmetric gyroscopic matrix is the same,

$$\vec{\mathbf{G}}=\frac{1}{|\gamma|M_s}\begin{pmatrix}0 & -1\\ 1 & 0\end{pmatrix}. \tag{2.53}$$

In the symmetric stiffness matrix, the natural frequency ω_H in the two diagonal elements of the stiffness matrix has been replaced by the stiffness frequencies ω_x and ω_y, respectively, so that

$$\vec{\mathbf{K}}=\frac{1}{|\gamma|M_s}\begin{pmatrix}\omega_x & 0\\ 0 & \omega_y\end{pmatrix}. \tag{2.54}$$

The equations of motions in Eq. (2.49) then become, in Smith matrix form,

$$\vec{\mathbf{G}}\frac{d\mathbf{m}(t)}{dt}+\vec{\mathbf{K}}\mathbf{m}(t)=\mathbf{h}_{ext}(t),$$

and will now be solved with the complex amplitude method.

2.4.c Magnetization response in an ellipsoidal sample

As in the treatment for the infinite medium in Section 2.3.c, a harmonic driving field $\mathbf{h}_{ext}(t)$ with driving frequency ω and harmonic magnetization response $\mathbf{m}(t)$ can be expressed in terms of complex amplitudes:

$$h_{ext-x}(t) = \mathrm{Re}\left(h_{ext-x0}e^{i\omega t}\right), \tag{2.55}$$

$$h_{ext-y}(t) = \mathrm{Re}\left(h_{ext-y0}e^{i\omega t}\right), \tag{2.56}$$

$$m_x(t) = \mathrm{Re}\left(m_{x0}e^{i\omega t}\right), \tag{2.57}$$

and

$$m_y(t) = \mathrm{Re}\left(m_{y0}e^{i\omega t}\right). \tag{2.58}$$

Substitution into the equations of motion in Eq. (2.49) yields a linear system for the complex magnetization amplitudes,

$$\frac{1}{|\gamma|M_s}\begin{pmatrix}\omega_x & -i\omega\\ i\omega & \omega_y\end{pmatrix}\begin{pmatrix}m_{x0}\\ m_{y0}\end{pmatrix} = \begin{pmatrix}h_{ext-x0}\\ h_{ext-y0}\end{pmatrix}, \tag{2.59}$$

so that

$$\begin{aligned}\begin{pmatrix}m_{x0}\\ m_{y0}\end{pmatrix} &= |\gamma|M_s\begin{pmatrix}\omega_x & -i\omega\\ i\omega & \omega_y\end{pmatrix}^{-1}\begin{pmatrix}h_{ext-x0}\\ h_{ext-y0}\end{pmatrix}\\ &= \frac{|\gamma|M_s}{\omega_x\omega_y-\omega^2}\begin{pmatrix}\omega_y & i\omega\\ -i\omega & \omega_x\end{pmatrix}\begin{pmatrix}h_{ext-x0}\\ h_{ext-y0}\end{pmatrix}.\end{aligned} \tag{2.60}$$

The susceptibility tensor for the complex amplitudes in Cartesian coordinates is therefore given by

$$\ddot{\chi}(\omega) = \frac{|\gamma|M_s}{\omega_x\omega_y-\omega^2}\begin{pmatrix}\omega_y & i\omega\\ -i\omega & \omega_x\end{pmatrix}. \tag{2.61}$$

From this equation is clear that the magnetization response diverges at the Kittel resonance frequency (Kittel [1949]),

$$\omega_{Kittel} = \sqrt{\omega_x \omega_y} \,. \tag{2.62}$$

As in the case of an infinite medium, the resonance frequency of the driven precession coincides with the natural frequency of the undriven precession. This natural frequency is easily determined from the Smith matrix form of the equations of motion in Eq. (2.49), when the microwave driving field is set to zero.

$$\frac{1}{|\gamma| M_s}\begin{pmatrix} 0 & -1 \\ 1 & 0 \end{pmatrix}\begin{pmatrix} dm_x(t)/dt \\ dm_y(t)/dt \end{pmatrix} + \frac{1}{|\gamma| M_s}\begin{pmatrix} \omega_x & 0 \\ 0 & \omega_y \end{pmatrix}\begin{pmatrix} m_x(t) \\ m_y(t) \end{pmatrix} = \begin{pmatrix} 0 \\ 0 \end{pmatrix}. \tag{2.63}$$

Substitution of the complex amplitude approach

$$m_x(t) = \mathrm{Re}\left(m_{x0} e^{i\omega_0 t}\right) \tag{2.64}$$

and

$$m_y(t) = \mathrm{Re}\left(m_{y0} e^{i\omega_0 t}\right) \tag{2.65}$$

into Eq. (2.63) yields the linear system

$$i\omega_0 \begin{pmatrix} 0 & -1 \\ 1 & 0 \end{pmatrix}\begin{pmatrix} m_{x0} \\ m_{y0} \end{pmatrix} + \begin{pmatrix} \omega_x & 0 \\ 0 & \omega_y \end{pmatrix}\begin{pmatrix} m_{x0} \\ m_{y0} \end{pmatrix} = \begin{pmatrix} 0 \\ 0 \end{pmatrix}, \tag{2.66}$$

that is,

$$\begin{pmatrix} \omega_x & -i\omega_0 \\ i\omega_0 & \omega_y \end{pmatrix}\begin{pmatrix} m_{x0} \\ m_{y0} \end{pmatrix} = \begin{pmatrix} 0 \\ 0 \end{pmatrix}. \tag{2.67}$$

This linear system has a nontrivial solution if and only if the determinant is zero:

$$\omega_x \omega_y - \omega_0^2 = 0 \,. \tag{2.68}$$

The two solutions for the natural frequency are

$$\omega_0 = \pm\sqrt{\omega_x \omega_y}\,. \tag{2.69}$$

What is the physical meaning of the negative frequency solution? Consider the magnetization response for both the positive and the negative frequency solution. For the positive natural frequency, $\omega_{0+} = \sqrt{\omega_x \omega_y}$, the complex amplitude of the magnetization response has the form

$$\begin{pmatrix} m_{x0+} \\ m_{y0+} \end{pmatrix} = c e^{i\varphi} \begin{pmatrix} \sqrt{\omega_y} \\ -i\sqrt{\omega_x} \end{pmatrix} \tag{2.70}$$

with arbitrary real constants c and φ. For the negative natural frequency, $\omega_{0-} = -\sqrt{\omega_x \omega_y}$, the complex amplitude of the magnetization response has the form

$$\begin{pmatrix} m_{x0-} \\ m_{y0-} \end{pmatrix} = c e^{-i\varphi} \begin{pmatrix} \sqrt{\omega_y} \\ i\sqrt{\omega_x} \end{pmatrix} \tag{2.71}$$

with arbitrary real constants c and φ. Since the complex amplitudes m_{x0-} and m_{y0-} of the negative frequency solution are complex conjugate to the corresponding complex amplitudes m_{x0+} and m_{y0+} of the positive frequency solution, the time-dependent transverse magnetization components are the same for both frequencies:

$$m_x(t) = c\sqrt{\omega_y}\cos\left(\sqrt{\omega_x \omega_y}\,t + \varphi\right) \tag{2.72}$$

and

$$m_y(t) = c\sqrt{\omega_x}\sin\left(\sqrt{\omega_x \omega_y}\,t + \varphi\right). \tag{2.73}$$

Both the positive and the negative frequency leads to the same physical magnetization response! Therefore, the negative frequency solution can be omitted as redundant.

2.5 Internal energy and stiffness matrix

2.5.a Internal energy in an ellipsoidal sample

The potential magnetic energy in a uniformly magnetized ferromagnetic sample consists of the demagnetizing energy due to the static and dynamic demagnetization fields and the Zeeman energy due to the static applied field. Since the equation of motion conserves the magnitude of the magnetization, the potential energy can be expressed as a quadratic form in the two transverse magnetization components alone. Furthermore it is shown in the small signal limit that for an ellipsoidal sample, the stiffness matrix in the equation of motion is exactly the matrix by which the internal energy is expressed as a quadratic form in the magnetization components. Recall from Eq. (2.39) that the demagnetizing field in an ellipsoidal sample can be written as

$$\mathbf{H}_{demag}(t) = -4\pi\vec{\mathbf{N}}\cdot\mathbf{M}(t) = -4\pi\begin{pmatrix} N_x & 0 & 0 \\ 0 & N_y & 0 \\ 0 & 0 & N_z \end{pmatrix}\cdot\mathbf{M}(t). \tag{2.74}$$

Since the demagnetizing field is the negative gradient of the demagnetizing energy, the latter is given by

$$\mathbf{U}_{demag}(t) = 2\pi\left[N_x M_x^2(t) + N_y M_y^2(t) + N_z M_z^2(t)\right]. \tag{2.75}$$

The Zeeman energy corresponding to the static external field H_{ext} in $z-$direction is

$$\mathbf{U}_{Zeeman}(t) = -H_{ext} M_z(t). \tag{2.76}$$

The potential energy $\mathbf{U}_{pot}(t)$ is the sum of the demagnetizing and the Zeeman energy, therefore

$$\mathbf{U}_{pot}(t) = 2\pi\left[N_x M_x^2(t) + N_y M_y^2(t) + N_z M_z^2(t)\right] - H_{ext} M_z(t). \tag{2.77}$$

Note that the "energies" here referred to are actually volume densities of energies, since the magnetization is a volume density (of the magnetic moment) itself. Now it will be shown that in the

small signal limit, the potential energy can be expressed with the stiffness fields X_H and Y_H in the form,

$$\mathbf{U}_{pot}(t) = \frac{1}{2}\frac{X_H}{M_s}m_x^2(t) + \frac{1}{2}\frac{Y_H}{M_s}m_y^2(t), \tag{2.78}$$

where $m_x(t)$ and $m_y(t)$ are the transverse magnetization components in the small signal limit.

The stiffness fields X_H and Y_H are the same stiffness fields developed earlier in the precession analysis. Recall that for an ellipsoidal sample they are given in Eqs. (2.45) and (2.46) by

$$X_H = H_{ext} + 4\pi(N_x - N_z)M_s \tag{2.79}$$

and

$$Y_H = H_{ext} + 4\pi(N_y - N_z)M_s. \tag{2.80}$$

The approximation in Eq. (2.78) follows directly from the exact formula in Eq. (2.77) with the approximation of the longitudinal magnetization component developed earlier in Eq. (2.18),

$$M_z(t) \approx M_s\left[1 - \frac{1}{2}\frac{m_x^2(t) + m_y^2(t)}{M_s^2}\right]. \tag{2.81}$$

One obtains the small signal approximation of the internal energy as

$$\begin{aligned}
\mathbf{U}_{pot} &= 2\pi\left(N_x m_x^2 + N_y m_y^2 + N_z M_z^2\right) - H_{ext}M_z \\
&\approx 2\pi\left[N_x m_x^2 + N_y m_y^2 + N_z\left(M_s^2 - m_x^2 - m_y^2\right)\right] - H_{ext}M_s\left(1 - \frac{1}{2}\frac{m_x^2 + m_y^2}{M_s^2}\right) \\
&= \frac{1}{2}\frac{H_{ext} + 4\pi(N_x - N_z)M_s}{M_s}m_x^2 + \frac{1}{2}\frac{H_{ext} + 4\pi(N_y - N_z)M_s}{M_s}m_y^2 + 2\pi N_z M_s^2 - H_{ext}M_s \\
&= \frac{1}{2}\frac{X_H}{M_s}m_x^2 + \frac{1}{2}\frac{Y_H}{M_s}m_y^2 + 2\pi N_z M_s^2 - H_{ext}M_s.
\end{aligned} \tag{2.82}$$

In this equation the time dependencies were not written. The last two terms are constant, and can be omitted, since any potential energy, or potential energy density, is only determined up to an additive constant. If this constant is dropped, one obtains the potential energy in the simple form given in Eq. (2.78).

2.5.b The role of the stiffness matrix

Recall the stiffness matrix,

$$\vec{\mathbf{K}} = \begin{pmatrix} \frac{X_H}{M_s} & 0 \\ 0 & \frac{Y_H}{M_s} \end{pmatrix} \tag{2.83}$$

from the equations of motion in Smith matrix form. With the stiffness matrix, the potential energy for an ellipsoidal sample in the small signal limit takes the vector-matrix form

$$U_{pot}(t) = \frac{1}{2}\left[\mathbf{m}(t)\right]^T \vec{\mathbf{K}} \left[\mathbf{m}(t)\right], \tag{2.84}$$

where $\mathbf{m}(t) = \left[m_x(t), m_y(t)\right]^T$ is the vector of the transverse magnetization components.

The goal of this section is to show that this connection between the potential energy and the stiffness matrix is not a coincidence. Rather, the form of the potential energy in Eq. (2.84) is a consequence of the equations of motion in the small signal limit. Recall that these are given by

$$\vec{\mathbf{G}} \frac{d\mathbf{m}(t)}{dt} + \vec{\mathbf{K}}\, \mathbf{m}(t) = \mathbf{h}_{ext}(t). \tag{2.85}$$

Consider the power transferred into the system by the external microwave driving field,

$$P_{in}(t) = \mathbf{h}_{ext}(t) \cdot \frac{d\mathbf{m}(t)}{dt}. \tag{2.86}$$

This formula is analogous to the rule "power equals force times velocity" in classical mechanics.

With the equation of motion in Eq. (2.85), the input power can be readily expressed in terms of the magnetization response alone,

$$\begin{aligned} P_{in}(t) &= \left(\vec{\vec{\mathbf{G}}} \frac{d\mathbf{m}(t)}{dt} + \vec{\vec{\mathbf{K}}}\, \mathbf{m}(t) \right) \cdot \frac{d\mathbf{m}(t)}{dt} \\ &= \left[\vec{\vec{\mathbf{G}}} \frac{d\mathbf{m}(t)}{dt} \right] \cdot \frac{d\mathbf{m}(t)}{dt} + \left[\vec{\vec{\mathbf{K}}}\, \mathbf{m}(t) \right] \cdot \frac{d\mathbf{m}(t)}{dt}. \end{aligned} \tag{2.87}$$

This equation is more conveniently written, with matrix multiplications instead of inner products, as

$$P_{in}(t) = \left[\frac{d\mathbf{m}(t)}{dt} \right]^T \vec{\vec{\mathbf{G}}} \frac{d\mathbf{m}(t)}{dt} + \left[\frac{d\mathbf{m}(t)}{dt} \right]^T \vec{\vec{\mathbf{K}}}\, \mathbf{m}(t). \tag{2.88}$$

The first term on the right-hand side of this equation is zero, because $\mathbf{x}^T \vec{\vec{\mathbf{A}}}^{antisym} \mathbf{x} = 0$ for any anti-symmetric $n \times n$ matrix $\vec{\vec{\mathbf{A}}}^{antisym}$ and any compatible (that is $n \times 1$) column vector $\mathbf{x}$. The proof of this fact proceeds as follows:

Any scalar $\mathbf{x}^T \vec{\vec{\mathbf{A}}}^{antisym} \mathbf{x}$ can be considered as a 1×1 matrix, which is its own transpose. That is,

$$\mathbf{x}^T \vec{\vec{\mathbf{A}}}^{antisym} \mathbf{x} = \left(\mathbf{x}^T \vec{\vec{\mathbf{A}}}^{antisym} \mathbf{x} \right)^T . \tag{2.89}$$

By the rules for taking the transposition of a matrix product, this implies the further connection,

$$\mathbf{x}^T \vec{\vec{\mathbf{A}}}^{antisym} \mathbf{x} = \mathbf{x}^T \left(\vec{\vec{\mathbf{A}}}^{antisym} \right)^T \mathbf{x} = = -\mathbf{x}^T \vec{\vec{\mathbf{A}}}^{antisym} \mathbf{x} . \tag{2.90}$$

The last step used the fact that the the transpose of an antisymmetric matrix is its negative. The only number that is its own negative is zero. Therefore, $\mathbf{x}^T \vec{\vec{\mathbf{A}}}^{antisym} \mathbf{x} = 0$, which we set out to prove.

The second term on the right side of Eq. (2.88) can be written as a time derivative because of a generalization of the product rule, $\frac{d}{dt} \left\{ \left[\mathbf{m}(t) \right]^T \vec{\vec{\mathbf{K}}}\, \mathbf{m}(t) \right\} = 2 \left[d\mathbf{m}(t)/dt \right]^T \vec{\vec{\mathbf{K}}}\, \mathbf{m}(t)$, which is valid because the matrix $\vec{\vec{\mathbf{K}}}$ is symmetric. This leads to a compact notation for the power into the system,

$$P_{in}(t)=\frac{d}{dt}\left\{\frac{1}{2}\left[\mathbf{m}(t)\right]^{T}\ \vec{\mathbf{K}}\,\mathbf{m}(t)\right\}. \tag{2.91}$$

Since the undamped torque equation of motion dissipates no energy, the input power $P_{in}(t)$ is equal to the time rate of change of the potential energy. Hence in Eq. (2.91) the quantity in braces must be the potential energy, and one has, therefore,

$$U_{pot}(t)=\frac{1}{2}\left[\mathbf{m}(t)\right]^{T}\ \vec{\mathbf{K}}\,\mathbf{m}(t). \tag{2.92}$$

This representation of the potential energy remains valid if, in order to incorporate magnetocrystalline anisotropy into the equations of motion, a more general form of the stiffness matrix is used. In fact, the stiffness matrix can be defined as the matrix of second partial derivatives of the potential magnetic energy with respect to the magnetization components, evaluated at the equilibrium $\left(m_x,m_y\right)^{T}=(0,0)^{T}$ in the absence of damping.

$$\vec{\mathbf{K}}=\begin{pmatrix} \left.\dfrac{\partial^2 U_{pot}\left(m_x,m_y\right)}{\partial m_x^2}\right|_{\substack{m_x=0\\m_y=0}} & \left.\dfrac{\partial^2 U_{pot}\left(m_x,m_y\right)}{\partial m_x \partial m_y}\right|_{\substack{m_x=0\\m_y=0}} \\ \left.\dfrac{\partial^2 U_{pot}\left(m_x,m_y\right)}{\partial m_y \partial m_x}\right|_{\substack{m_x=0\\m_y=0}} & \left.\dfrac{\partial^2 U_{pot}\left(m_x,m_y\right)}{\partial m_y^2}\right|_{\substack{m_x=0\\m_y=0}} \end{pmatrix}. \tag{2.93}$$

The stiffness matrix is symmetric, because the mixed partial derivatives of the potential magnetic energy are equal. To second order in the magnetization components, the Taylor expansion of the potential magnetic energy yields,

$$U_{pot}(\mathbf{m})=U_{pot}(\mathbf{0})+\left[\nabla U_{pot}(\mathbf{0})\right]^{T}\mathbf{m}+\frac{1}{2}\mathbf{m}^{T}\vec{\mathbf{K}}\mathbf{m}. \tag{2.94}$$

Since the potential magnetic energy attains a minimum at the stable equilibrium of zero transverse magnetization, the gradient $\nabla U_{pot}(\mathbf{0})$ is zero, and the stiffness matrix $\vec{\mathbf{K}}$ is positive definite. Without loss of generality the potential energy, defined only up to an additive constant, was set to

zero at the equilibrium. Thus in the small signal limit the potential energy is the quadratic form given above in Eq. (2.92).

2.6 Static and instantaneous equilibrium

2.6.a Static equilibrium

If all applied fields are static, one has the usual conditions for magnetostatic equilibrium in which the magnetization vector is aligned with the static internal field. In the small signal limit formulation, one then takes $h_{ext-x}(t) = h_{ext-x}^{(static)}$ and $h_{ext-y}(t) = h_{ext-y}^{(static)}$, and solves the magnetostatic equilibrium problem for $m_x^{(static)}$ and $m_y^{(static)}$. For the actual dynamic external fields $h_{ext-x}(t)$ and $h_{ext-y}(t)$, one can do the same analysis, but the resulting transverse magnetization components $m_x^{(eq)}(t)$ and $m_y^{(eq)}(t)$ will correspond to an "instantaneous" equilibrium. The actual magnetization components $m_x(t)$ and $m_y(t)$ will, in general, be different from those of the instantaneous equilibrium, $m_x^{(eq)}(t)$ and $m_y^{(eq)}(t)$. The time dependencies of $m_x^{(eq)}(t)$ and $m_y^{(eq)}(t)$ derive from the time dependencies of $h_{ext-x}(t)$ and $h_{ext-y}(t)$, and have nothing to do with the actual $m_x(t)$ and $m_y(t)$.

To calculate the static equilibrium for a small static transverse applied field $\left(h_{ext-x}^{(static)}, h_{ext-y}^{(static)}\right)^T$ and a static applied field H_{ext} in z-direction, consider the internal field that will be present at equilibrium. This field is given, in components, as

$$h_{int-x}^{(static)} = h_{ext-x}^{(static)} - 4\pi N_x m_x^{(static)}, \tag{2.95}$$

$$h_{int-y}^{(static)} = h_{ext-y}^{(static)} - 4\pi N_y m_y^{(static)}, \tag{2.96}$$

and

$$H_{int} = H_{ext} - 4\pi M_s N_z. \tag{2.97}$$

For the equilibrium magnetization to be collinear with the internal field in equilibrium, one must have

$$\frac{m_x^{(static)}}{M_s} = \frac{h_{int-x}^{(static)}}{H_{int}} \text{ and } \frac{m_y^{(static)}}{M_s} = \frac{h_{int-y}^{(static)}}{H_{int}}. \tag{2.98}$$

In Fig. 2-4, the x-collinearity is illustrated. The first diagram shows a net x-z magnetization vector, formed by the x- and z-component of the equilibrium magnetization. The second diagram shows the total x-z-field vector, formed by the x- and z-component of the internal field in equilibrium. The similarity of the two right triangles is equivalent to Eq. (2.98). The third diagram

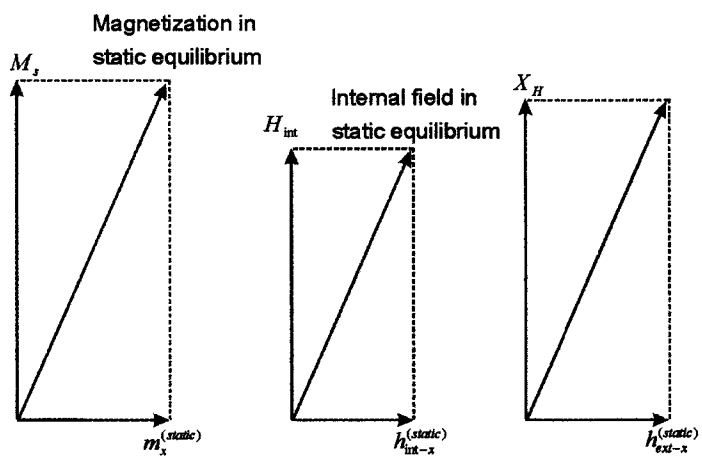

Figure 2-4: In static equilibrium, the equilibrium magnetization is collinear with the internal field. The triangles formed by the x- and z-components of the equilibrium magnetization (left triangle) and the internal field (center triangle) must be similar. Both triangles are similar to the one formed by the x-component of the static applied field $h_{ext-x}^{(static)}$ and the stiffness field X_H (right triangle). This shows the role of the stiffness field as an effective z-direction field for the static equilibrium. The three triangles formed by the corresponding y- and z-components are similar as well.

shows the vector formed by the x-component of the static applied field in x-direction and the stiffness field X_H in z-direction. This right triangle is similar to the first two in the figure.

$$\frac{m_x^{(static)}}{M_s} = \frac{h_{ext-x}^{(static)} - 4\pi N_x m_x^{(static)}}{H_{ext} - 4\pi M_s N_z} \tag{2.99}$$

and

$$\frac{m_y^{(static)}}{M_s} = \frac{h_{ext-y}^{(static)} - 4\pi N_y m_y^{(static)}}{H_{ext} - 4\pi M_s N_z}. \tag{2.100}$$

Solved for the components of the equilibrium magnetization, one obtains,

$$m_x^{(static)} = \frac{M_s}{H_{ext} + 4\pi M_s (N_x - N_z)} h_{ext-x}^{(static)} = \frac{M_s}{X_H} h_{ext-x}^{(static)} \tag{2.101}$$

and

$$m_y^{(static)} = \frac{M_s}{H_{ext} + 4\pi M_s (N_y - N_z)} h_{ext-y}^{(static)} = \frac{M_s}{Y_H} h_{ext-y}^{(static)}. \tag{2.102}$$

Therefore, the static equilibrium can also be written in the form

$$\frac{m_x^{(static)}}{M_s} = \frac{h_{int-x}^{(static)}}{H_{int}} = \frac{h_{ext-x}^{(static)}}{X_H} \tag{2.103}$$

and

$$\frac{m_y^{(static)}}{M_s} = \frac{h_{int-y}^{(static)}}{H_{int}} = \frac{h_{ext-y}^{(static)}}{Y_H}. \tag{2.104}$$

This form shows that the previously derived dynamic stiffness fields X_H and Y_H also have a clear static role. They take the place of the z-direction field when equilibrium is expressed by the external field components $h_{ext-x}^{(static)}$ and $h_{ext-y}^{(static)}$ instead of the internal field components $h_{int-x}^{(static)}$ and $h_{int-y}^{(static)}$.

2.6.b Instantaneous equilibrium

Instantaneous equilibrium is determined in precisely the same way as the static equilibrium, with the static applied transverse field $\left[h_{ext-x}^{(static)}, h_{ext-y}^{(static)}\right]^T$ replaced by the time-dependent applied transverse field $\left[h_{ext-x}(t), h_{ext-y}(t)\right]^T$, the static equilibrium of magnetization $\left[m_x^{(static)}, m_y^{(static)}\right]^T$ replaced by the instantaneous equilibrium $\left[m_x^{(eq)}(t), m_y^{(eq)}(t)\right]^T$, and the internal static field $\left[h_{\text{int}-x}^{(static)}, h_{\text{int}-y}^{(static)}\right]^T$ replaced by the time-dependent internal field $\left[h_{\text{int}-x}(t), h_{\text{int}-y}(t)\right]^T$. Exactly as for the static equilibrium discussed above, one can express the instantaneous equilibrium in terms of the internal field as well as in terms of the external applied field:

$$\frac{m_x^{(eq)}(t)}{M_s} = \frac{h_{int-x}(t)}{H_{\text{int}}} = \frac{h_{ext-x}(t)}{X_H} \tag{2.105}$$

and

$$\frac{m_y^{(eq)}(t)}{M_s} = \frac{h_{int-y}(t)}{H_{int}} = \frac{h_{ext-y}(t)}{Y_H}. \tag{2.106}$$

Equivalently, one can write

$$h_{int-x}^{(eq)}(t) - \frac{m_x^{(eq)}(t)}{M_s} H_{int} = h_{ext-x}(t) - \frac{m_x^{(eq)}(t)}{M_s} X_H = 0, \tag{2.107}$$

and

$$h_{int-y}(t) - \frac{m_y^{(eq)}(t)}{M_s} H_{int} = h_{ext-y}(t) - \frac{m_y^{(eq)}(t)}{M_s} Y_H = 0. \tag{2.108}$$

Note that in Eqs. (2.107) and (2.108) the first equality remains valid when not the instantaneous equilibria of the magnetization and of the internal field are considered, but the actual quantities. For with the stiffness fields X_H and Y_H defined in Eqs. (2.45) and (2.46), and the relationship in Eq.

(2.97) between the internal static field and the external applied static field, one obtains

$$\begin{aligned} h_{int\text{-}x}(t)-\frac{m_x(t)}{M_s}H_{int} &= h_{ext-x}(t)-4\pi N_x m_x(t)-\frac{m_x(t)}{M_s}H_{int} \\ &= h_{ext-x}(t)-\frac{m_x(t)}{M_s}\left(H_{\text{int}}+4\pi N_x M_s\right) \\ &= h_{ext-x}(t)-\frac{m_x(t)}{M_s}\left(H_{ext}-4\pi N_z M_s+4\pi N_x M_s\right) \\ &= h_{ext-x}(t)-\frac{m_x(t)}{M_s}X_H \end{aligned} \tag{2.109}$$

and, similarly,

$$\begin{aligned} h_{int\text{-}y}(t)-\frac{m_y(t)}{M_s}H_{int} &= h_{ext-y}(t)-4\pi N_y m_y(t)-\frac{m_y(t)}{M_s}H_{int} \\ &= h_{ext-y}(t)-\frac{m_y(t)}{M_s}\left(H_{\text{int}}+4\pi N_y M_s\right) \\ &= h_{ext-y}(t)-\frac{m_y(t)}{M_s}\left(H_{ext}-4\pi N_z M_s+4\pi N_y M_s\right) \\ &= h_{ext-y}(t)-\frac{m_y(t)}{M_s}Y_H. \end{aligned} \tag{2.110}$$

The significance of Eqs. (2.109) and (2.110) will be understood in Chapter 3 in the discussion of phenomenological damping models. For each damping model the physical concepts that drive the damping yield the equations of motion in terms of the internal field components. Then the internal field components $h_{int\text{-}x}(t)$, $h_{int\text{-}y}(t)$ and H_{int} are expressed by the components $h_{ext-x}(t)$ and $h_{ext-y}(t)$ of the external microwave driving field and by the stiffness fields X_H and Y_H. In this way the equations of motion can be brought into a form that does not contain any internal field components.

2.7 Summary and Outlook

In this chapter the Smith matrix formulation was introduced as the standard form of the equation of motion of the undamped magnetization precession in a uniformly magnetized ferromagnetic

sample. The Smith matrix form represents the linear system of two first-order differential equations in a form similar to the simple harmonic oscillator in one dimension. In this form, the equation of motion is solved for the external driving field (or driving force) on the right side of the equation. The Smith matrix form allows a simple derivation of the instantaneous internal magnetic energy in the sample. In Chapter 3, a damping term is added in the Smith matrix form. The form of this damping term depends on which particular phenomenological damping model is used. For the damped magnetic precession the Smith matrix form is particularly suited to derive the instantaneous loss power that is dissipated in the sample. The analysis of loss for the damped magnetic precession is carried out in Chapter 4.

Chapter 3

Five phenomenological models of magnetization damping, analyzed and compared in the small-signal limit

Table of contents:

3.1 Introduction

Damping causes the magnetization to relax at every instant toward its equilibrium state of lowest magnetic energy in the direction of the internal magnetic field. Damping dissipates some of the magnetic potential energy and converts it to heat. Chapter 2 developed the equations of motion for the transverse magnetization response without energy dissipation. In order to model the damped response, a small damping term can be added to the undamped equations of motion. This chapter examines five phenomenological models of magnetization damping. The adjective "phenomenological" implies that these models are not derived from the microscopic mechanisms of relaxation. Rather, they represent simple heuristic constructions that allow for precession decay, or - in the case of the steady state response to a microwave driving field - microwave energy loss. The objective of this chapter is to develop, analyze, and compare five particular archival phenomenological models with respect to the underlying physical concepts, as far as such concepts exist, as well as the geometry of the magnetization trajectories, the decay rates of the undriven precession, and the external susceptibility tensors of the microwave response.

Section 3.2 reviews the fields that are present in a sample of ellipsoidal shape. These are

the static field that is applied along one of the principal axes, a general elliptically polarized and transverse microwave driving field in the plane perpendicular to the static applied field, and the demagnetizing fields associated with the magnetization response. This section also revisits the concept of instantaneous equilibrium as it relates to the transverse magnetization response. In the calculation of this equilibrium, the stiffness fields from Chapter 2 play an important role.

Section 3.3 introduces the five specific damping models that have been developed over a span of about 70 years to analyze decay and loss in magnetic systems. In the chronological order of their publication, these models are:

a) Landau-Lifshitz (LL) damping (Landau and Lifshitz, 1935)

b) Bloch-Bloembergen (BB) damping (Bloembergen, 1950)

c) Codrington-Olds-Torrey (COT) damping (Codrington, Olds and Torrey, 1954)

d) Gilbert (G) damping (Gilbert, 1955)

e) Modified Bloch-Bloembergen (MBB) damping (Lax and Button, 1962)

The five damping models may be classified into three categories, depending on "what drives the relaxation".

For *field-driven damping*, the transverse magnetization response is driven by the internal field component perpendicular to the magnetization. This is the case for the Landau-Lifshitz damping model.

For *viscous damping*, the transverse magnetization response is driven by the viscous drag on magnetization. The damping is proportional in magnitude to the time rate of change of the magnetization. The Gilbert damping model belongs to this group.

For *magnetization-driven damping*, the transverse magnetization response is driven by the magnetization component perpendicular to some chosen field: the static component of the internal field for Bloch-Bloembergen damping, the internal field for Codrington-Olds-Torrey damping or the instantaneous equilibrium of the magnetization for Modified Bloch-Bloembergen damping.

Equations of motion are developed in the small signal limit for each of the five models. This is done by letting the damping contribution to the rate of change of the magnetization depend linearly on "what drives the relaxation". For each model, the equations of motion contain one or two scalar damping parameters which may be given either as relaxation times, relaxation rates, or in dimensionless form. The equations of motion are presented in two forms:

(a) one in which the equations are solved for the time derivative of the transverse magnetization vector $\mathbf{m}(t)=\left[m_x(t),m_y(t)\right]^T$ in the small signal limit, and

(b) one in which the equations are solved for the externally applied transverse driving field components.

Section 3.4 analyzes the precession decay response from a geometrical perspective. For each of the five models the trajectory of the damped, undriven, transverse magnetization precession decay response is examined. In all cases, the decay response consists of a stretched logarithmic spiral in the transverse plane. Moreover, this section examines the decay rate formulae that follow from the five damping models. For LL, G and COT damping, the relaxation rate changes with the sample shape and is proportional to the arithmetic mean of the Kittel stiffness frequencies. For BB and MBB damping, on the other hand, the relaxation rate is independent of the sample geometry.

Section 3.5 presents the equations of motion of the damped precession in the Smith matrix form, following the work of Neil Smith in Smith [2002]. The Smith gyroscopic and stiffness matrices were already developed in Chapter 2 for the undamped magnetization response. The damping matrix is introduced here. The Smith matrix formulation provides a useful way to calculate the external susceptibility tensor and the instantaneous and time averaged loss, and to obtain correlations between thermal noise components of the internal field. These applications are covered in Chapters 4 and 5, respectively.

Section 3.6 develops analytical expressions for the complete transverse magnetization response and the corresponding external susceptibility tensors corresponding to the five models. While these susceptibility components are well documented in the archival literature, the approach here, based on Smith matrices, provides a useful way to develop those response functions in simple form.

Section 3.7 summarizes the key results of the chapter.

3.2 Review: Internal field and instantaneous magnetization equilibrium in an ellipsoidal sample

Chapter 2 explained the importance of the total internal field for the *precessional* motion of the undamped magnetization response. Recall that at every instant of time, the undamped magnetic precession, whether driven or undriven, can be viewed as a circular precession about the instantaneous direction of the internal field. This internal field is of equal importance for the *relaxation* of the magnetization vector in the damped response analysis. The relaxation or decay

seeks to decrease the radius of the instantaneous precession circle, and to align the magnetization response with the instantaneous direction of the internal field. This is true for all of the models considered here except the BB model.

In parallel with the analysis of the undamped magnetization precession in Chapter 2, this Chapter considers the damped precession for an ellipsoidal sample without magnetocrystalline anisotropy. However the results are easily generalized to include anisotropic materials through the inclusion of additional terms in the stiffness matrix in the equations of motion.

Figure 3-1 depicts the magnetization and field components in an ellipsoidal sample, as developed in Chapter 2. The sample is subjected to a static applied field of magnitude H_{ext} in the z-direction, called the longitudinal direction. This static applied field must be large enough to magnetize the sample to saturation, so that the z-component of the magnetization is M_s, the saturation magnetization. In the plane perpendicular to the static applied field, called the transverse plane, there is an additional small time dependent field with x- and y-components $h_{ext-x}(t)$ and $h_{ext-y}(t)$. This transverse field is taken to be small compared with the static applied field. The corresponding transverse magnetization response components $m_x(t)$ and $m_y(t)$ are taken to be small compared to M_s. This set of assumptions is called the *small signal limit.*

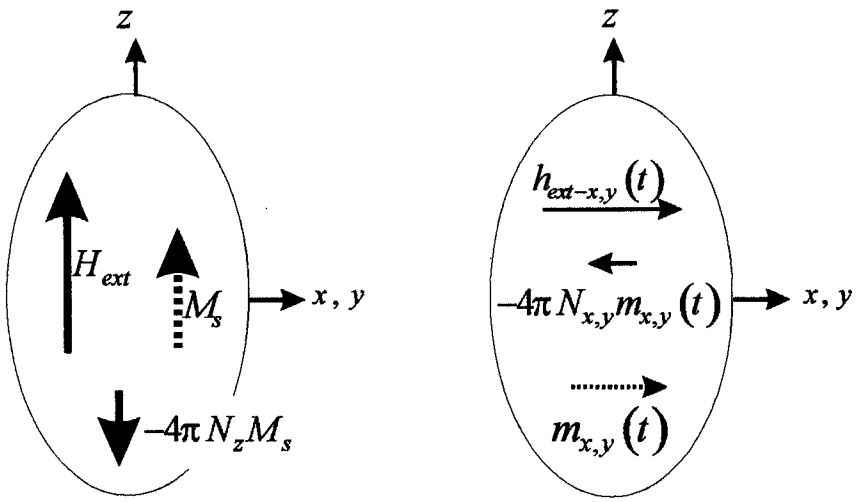

Figure 3-1: Internal field and magnetization components in an ellipsoidal sample. Parallel to the z-axis are the static external field, the static magnetization and its demagnetizing field. Parallel to the x-axis are the x-component of the applied time dependent transverse microwave field, the x- component of the dynamic magnetization response, and its demagnetizing field. Parallel to the y- axis are the y-component of the applied microwave field, the y-component of the dynamic magnetization response, and its demagnetizing field.

Recall from Chapter 2 that the sample also experiences demagnetizing fields. One has a static demagnetizing field of magnitude $4\pi N_z M_s$ in the negative z-direction, and time-varying dynamic demagnetizing fields $4\pi N_x m_x(t)$ in the negative x-direction and $4\pi N_y m_y(t)$ in the negative y-direction. The three constants N_x, N_y, and N_z are the demagnetizing factors of the ellipsoidal sample in the x-, y- and z-directions, respectively, the directions of the principal axes. The internal field, therefore, consists of its static component,

$$H_{\text{int}} = H_{ext} - N_z \cdot 4\pi M_s, \tag{3.1}$$

in the z-direction (or longitudinal direction), and the time-dependent transverse components given by

$$h_{\text{int}-x}(t) = h_{ext-x}(t) - N_x \cdot 4\pi m_x(t), \tag{3.2}$$

and

$$h_{\text{int}-y}(t) = h_{ext-y}(t) - N_y \cdot 4\pi m_y(t). \tag{3.3}$$

In vector form, one has an internal field

$$\mathbf{H}_{\text{int}}(t) = \begin{pmatrix} h_{int-x}(t) \\ h_{int-y}(t) \\ H_{int} \end{pmatrix}. \tag{3.4}$$

Now, consider again the instantaneous equilibrium magnetization condition for a given external applied field $\left[h_{ext-x}(t), h_{ext-y}(t), H_{ext}\right]^T$. This instantaneous equilibrium condition corresponds to a magnetization vector that lines up with the internal field, which includes the demagnetizing field of the magnetization vector. In the small signal limit, the corresponding values of the transverse magnetization components of the instantaneous equilibrium were shown in Chapter 2 to be given by

$$m_x^{(eq)}(t) = \frac{M_s}{X_H} h_{ext-x}(t) \tag{3.5}$$

and

$$m_y^{(eq)}(t) = \frac{M_s}{Y_H} h_{ext-y}(t). \tag{3.6}$$

It is important to emphasize that $m_x^{(eq)}(t)$ and $m_y^{(eq)}(t)$ are not the actual values of the transverse magnetization components m_x and m_y at time t. Rather, $m_x^{(eq)}(t)$ and $m_y^{(eq)}(t)$ are the values that m_x and m_y would attain, if the system were at static equilibrium. The instantaneous equilibrium is of central importance in the damped equations of motion in the small signal limit. The next section will demonstrate that for all of the damping models, except for the Bloch-Bloembergen model, the equations of motion have the form

$$\frac{dm_x(t)}{dt} = -A_y\left[m_y(t) - m_y^{(eq)}(t)\right] - B_x\left[m_x(t) - m_x^{(eq)}(t)\right] \tag{3.7}$$

and

$$\frac{dm_y(t)}{dt} = +A_x\left[m_x(t) - m_x^{(eq)}(t)\right] - B_y\left[m_y(t) - m_y^{(eq)}(t)\right] \tag{3.8}$$

with positive parameters A_x, A_y, B_x, and B_y. In these two equations the first terms on the right side are precession terms, and describe the elliptical precession of the transverse magnetization about its instantaneous equilibrium. The second terms are damping terms, and describe the relaxation of the transverse magnetization components toward their instantaneous equilibrium values. One can see from the form of these equations that the damping is driven by the differences between $m_{x,y}(t)$ and $m_{x,y}^{(eq)}(t)$, respectively, or, in other words, by the difference between $m_{x,y}$ themselves and what $m_{x,y}$ would be in static equilibrium.

Recall also from Eqs. (2.112) and (2.113) that at every instant of time, the internal field $\mathbf{h}_{\text{int}} = \left[h_{\text{int}-x}(t), h_{\text{int}-y}(t), H_{\text{int}}\right]^T$ is related to the applied field $\mathbf{h}_{ext} = \left[h_{ext-x}(t), h_{ext-y}(t), H_{ext}\right]^T$ by the pair of equations,

$$h_{\text{int}-x}(t)-\frac{m_x(t)}{M_s}H_{\text{int}}=h_{ext-x}(t)-\frac{m_x(t)}{M_s}X_H\,, \tag{3.9}$$

and

$$h_{int-y}(t)-\frac{m_y(t)}{M_s}H_{\text{int}}=h_{ext-y}(t)-\frac{m_y(t)}{M_s}Y_H\,. \tag{3.10}$$

Notice that in both equations the right and left sides have a similar form. The applied field components $h_{ext-x}(t)$ and $h_{ext-y}(t)$ on the right side correspond to the internal field components $h_{\text{int}-x}(t)$ and $h_{\text{int}-y}(t)$ on the left side, and the stiffness fields X_H and Y_H on the right side correspond to the static internal field H_{int} on the left side. For each damping model the physical concepts that drive the damping yield the equations of motion in terms of the internal field components. Then the internal field components $h_{\text{int}-x}(t)$, $h_{\text{int}-y}(t)$ and H_{int} are, through application of Eqs. (3.9) and (3.10), expressed by the components $h_{ext-x}(t)$ and $h_{ext-y}(t)$ of the external microwave driving field and by the stiffness fields X_H and Y_H. In this way the equations of motion are brought into a form that does not contain any internal field components. Rather, they relate the transverse magnetization response $\left[m_x(t),m_y(t)\right]^T$ to the transverse microwave driving field $\left[h_{ext-x}(t),h_{ext-y}(t)\right]^T$.

3.3 Damped precession in the small signal limit

This section discusses the physical concepts behind the five damping models. For each model, the coupled equations of motion are developed in the small signal limit. This treatment of the small signal limit differs from the traditional approach, which starts with the damped

equations of motion in the full three-dimensional vector form, and then linearizes these equations and arrives at a reduced, two-dimensional system for the two transverse components of the magnetization response. The advantage of starting with the small signal limit is that the simple physical origins of the transverse damping terms are made clear. The reduced 2D system is obtained directly from these concepts without the ad hoc postulation of the 3D form.

For each damping model, the total time rate of change of the transverse magnetization response, $d\mathbf{m}(t)/dt$, consists of a precessional part and a damping part.

$$\frac{d\mathbf{m}(t)}{dt} = \mathbf{T}(t) + \left[\frac{d\mathbf{m}(t)}{dt}\right]_{damping}. \tag{3.11}$$

The precessional part $\mathbf{T}(t)$ of $d\mathbf{m}(t)/dt$ is given in components by

$$T_x(t) = -|\gamma|\left[Y_H m_y(t) - M_s h_y(t)\right] \tag{3.12}$$

and

$$T_y(t) = +|\gamma|\left[X_H m_x(t) - M_s h_x(t)\right]. \tag{3.13}$$

The damping part $\left[d\mathbf{m}(t)/dt\right]_{damping}$ is now derived for each damping model from the different physical considerations indicated in the introduction to this chapter.

3.3.a Landau-Lifshitz (LL) damping, driven by the internal field component perpendicular to the magnetization

The first model of damped precession dynamics in a ferromagnetic sample was published by Landau and Lifshitz [1935] in their paper "On the theory of the dispersion of magnetic

permeability in ferromagnetic bodies", which appeared in English in the "Physikalische Zeitschrift der Sowjetunion". Their model supplemented the undamped torque equation of motion, developed in Chapter 2, with an additional damping term that is proportional to the component of the internal field perpendicular to the magnetization.

LL damping is field-driven. At every instant of time t, the rate of change of the total magnetization vector $\mathbf{M}(t)$ due to damping is taken to be proportional to the component of the internal field $\mathbf{H}_{\text{int}}(t)$ perpendicular to $\mathbf{M}(t)$. Since $d\mathbf{M}(t)/dt$ is orthogonal to $\mathbf{M}(t)$, the magnitude of $\mathbf{M}(t)$ remains constant in time and can be taken to be the saturation magnetization M_s. The geometry of the problem is shown in Fig. 3-2. Here, $\theta(t)$ is the angle between $\mathbf{H}_{\text{int}}(t)$ and $\mathbf{M}(t)$. The components of $\mathbf{H}_{\text{int}}(t)$ that are parallel and perpendicular to $\mathbf{M}(t)$, are named $\mathbf{H}_{\|M}(t)$ and $\mathbf{H}_{\perp M}(t)$, respectively. The parallel component of $\mathbf{H}_{\text{int}}(t)$ is given by

$$\mathbf{H}_{\|M}(t) = \frac{\mathbf{H}_{\text{int}}(t)\cdot\mathbf{M}(t)}{M_s^2}\ \mathbf{M}(t). \tag{3.14}$$

By vector subtraction, the perpendicular component of $\mathbf{H}_{\text{int}}(t)$ is then given by

$$\mathbf{H}_{\perp M}(t) = \mathbf{H}_{\text{int}}(t) - \mathbf{H}_{\|M}(t) = \mathbf{H}_{\text{int}}(t) - \frac{\mathbf{H}_{\text{int}}(t)\cdot\mathbf{M}(t)}{M_s^2}\ \mathbf{M}(t). \tag{3.15}$$

The damping part of $d\mathbf{M}(t)/dt$ is taken to be proportional to $\mathbf{H}_{\perp M}(t)$ with a proportionality factor λ_{LL}. The full LL equation of motion in vector form is then given by

$$\begin{aligned}\frac{d\mathbf{M}(t)}{dt} &= \mathbf{T}(t) + \lambda_{LL}\mathbf{H}_{\perp M}(t) \\ &= -|\gamma|\mathbf{M}(t)\times\mathbf{H}_{\text{int}}(t) + \lambda_{LL}\left[\mathbf{H}_{\text{int}}(t) - \frac{\mathbf{H}_{\text{int}}(t)\cdot\mathbf{M}(t)}{M_s^2}\mathbf{M}(t)\right].\end{aligned} \tag{3.16}$$

This is the actual form used in the original paper in Landau and Lifshitz (1935). Nowadays, the perpendicular component of the total field, which is contained in the brackets of Eq. (3.16), is often written as a triple cross product, by application of the vector identity $\mathbf{a}\times(\mathbf{b}\times\mathbf{c})=\mathbf{c}(\mathbf{a}\cdot\mathbf{b})-\mathbf{b}(\mathbf{a}\cdot\mathbf{c})$. In this modern form, the LL equation becomes

$$\frac{d\mathbf{M}(t)}{dt}=-|\gamma|\mathbf{M}(t)\times\mathbf{H}_{\text{int}}(t)-\frac{\lambda_{LL}}{M_s^2}\mathbf{M}(t)\times\left[\mathbf{M}(t)\times\mathbf{H}_{\text{int}}(t)\right]. \tag{3.17}$$

From this form of the LL equation, it is more obvious than from Eq. (3.16) that $d\mathbf{M}(t)/dt$ is indeed orthogonal to $\mathbf{M}(t)$. Notice further that the magnitude ratio of the damping term and the torque term in Eq. (3.17) is given by a ratio parameter

$$\alpha_{LL} = \frac{\frac{\lambda_{LL}}{M_s}\left|\mathbf{M}(t)\times\mathbf{H}_{\text{int}}(t)\right|}{|\gamma|\left|\mathbf{M}(t)\times\mathbf{H}_{\text{int}}(t)\right|} = \frac{\lambda_{LL}}{|\gamma|M_s}. \tag{3.18}$$

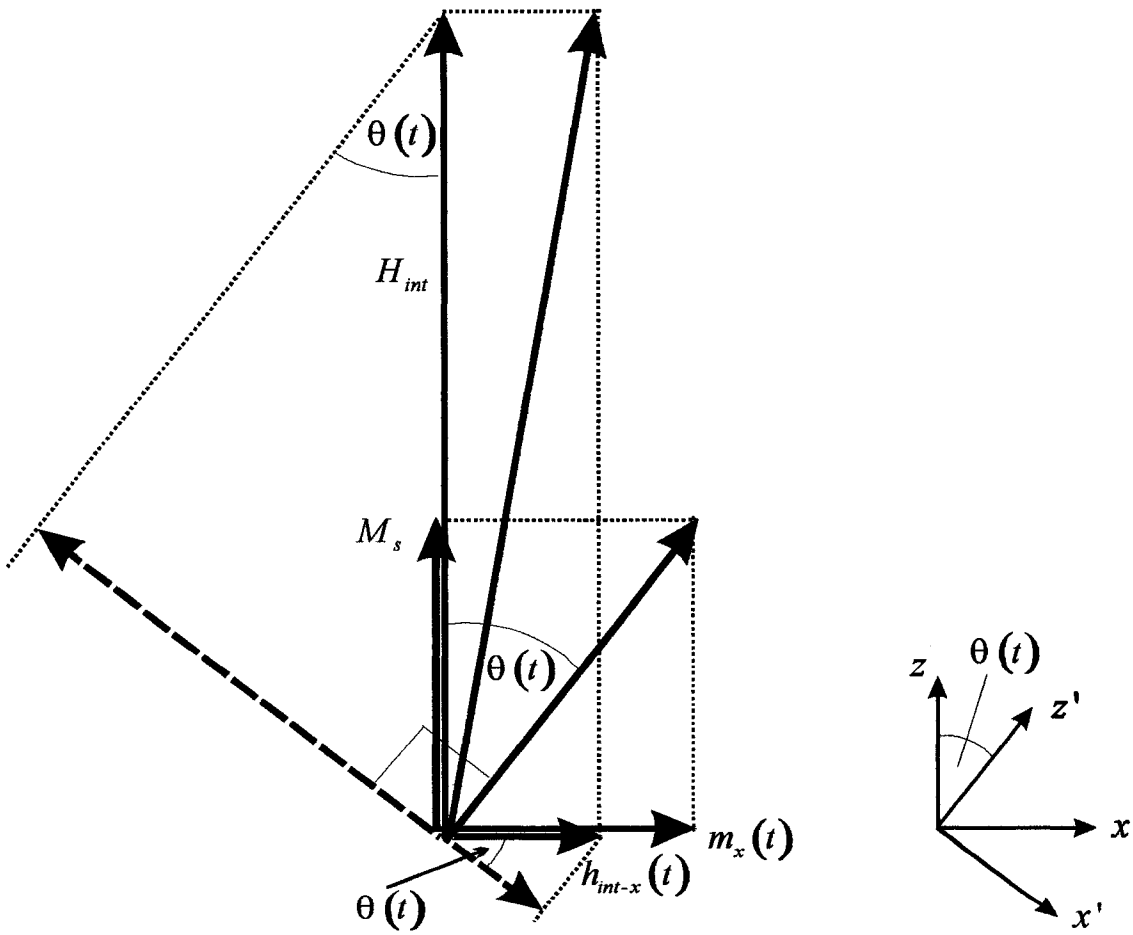

Figure 3-3: Construction of the LL damping term in the small signal limit. The x-z projection $\mathbf{M}_{x-z} \approx M_s$ of the magnetization makes an angle $\theta(t)$ with the static internal field H_{int}. In the small signal limit, the LL damping contribution to $dm_x(t)/dt$ is approximated by the component of $\left[h_{\text{int}-x}(t), H_{\text{int}}\right]^T$ perpendicular to $\left[m_x(t), M_s\right]^T$ in the x-z plane.

This dimensionless ratio α_{LL} is often called the dimensionless LL damping parameter. In terms of α_{LL}, the LL equation is

$$\frac{d\mathbf{M}(t)}{dt} = -|\gamma|\mathbf{M}(t)\times\mathbf{H}_{\text{int}}(t) - \frac{\alpha_{LL}|\gamma|}{M_s}\mathbf{M}(t)\times\left[\mathbf{M}(t)\times\mathbf{H}_{\text{int}}(t)\right]. \tag{3.19}$$

One may obtain the small signal limit form of the LL equation, for the x- and y-components only, in two ways. The standard way is simply to expand Eq. (3.19) in component form, and then keep only the linear terms in $h_{ext-x}(t)$, $h_{ext-y}(t)$, $m_x(t)$ and $m_y(t)$. A second way is to work directly from diagrams similar to those in Fig. 3-2 and to work out the component equations in the small signal limit directly. This second approach is used now for the LL damping model. Consider the diagram in Fig. 3-3 above. The x-z projection $\mathbf{M}_{x-z} \approx M_s$ of the total magnetization makes an angle $\theta(t)$ with the static internal field H_{int}. Consider now a rotation of the x-z coordinate system to an x'-z'-coordinate system such that the z' axis is in the direction of $\mathbf{M}_{x-z}$. While $\theta(t) \ll 90^0$ is true in the small signal limit, the size of the angle is exaggerated here for clarity. The x-z projection of the internal field consists of the static component H_{int} in the z-direction and the time-dependent component $h_{\text{int}-x}(t)$ in the x-direction. These two internal field components are now resolved along the x'-direction. Their x'-components are depicted as dashed arrows in Fig. 3-3. The x'-component of H_{int} is $-H_{\text{int}}\sin\theta(t)$, and the x'-component of $h_{\text{int}-x}(t)$ is $h_{\text{int}-x}(t)\cos\theta(t)$. The x'-component vector of $\mathbf{H}_{\text{int},x-z}$ is the sum of these two contributions. By projection of the sum of these two contributions onto the x-axis and multiplication by a suitable rate parameter, one obtains the damping term in $dm_x(t)/dt$. The reader sees by linearization of the full nonlinear LL equation in Eq. (3.17) that the rate parameter

is given by the LL damping parameter λ_{LL}. As a result, one obtains the equation of motion,

$$\frac{dm_x(t)}{dt} = T_x(t) + \lambda_{LL}\left[-H_{\text{int}}\sin\theta(t) + h_{\text{int}-x}(t)\cos\theta(t)\right]\cos\theta(t). \tag{3.20}$$

The last cosine on the right side is obtained by the projection onto the x-axis. In the small signal limit, terms of second or higher order in the transverse magnetization components are neglected, so that

$$\cos\theta(t) \approx 1 \tag{3.21}$$

and

$$\sin\theta(t) \approx \theta(t) \approx \tan\theta(t) = \frac{m_x(t)}{M_s}. \tag{3.22}$$

As a consequence, Eq. (3.20) becomes

$$\frac{dm_x(t)}{dt} = T_x(t) + \lambda_{LL}\left[-H_{\text{int}}\frac{m_x(t)}{M_s} + h_{\text{int}-x}(t)\right]. \tag{3.23}$$

The corresponding equation for the y-component of the magnetization is

$$\frac{dm_y(t)}{dt} = T_y(t) + \lambda_{LL}\left[-H_{\text{int}}\frac{m_y(t)}{M_s} + h_{\text{int}-y}(t)\right]. \tag{3.24}$$

Recall the internal-to-external field conversions reviewed earlier in Eqs. (3.9) and (3.10), which are given by

$$h_{\text{int}-x}(t) - \frac{m_x(t)}{M_s}H_{\text{int}} = h_{ext-x}(t) - \frac{m_x(t)}{M_s}X_H, \tag{3.25}$$

and

$$h_{int-y}(t)-\frac{m_y(t)}{M_s}H_{\text{int}}=h_{ext-y}(t)-\frac{m_y(t)}{M_s}Y_H\,. \tag{3.26}$$

With these relationships, the LL equations of motion in the small signal limit become

$$\frac{dm_x(t)}{dt}=T_x(t)-\frac{\lambda_{LL}}{M_s}\left[X_H m_x(t)-M_s h_{ext-x}(t)\right], \tag{3.27}$$

and

$$\frac{dm_y(t)}{dt}=T_y(t)-\frac{\lambda_{LL}}{M_s}\left[Y_H m_y(t)-M_s h_{ext-y}(t)\right]. \tag{3.28}$$

When the torque terms are written out explicitly, a striking similarity of the damping and the torque terms can be noticed.

$$\frac{dm_x(t)}{dt}=-|\gamma|\left[Y_H m_y(t)-M_s h_{ext-y}(t)\right]-\frac{\lambda_{LL}}{M_s}\left[X_H m_x(t)-M_s h_{ext-x}(t)\right] \tag{3.29}$$

and

$$\frac{dm_y(t)}{dt}=+|\gamma|\left[X_H m_x(t)-M_s h_{ext-x}(t)\right]-\frac{\lambda_{LL}}{M_s}\left[Y_H m_y(t)-M_s h_{ext-y}(t)\right]. \tag{3.30}$$

A simple rearrangement leads to the form

$$\begin{aligned}\frac{dm_x(t)}{dt}&=-|\gamma|Y_H\left[m_y(t)-\frac{M_s}{Y_H}h_{ext-y}(t)\right]-\frac{\lambda_{LL}X_H}{M_s}\left[m_x(t)-\frac{M_s}{X_H}h_{ext-x}(t)\right]\\&=-|\gamma|Y_H\left[m_y(t)-m_y^{(eq)}(t)\right]-\frac{\lambda_{LL}X_H}{M_s}\left[m_x(t)-m_x^{(eq)}(t)\right]\end{aligned} \tag{3.31}$$

and

$$\frac{dm_y(t)}{dt} = +|\gamma| X_H \left[m_x(t) - \frac{M_s}{X_H} h_{ext-x}(t) \right] - \frac{\lambda_{LL} Y_H}{M_s} \left[m_y(t) - \frac{M_s}{Y_H} h_{ext-y}(t) \right]$$

(3.32)

$$= +|\gamma| X_H \left[m_x(t) - m_x^{(eq)}(t) \right] - \frac{\lambda_{LL} Y_H}{M_s} \left[m_y(t) - m_y^{(eq)}(t) \right].$$

Here, one sees explicitly that at every instant the magnetization components $m_x(t)$ and $m_y(t)$ are driven toward their respective instantaneous equilibrium values

$$m_x^{(eq)}(t) = \frac{M_s}{X_H} h_{ext-x}(t) \tag{3.33}$$

and

$$m_y^{(eq)}(t) = \frac{M_s}{Y_H} h_{ext-y}(t). \tag{3.34}$$

Furthermore, observe in the damping terms of Eqs. (3.31) and (3.32) that the coefficients of the differences $m_x(t) - m_x^{(eq)}(t)$ and $m_y(t) - m_y^{(eq)}(t)$ are not equal! This provides a simple view of one of the key differences between the LL and BB (or MBB or COT) models. This observation will be given more thought later in the chapter.

Finally, when the damping terms are expressed in terms of the torque terms, one obtains,

$$\frac{dm_x(t)}{dt} = T_x(t) - \frac{\lambda_{LL}}{|\gamma| M_s} T_y(t) \tag{3.35}$$

and

$$\frac{dm_y(t)}{dt} = T_y(t) + \frac{\lambda_{LL}}{|\gamma| M_s} T_x(t) \tag{3.36}$$

Recall from Eq. (3.18) that $\lambda_{LL} / (|\gamma| M_s)$ is equal to the dimensionless damping parameter α_{LL}. One has, therefore,

$$\frac{dm_x(t)}{dt} = T_x(t) - \alpha_{LL} T_y(t) \tag{3.37}$$

and

$$\frac{dm_y(t)}{dt} = T_y(t) + \alpha_{LL} T_x(t). \tag{3.38}$$

In this form, one sees that in terms of the torque, α_{LL} also has a simple interpretation. It is the mixing ratio $|T_y(t)|/|T_x(t)|$ for $dm_x(t)/dt$ and $|T_x(t)|/|T_y(t)|$ for $dm_y(t)/dt$. One also sees that the damping contribution to $d\mathbf{m}(t)/dt$ is given by the vector $\alpha_{LL}\left[-T_y(t), T_x(t)\right]^T$, which is perpendicular to the precession contribution $\left[T_x(t), T_y(t)\right]^T$. This orthogonality of precession vector and damping vector in the small signal limit is illustrated in Fig. 3-4. It will be contrasted later on in this chapter with the Gilbert damping, for which the damping vector has a nonzero component opposing the precession vector, which leads to a slowdown in the precession.

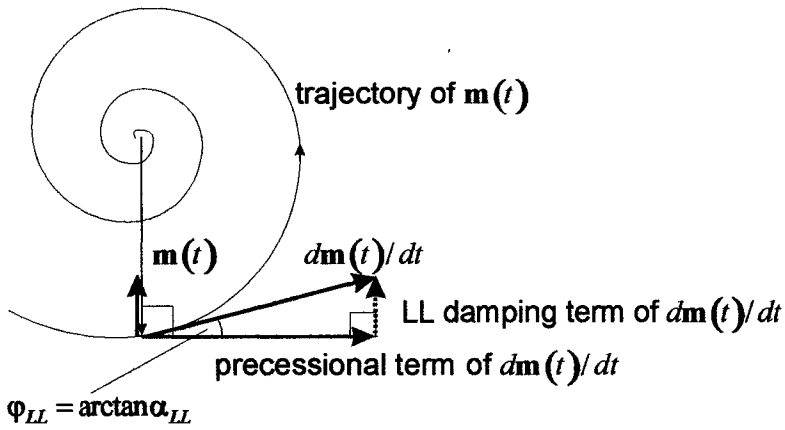

Figure 3-4: For Landau-Lifshitz damping, the transverse damping contribution to $d\mathbf{m}(t)/dt$ is perpendicular to the precession contribution. As a consequence, LL damping does not, to first order in the damping parameter, slow the precession. This is in contrast to Gilbert damping, which is discussed later in this chapter.

The reader is urged to appreciate the utility of this Landau-Lifshitz analysis in terms of small components. The small component analysis allows one to see the simple ingredients that go into the model, and the simple form of the decay drive terms that come out. Table 3-1 summarizes the various useful forms of the x-y component forms for the LL equations of motion in the small signal limit. The damping terms are cast in terms of internal fields, external fields and torques, respectively. For all three, the coefficients of both the x- and the y-damping terms are the same.

Internal field damping terms	$\frac{dm_x(t)}{dt} = T_x(t) + \lambda_{LL}\left[h_{\text{int}-x}(t) - \frac{H_{\text{int}}}{M_s}m_x(t)\right],$ $\frac{dm_y(t)}{dt} = T_y(t) + \lambda_{LL}\left[h_{\text{int}-y}(t) - \frac{H_{\text{int}}}{M_s}m_y(t)\right].$
External applied field damping terms	$\frac{dm_x(t)}{dt} = T_x(t) + \lambda_{LL}\left[h_{ext-x}(t) - \frac{X_H}{M_s}m_x(t)\right],$ $\frac{dm_y(t)}{dt} = T_y(t) + \lambda_{LL}\left[h_{ext-y}(t) - \frac{Y_H}{M_s}m_y(t)\right].$
Torque damping terms	$\frac{dm_x(t)}{dt} = T_x(t) - \alpha_{LL}T_y(t),$ $\frac{dm_y(t)}{dt} = T_y(t) + \alpha_{LL}T_x(t).$

Table 3-1: Forms of the Landau-Lifshitz equations of motion in the small signal limit.

3.3.b Bloch-Bloembergen (BB) damping, driven by the magnetization component perpendicular to the static internal field

Unlike the Landau-Lifshitz damping model, the Bloch-Bloembergen damping does not conserve the magnitude of the magnetization vector. It allows for two relaxation processes to proceed simultaneously with different relaxation rates. The first process, called transverse

relaxation, strives to exponentially reduce the transverse magnetization components to zero. Its time constant is denoted as T_2. The other process, called longitudinal relaxation, strives to exponentially decrease the difference between the longitudinal magnetization component and its limiting value M_s, the saturation magnetization. This longitudinal process has the time constant T_1. The equations of motion of the magnetization precession with BB damping are consequently given as

$$\frac{dM_x(t)}{dt} = -|\gamma|\left[\mathbf{M}(t)\times\mathbf{H}_{\text{int}}(t)\right]_x - \frac{1}{T_2}M_x(t), \tag{3.39}$$

$$\frac{dM_y(t)}{dt} = -|\gamma|\left[\mathbf{M}(t)\times\mathbf{H}_{\text{int}}(t)\right]_y - \frac{1}{T_2}M_y(t), \tag{3.40}$$

and

$$\frac{dM_z(t)}{dt} = -|\gamma|\left[\mathbf{M}(t)\times\mathbf{H}_{\text{int}}(t)\right]_z - \frac{1}{T_1}\left[M_z(t)-M_s\right]. \tag{3.41}$$

In the small signal limit, one usually considers only the relaxation of the transverse magnetization components and sets $M_z(t)$ to M_s. The corresponding equations of motion for the transverse magnetization components $m_x(t)$ and $m_y(t)$ are given by

$$\frac{dm_x(t)}{dt} = T_x(t) - \frac{1}{T_2}m_x(t). \tag{3.42}$$

and

$$\frac{dm_y(t)}{dt} = T_y(t) - \frac{1}{T_2}m_y(t). \tag{3.43}$$

These equations of motion specify a relaxation of the transverse magnetization components

that is driven by the transverse magnetization components themselves. In contrast to the LL damping, no field components appear in the BB damping terms. One can see that this form, with the torque terms neglected, gives simple exponential decay with both $m_x(t)$ and $m_y(t)$ proportional to $\exp(-t/T_2)$. The problem here is that for any nonzero driving field components $h_{ext-x}(t)$ or $h_{ext-y}(t)$, the instantaneous magnetization equilibrium components $m_x^{(eq)}(t)$ or $m_y^{(eq)}(t)$ are nonzero as well, and the BB decay is never to the instantaneous equilibrium, but to the static internal field. But why should the magnetization vector relax toward the direction of the static internal field, instead of the internal field? Rather, if the relaxation is driven by the magnetization and not the field, then the magnetization should relax at every instant of time toward the internal field (Codrington-Olds-Torrey's model), or toward the instantaneous magnetization equilibrium defined by the external applied field (Modified Bloch-Bloembergen model). Both models avoid the unphysical characteristics of the BB damping model and are analyzed in 3.3.c and 3.3.e, respectively. With the torque terms written explicitly and with the notation $\lambda_{BB} = 1/T_2$, Eqs. (3.42) and (3.43) become

$$\frac{dm_x(t)}{dt} = -|\gamma|\left[Y_H m_y(t) - M_s h_{ext-y}(t)\right] - \lambda_{BB} m_x(t) \tag{3.44}$$

and

$$\frac{dm_y(t)}{dt} = +|\gamma|\left[X_H m_x(t) - M_s h_{ext-x}(t)\right] - \lambda_{BB} m_y(t), \tag{3.45}$$

respectively. Notice that the damping terms do not contain the external microwave driving field components $h_{ext-x}(t)$ and $h_{ext-y}(t)$ at all. This is the algebraic expression of the fact that the

magnetization always relaxes to the direction of the static field instead of the instantaneous equilibrium direction. In Chapter 4 it will be shown that this concept leads to negative loss in certain special cases of the sample geometry and the polarization of the microwave driving field.

3.3.c Codrington-Olds-Torrey's (COT) damping, driven by the magnetization component perpendicular to the total internal field

At the 1954 Spring Meeting of the American Physical Society at Washington, D. C., Codrington, Olds, and Torrey from Rutgers University gave a contributed paper with the title

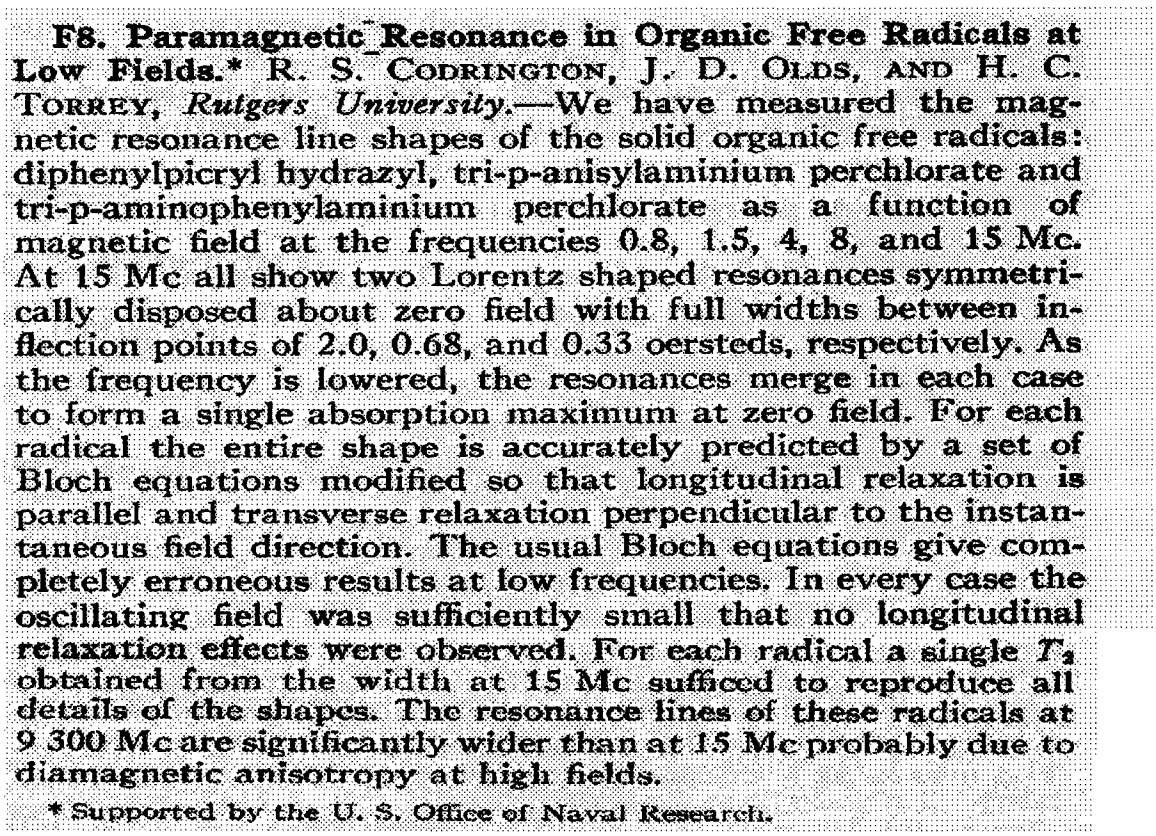

F8. Paramagnetic Resonance in Organic Free Radicals at Low Fields.* R. S. CODRINGTON, J. D. OLDS, AND H. C. TORREY, *Rutgers University*.—We have measured the magnetic resonance line shapes of the solid organic free radicals: diphenylpicryl hydrazyl, tri-p-anisylaminium perchlorate and tri-p-aminophenylaminium perchlorate as a function of magnetic field at the frequencies 0.8, 1.5, 4, 8, and 15 Mc. At 15 Mc all show two Lorentz shaped resonances symmetrically disposed about zero field with full widths between inflection points of 2.0, 0.68, and 0.33 oersteds, respectively. As the frequency is lowered, the resonances merge in each case to form a single absorption maximum at zero field. For each radical the entire shape is accurately predicted by a set of Bloch equations modified so that longitudinal relaxation is parallel and transverse relaxation perpendicular to the instantaneous field direction. The usual Bloch equations give completely erroneous results at low frequencies. In every case the oscillating field was sufficiently small that no longitudinal relaxation effects were observed. For each radical a single T_2 obtained from the width at 15 Mc sufficed to reproduce all details of the shapes. The resonance lines of these radicals at 9 300 Mc are significantly wider than at 15 Mc probably due to diamagnetic anisotropy at high fields.

* Supported by the U. S. Office of Naval Research.

Figure 3.5: Codrington-Olds-Torrey's abstract in Phys. Rev. **95**, 607 (1954).

"Paramagnetic Resonance in Organic Free Radicals at Low Fields". The abstract of this paper was published in Codrington, Olds, and Torrey [1954] and is photographically reproduced here in Fig. 3-5. Unfortunately, this abstract is not accessible from the Physical Review web archives.

In this abstract, Codrington, Olds and Torrey briefly allude to a new damping model that consists of "... a set of Bloch equations modified so that longitudinal relaxation is parallel and transverse relaxation perpendicular to the instantaneous field direction." They continue, "The usual Bloch equations give completely erroneous results at low frequencies." The COT abstract does not give any more than the above words. The full COT equations of motion were first given in explicit form by Wangsness [1956], written as

$$\frac{d\mathbf{M}(t)}{dt} = -|\gamma|\mathbf{M}(t)\times\mathbf{H}_{\text{int}}(t) - \frac{1}{T_1}\left(\mathbf{M}(t)\times\frac{\mathbf{H}_{\text{int}}(t)}{|\mathbf{H}_{\text{int}}(t)|} - M_s\right)\times\frac{\mathbf{H}_{\text{int}}(t)}{|\mathbf{H}_{\text{int}}(t)|} - \frac{1}{T_2}\frac{\mathbf{H}_{\text{int}}(t)}{|\mathbf{H}_{\text{int}}(t)|}\times\left(M(t)\times\frac{\mathbf{H}_{\text{int}}(t)}{|\mathbf{H}_{\text{int}}(t)|}\right). \tag{3.46}$$

Note that there are two damping terms! The first term is the precession term of the torque equation of motion. The second term is a longitudinal damping torque in the direction of the internal field $\mathbf{H}_{\text{int}}(t)$, with relaxation time constant T_1. The third term is a transverse damping torque perpendicular to the internal field, with relaxation time constant T_2.

The COT damping model is very similar to the LL model, but with reversed roles for the magnetization and the internal field. Whereas LL damping is driven by the internal field component perpendicular to the total magnetization, the COT damping is driven by the negative of the magnetization component perpendicular to the internal field. Figure 3-6 illustrates how, in this sense, LL damping and COT damping are reciprocal to each other.

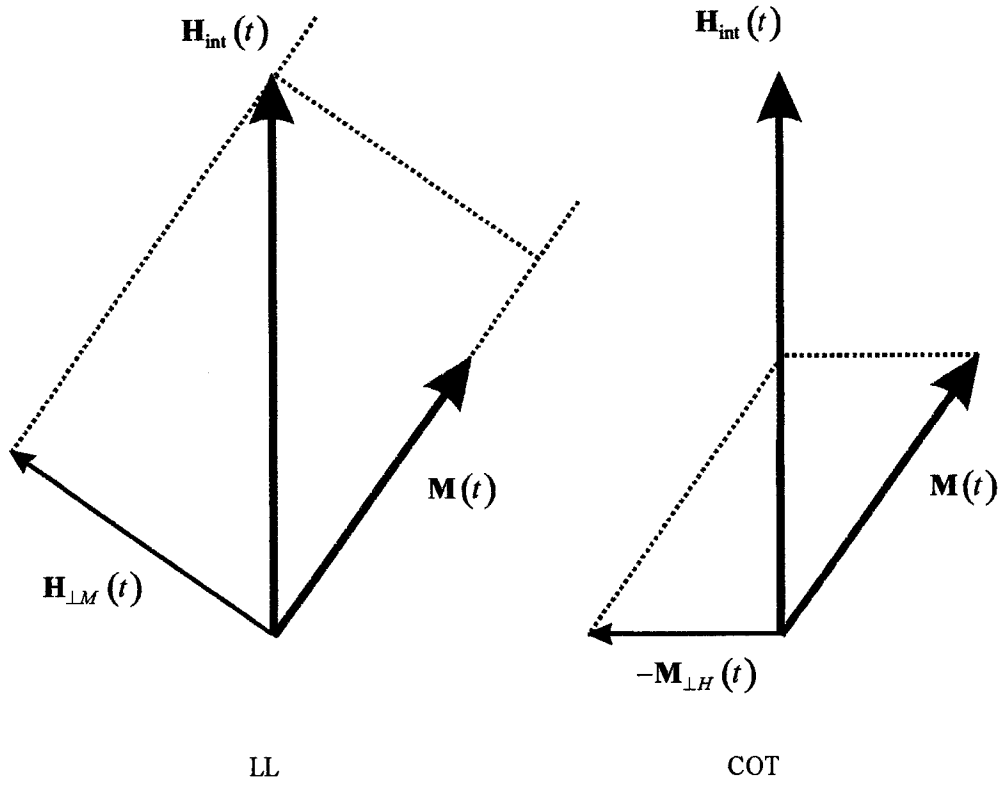

Figure 3-6: The two diagrams illustrate how LL damping and COT damping are reciprocal to each other. Left diagram: The LL damping term is proportional to the component $\mathbf{H}_{\perp M}(t)$ of the internal field that is perpendicular to the total magnetization. Right diagram: The COT damping term is proportional to the negative of the magnetization component $\mathbf{M}_{\perp H}(t)$ that is perpendicular to the internal field.

Figure 3-7 gives a working diagram for the construction of the x damping term. The x-z projection $\mathbf{H}_{x-z}$ of the internal field defines a z'-axis that makes an angle φ with the z- axis. The left diagram in the figure shows the x'-z' coordinate system that is obtained by a rotation of the x-z system by the angle φ. In this way the x'-axis is in a direction perpendicular to the

projection $\mathbf{H}_{x-z}$ of the total internal field. The x'-component of $\mathbf{M}_{x-z}(t)$ is now obtained as

$$M_{x'}(t) = m_x(t)\cos\varphi - M_s \sin\varphi . \tag{3.47}$$

In the small signal limit, the angle φ is small, so that one has the approximations

$$\cos\varphi \approx 1 \tag{3.48}$$

and

$$\sin\varphi \approx \varphi \approx \tan\varphi = \frac{h_{\text{int}-x}(t)}{H_{\text{int}}}. \tag{3.49}$$

Substitution into Eq. (3.47) yields the x'-component of the magnetization,

$$m_{x'}(t) \approx m_x(t) - M_s \frac{h_{\text{int}-x}(t)}{H_{\text{int}}}. \tag{3.50}$$

Similarly, one obtains

$$m_{y'}(t) \approx m_y(t) - M_s \frac{h_{\text{int}-y}(t)}{H_{\text{int}}}. \tag{3.51}$$

One has, then, in the small signal limit the COT response equations

$$\frac{dm_x(t)}{dt} = T_x(t) - \lambda_{COT}\left[m_x(t) - \frac{M_s}{H_{\text{int}}} h_{\text{int}-x}(t) \right] \tag{3.52}$$

and

$$\frac{dm_y(t)}{dt} = T_y(t) - \lambda_{COT}\left[m_y(t) - \frac{M_s}{H_{\text{int}}} h_{\text{int}-y}(t) \right]. \tag{3.53}$$

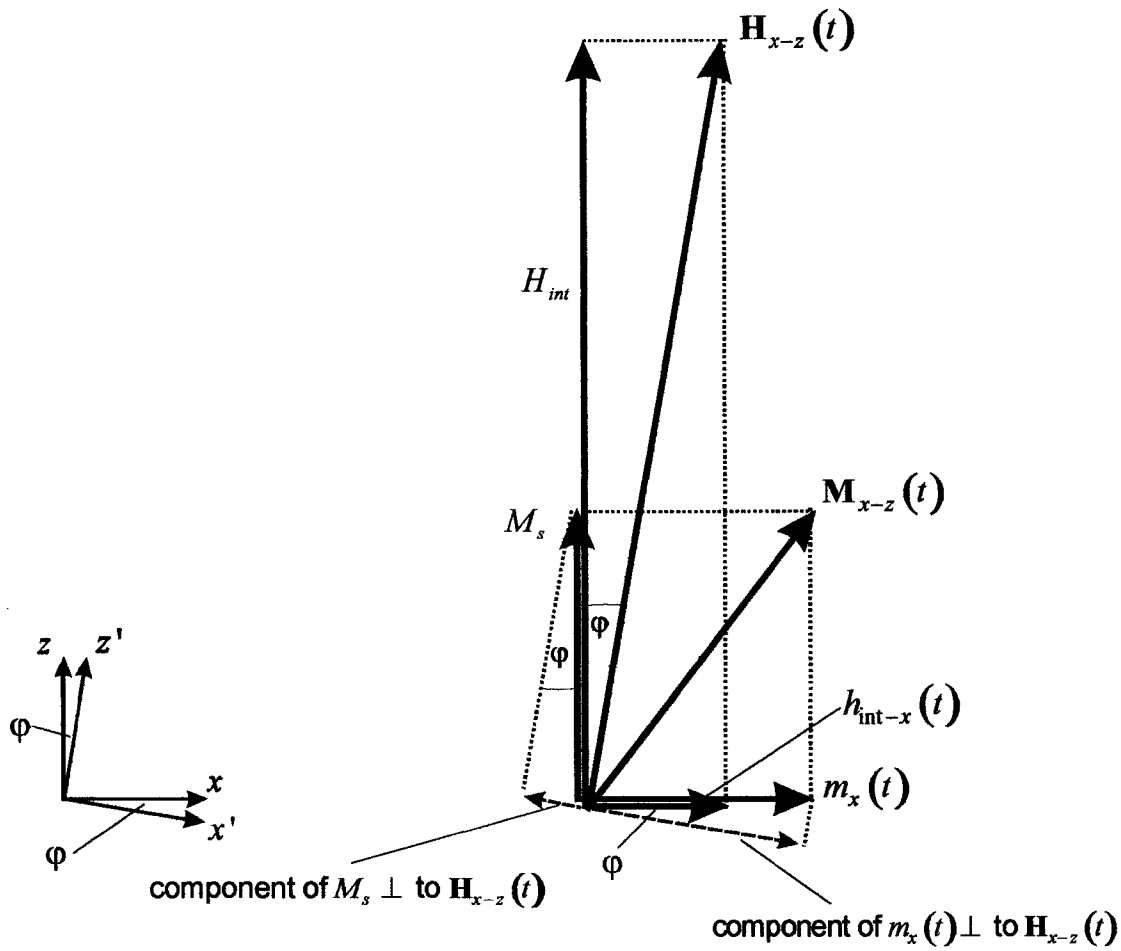

Figure 3-7: The projection of the magnetization and the internal field into the x-z plane yields the vectors $\mathbf{M}_{x-z}(t)$ and $\mathbf{H}_{x-z}(t)$, respectively. The dashed vectors are the components of M_s and of $m_x(t)$ perpendicular to $\mathbf{H}_{x-z}(t)$. Their sum is the component of $\mathbf{M}_{x-z}(t)$ perpendicular to $\mathbf{H}_{x-z}(t)$, and is proportional to the damping contribution to $dm_x(t)/dt$ in the COT equations of motion in the small signal limit.

A purely algebraic derivation of Eqs. (3.52) and (3.53) by linearization of the full nonlinear system (3.46) reveals that the COT rate parameter λ_{COT} is simply the reciprocal of the transverse relaxation time T_2,

$$\lambda_{COT} = \frac{1}{T_2} \tag{3.54}$$

If one uses the connections from Eqs. (3.2) and (3.3),

$$h_{\text{int}-x}(t) = h_{ext-x}(t) - 4\pi N_x m_x(t) \tag{3.55}$$

and

$$h_{\text{int}-y}(t) = h_{ext-y}(t) - 4\pi N_y m_y(t), \tag{3.56}$$

one can reduce the COT equations of motion to the form

$$\frac{dm_x(t)}{dt} = T_x(t) - \lambda_{COT}\frac{M_s}{H_{\text{int}}}\left[h_{ext-x}(t) - \frac{X_H}{M_s}m_x(t)\right] \tag{3.57}$$

and

$$\frac{dm_y(t)}{dt} = T_y(t) - \lambda_{COT}\frac{M_s}{H_{\text{int}}}\left[h_{ext-y}(t) - \frac{Y_H}{M_s}m_y(t)\right]. \tag{3.58}$$

The above match the LL equations with the replacement

$$\lambda_{LL} \leftrightarrow \lambda_{COT}\frac{M_s}{H_{\text{int}}}. \tag{3.59}$$

With this transformation, all results obtained for LL damping go over into corresponding results for COT damping. Therefore COT damping may be viewed in the small signal limit as a type of LL damping, where the LL damping parameter is inversely proportional to the magnitude of the static internal field.

One can also use algebraic replacements, based on the LL results, rather than geometry, to obtain the COT equations of motion in the small signal limit. Recall that the COT damping is

similar to the LL damping with reversed roles of the magnetization and the internal field. Therefore, to obtain the COT equations in the small signal limit, one must in the LL damping terms interchange $m_x(t)$ with $h_{\text{int}-x}(t)$, $m_y(t)$ with $h_{\text{int}-y}(t)$ and M_s with H_{int}. Also the LL rate parameter λ_{LL} must be replaced by the COT rate parameter λ_{COT}. By this procedure one obtains the COT equations (3.52) and (3.53) that were derived from geometrical considerations above.

3.3.d Gilbert (G) damping, driven by the rate of change of the magnetization

Gilbert [1955] proposed a model of magnetic damping in which the precessing magnetization vector experiences a viscous drag torque that dissipates energy. The original vector form of the Gilbert equation may be written as

$$\frac{d\mathbf{M}(t)}{dt} = -|\gamma|\mathbf{M}(t)\times\mathbf{H}_{\text{int}}(t) + \frac{\alpha_G}{M_s}\mathbf{M}(t)\times\frac{d\mathbf{M}(t)}{dt}. \tag{3.60}$$

The precessional response from this equation is depicted graphically in Fig. 3-8. The diagram is constructed for an instantaneous free decay response in which $\mathbf{M}(t)$ is precessing around $\mathbf{H}_{\text{int}}(t)$, but is also spiraling in toward $\mathbf{H}_{\text{int}}(t)$. Because of the spiraling-in response, the total $d\mathbf{M}(t)/dt$ has a component directed opposite to the precession torque. This amounts to a slowing down of the precession response, in addition to the inward decay.

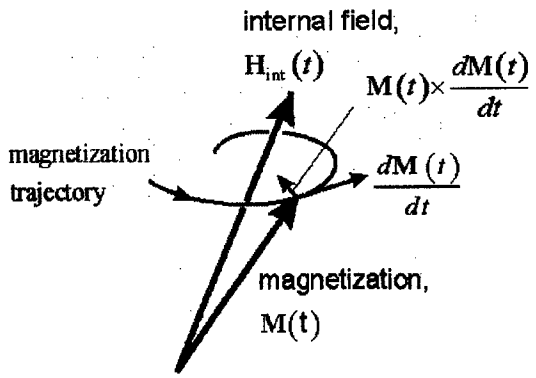

Figure 3-8: The Gilbert damping torque is proportional to $\mathbf{M}(t)\times d\mathbf{M}(t)/dt$, a vector perpendicular to the magnetization vector as well as to the magnetization trajectory.

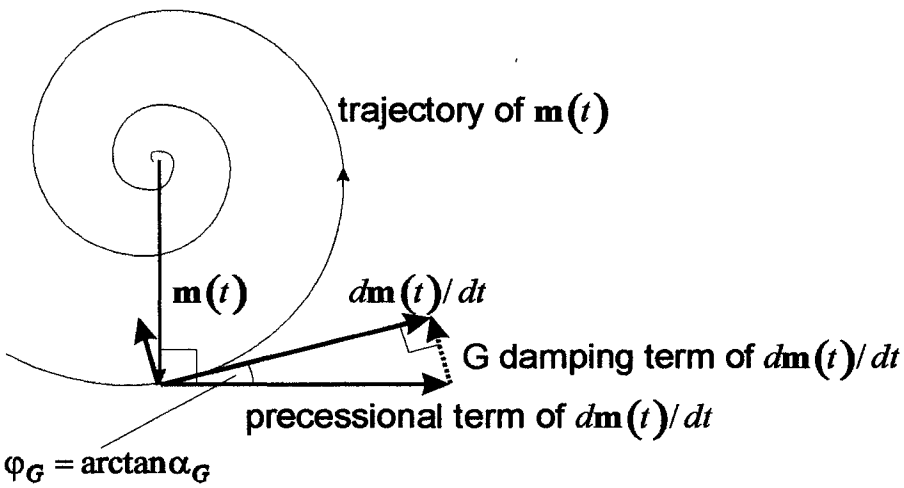

Figure 3-9: For Gilbert damping, the damping contribution to $d\mathbf{m}(t)/dt$ is perpendicular to $d\mathbf{m}(t)/dt$ itself, and has therefore a nonzero component opposing the precessional contribution. As a result, Gilbert damping slows down the precession.

Figure 3-9 shows a top view of the precession cone in the small signal limit. Similar to the 3-D situation, the time rate of change of the transverse magnetization, $d\mathbf{m}(t)/dt$, has a damping component that is perpendicular to $d\mathbf{m}(t)/dt$ itself. A linearization of the 3-D Gilbert equation in Eq. (3.60) shows that the Gilbert damping term in the equations of motion in the small signal limit can be characterized by two fundamental properties:

a) It is perpendicular to $d\mathbf{m}/dt$, such that the static internal field, $d\mathbf{m}/dt$ and the damping term of $d\mathbf{m}/dt$ form a right-handed system.

b) The magnitude of the damping term of $d\mathbf{m}/dt$ is proportional to the magnitude of $d\mathbf{m}/dt$ itself. The constant of proportionality will be called the dimensionless Gilbert damping parameter α_G. The α_G parameter is a direct analog to the LL parameter $\alpha_{LL} = \lambda_{LL}/|\gamma|M_s$ developed above.

The decay geometry for Gilbert damping is significantly different from that for LL damping. Recall that the damping torque for LL damping is perpendicular to the precession torque and has no effect on the precession response. This point of difference is often unappreciated because of the ability to transform algebraically the Gilbert equation into the form of the LL equation by a simple replacement of $|\gamma|$ by $|\gamma|/(1+\alpha_G^2)$. This transformation and some of the corresponding physical implications will be considered shortly. In the small signal limit, the Gilbert equations of motion take the form below.

$$\frac{dm_x(t)}{dt} = -|\gamma|\left[Y_H m_y(t) - M_s h_{ext-y}(t)\right] - \alpha_G \frac{dm_y(t)}{dt} \tag{3.61}$$

and

$$\frac{dm_y(t)}{dt} = +|\gamma|\left[X_H m_x(t) - M_s h_{ext-x}(t)\right] + \alpha_G \frac{dm_x(t)}{dt}. \tag{3.62}$$

The Gilbert damping term in vector form is $\alpha_G\left(-\frac{dm_y(t)}{dt}, \frac{dm_x(t)}{dt}\right)^T$. It depends only on the components of the rate of change of the magnetization, and not on the magnetization itself. It is orthogonal to the time rate of change of the magnetization $\left(\frac{dm_x(t)}{dt}, \frac{dm_y(t)}{dt}\right)$, but not orthogonal to the precession term. If Eqs. (3.61) and (3.62) are solved for the derivatives of the transverse magnetization components, one obtains

$$\frac{dm_x(t)}{dt} = -\frac{|\gamma|}{1+\alpha_G^2}\left[Y_H m_y(t) - M_s h_{ext-y}(t)\right] - \frac{\alpha_G|\gamma|}{1+\alpha_G^2}\left[X_H m_x(t) - M_s h_{ext-x}(t)\right] \tag{3.63}$$

and

$$\frac{dm_y(t)}{dt} = \frac{|\gamma|}{1+\alpha_G^2}\left[X_H m_x(t) - M_s h_{ext-x}(t)\right] - \frac{\alpha_G|\gamma|}{1+\alpha_G^2}\left[Y_H m_y(t) - M_s h_{ext-y}(t)\right]. \tag{3.64}$$

This system goes over into the Landau-Lifshitz equations of motion through two simple replacements, namely

$$\alpha_G \to \alpha_L \tag{3.65}$$

and

$$\frac{|\gamma|}{1+\alpha_G^2} \to |\gamma|. \tag{3.66}$$

In an algebraic sense, therefore, Gilbert damping can be considered to be a type of LL damping, where the gyromagnetic ratio decreases with the dimensionless damping parameter. As the reader may easily show, this equivalence between G and LL damping is valid even for the full nonlinear

equations of motion and is not limited to the small signal limit. However, in this thesis only the small signal limit response of the magnetization is considered.

In spite of the physical inequivalence of Landau-Lifshitz and Gilbert damping, the algebraic equivalence allows one to carry over much of the formal algebra to the Gilbert case. This includes expressions for the precession frequency and decay rates (to be considered shortly), and the Gilbert equation in Smith matrix form. One only needs to take the previously developed relations for the LL case and apply the replacements from Eqs. (3.65) and (3.66).

As the damping parameter α_G is increased, fundamental physical differences between the LL and G damping models become apparent. These differences stem from the fact that the Gilbert damping term has a precessional component, which in fact slows the precession. Consequently, in the case of Gilbert damping, with increasing α_G,

a) the natural frequency of the free precession decay is decreased,

b) the relaxation rate of the free precession decay increases to a maximum value at α_G=1 and then decreases asymptotically to zero. At the peak relaxation rate the damping is called critical damping.

The Gilbert damping model is the only one among the five damping models considered in this chapter that exhibits a critical damping phenomenon.

3.3.e Modified Bloch-Bloembergen (MBB) damping, driven by the magnetization component perpendicular to the instantaneous equilibrium of the magnetization

In contrast to the COT damping model, which relaxes the magnetization to the direction of the instantaneous internal field, the modified Bloch-Bloembergen damping model relaxes the magnetization to the direction of the instantaneous magnetization equilibrium defined by the external applied field. These two directions are not the same! As shown in Fig. 3-10, for MBB damping one resolves the net magnetization along the x'-direction based on the axis rotation angle $\zeta = h_{ext-x}(t)/X_H$. Recall from Fig. 3-7 that for COT damping one resolves the magnetization along an x'-direction based on an axis rotation angle $\varphi = h_{int-x}(t)/H_{int}$. These two angles are not the same. The angle φ depends on $m_x(t)$ through $h_{int-x}(t)$, whereas the angle ζ does not depend on $m_x(t)$ at all. This results for the following MBB equations of motion in the small signal limit,

$$\frac{dm_x(t)}{dt} = T_x(t) - \lambda_{MBB}\left[m_x(t) - \frac{M_s}{X_H}h_{ext-x}(t)\right] \tag{3.67}$$

and

$$\frac{dm_y(t)}{dt} = T_y(t) - \lambda_{MBB}\left[m_y(t) - \frac{M_s}{Y_H}h_{ext-y}(t)\right]. \tag{3.68}$$

Notice that the MBB equations of motion reduce to the BB equations of motion in the absence of the external applied transverse microwave field, that is for $h_{ext-x}(t) = h_{ext-y}(t) = 0$. The term "modified" was originally introduced to underscore the change in form so that $m_x(t)$ and $m_y(t)$ relax to their equilibrium values rather than to zero.

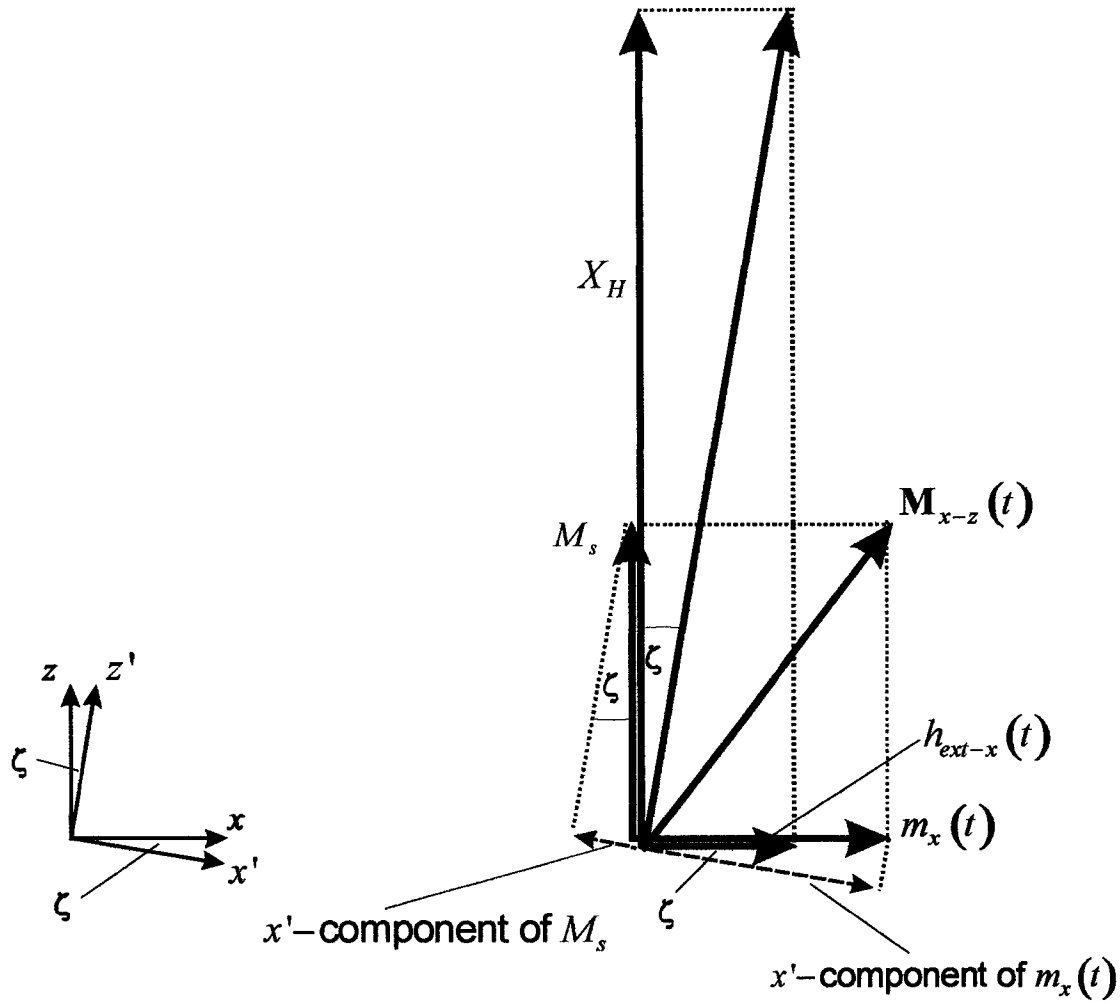

Figure 3-10: Construction of the MBB damping contribution to $dm_x(t)/dt$. The damping term is proportional to the x component of the magnetization component (dotted arrow) perpendicular to the direction $\left[h_x(t), X_H\right]^T$ of the instantaneous magnetization equilibrium.

As with the COT model, the small signal limit response of the MBB model may be cast into the LL form. One obtains,

$$\frac{dm_x(t)}{dt} = T_x(t) + \lambda_{MBB}\frac{M_s}{X_H}\left[h_{ext-x}(t) - \frac{X_H}{M_s}m_x(t)\right] \tag{3.69}$$

and

$$\frac{dm_y(t)}{dt} = T_y(t) + \lambda_{MBB}\frac{M_s}{Y_H}\left[h_{ext-y}(t) - \frac{Y_H}{M_s}m_y(t)\right]. \tag{3.70}$$

In this LL form, one sees a major problem. Instead of a single λ_{LL} multiplier for both the x- and the y-damping terms, one has two different coefficients that depend on the geometry and on the static internal field. Recall also that the COT equations in LL form gave a common multiplier $\lambda_{COT}M_s/H_{int}$. One can view the COT and MBB forms as moving further and further away from the original LL formulation with

$$\lambda_{LL}^{(COT)} = \lambda_{COT}\frac{M_s}{H_{\text{int}}}, \tag{3.71}$$

$$\lambda_{LL}^{(MBB,x)} = \lambda_{MBB}\frac{M_s}{X_H}, \tag{3.72}$$

and

$$\lambda_{LL}^{(MBB,y)} = \lambda_{MBB}\frac{M_s}{Y_H}. \tag{3.73}$$

One sees, therefore, that the damping parameters in these models (not to mention Gilbert) represent very different physical processes. There has been much discussion over the years about "which model is correct". The point to be emphasized here is that all five models are phenomenological in nature. The present analysis shows that the phenomenological bases of the LL, COT, G, BB and MBB models are all very different.

3.4 Trajectories of the free decay of the magnetization precession

Recall from Chapter 2 that the undamped, free magnetization precession in the small signal limit follows an elliptical trajectory in the transverse plane. "Undamped" means that no energy is dissipated at any instant of time, and "free" means that only a static field is applied, but no transverse microwave driving field. When damping is included, the magnetization trajectory is no longer a closed elliptical curve, but a compressed logarithmic spiral. The shape of the decompressed logarithmic spiral is controlled by a single parameter, the angular decay rate of the spiral. The functional dependence of the angular decay rate on the stiffness fields and the static internal field is established for each of the five damping models. As a byproduct, the decay parameters and relaxation rate of the free decay amplitude are obtained.

3.4.a Trajectory of the free precession decay with BB or MBB damping

Recall from Section 3.3.b that the equations of motion for the free precession decay with BB damping in an ellipsoidal sample with stiffness frequencies X_H and Y_H are

$$\frac{dm_x(t)}{dt} = -|\gamma| Y_H m_y(t) - \lambda_{BB} m_x(t), \tag{3.74}$$

and

$$\frac{dm_y(t)}{dt} = +|\gamma| X_H m_x(t) - \lambda_{BB} m_y(t). \tag{3.75}$$

Here λ_{BB} is the BB decay rate, namely $(1/T_2)_{BB}$. Recall that these equations also describe the free decay with MBB damping, since MBB damping coincides with BB damping in the absence of a transverse microwave driving field. It will now be shown that the magnetization trajectory is

a logarithmic spiral compressed along the transverse principal axes of the sample ellipsoid. The compression transformation that converts the precession ellipse of the undamped free decay into a circle is given by

$$\tilde{m}_x(t) = \sqrt{\omega_x}\, m_x(t) \tag{3.76}$$

and

$$\tilde{m}_y(t) = \sqrt{\omega_y}\, m_y(t). \tag{3.77}$$

Will the same compression transformation lead to rotational symmetry in the more general Eqs. (3.74) and (3.75) with the additional BB damping term? After application of the transformations in Eqs. (3.76) and (3.77), one obtains

$$\frac{d\tilde{m}_x(t)}{dt} = -\sqrt{\omega_x\omega_y}\,\tilde{m}_y(t) - \lambda_{BB}\tilde{m}_x(t) \tag{3.78}$$

and

$$\frac{d\tilde{m}_y(t)}{dt} = \sqrt{\omega_x\omega_y}\,\tilde{m}_x(t) - \lambda_{BB}\tilde{m}_y(t). \tag{3.79}$$

Notice that as for the undamped precession, both stiffness frequencies in the transformed system are equal to the Kittel frequency $|\gamma|^2\sqrt{X_H Y_H}$. Notice by comparison with the untransformed Eqs. (3.74) and (3.75) that the BB damping terms have not been changed through the transformation. For the undamped case, $\lambda_{BB}=0$, the "transformation to rotational symmetry" turns the precession ellipses into circles. What are the trajectories corresponding to the damped equations of motion in Eqs. (3.74) and (3.75)? They are compressed logarithmic spirals, as illustrated in Fig. 3.11. The proof follows below:

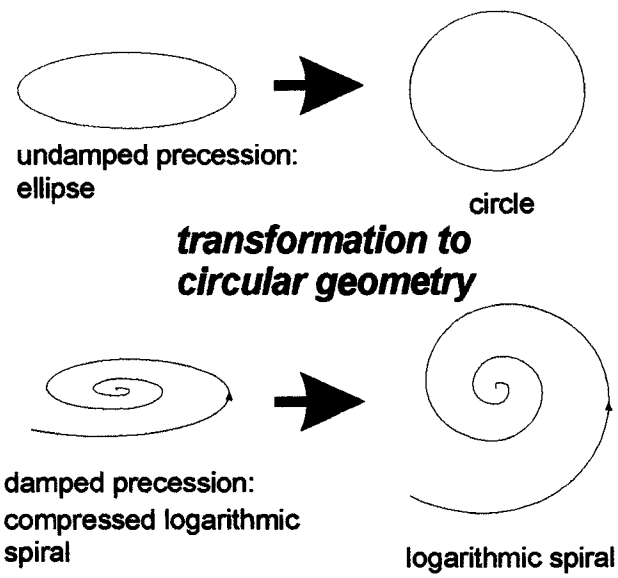

Figure 3-11: A linear transformation, explicitly given in Eqs. (3.76) and (3.77), transforms the precession ellipse of the undamped free precession into a circle. The same transformation converts the compressed spiral trajectory of the damped free precession into a logarithmic spiral. This transformation is called here "transformation to circular geometry". It is a linear compression along the coordinate axes.

Step 1: In order to obtain the time dependence of the magnitude $\left|\tilde{\mathbf{m}}(t)\right| = \sqrt{\left[\tilde{m}_x(t)\right]^2 + \left[\tilde{m}_y(t)\right]^2}$ of the transformed transverse magnetization vector, multiply Eq. (3.78) by $\tilde{m}_x(t)$ and Eq. (3.79) by $\tilde{m}_y(t)$, and then add the equations. One obtains

$$\tilde{m}_x(t)\frac{d\tilde{m}_x(t)}{dt} + \tilde{m}_y(t)\frac{d\tilde{m}_y(t)}{dt} = -\lambda_{BB}\left\{\left[\tilde{m}_x(t)\right]^2 + \left[\tilde{m}_x(t)\right]^2\right\}. \tag{3.80}$$

Now, recognize the left hand side as the time derivative of the quantity

$$\frac{1}{2}\left\{\left[\tilde{m}_x(t)\right]^2 + \left[\tilde{m}_x(t)\right]^2\right\} = \frac{1}{2}\left|\tilde{\mathbf{m}}(t)\right|^2. \tag{3.81}$$

Eq. (3.80) becomes

$$\frac{1}{2}\frac{d}{dt}\left|\tilde{\mathbf{m}}(t)\right|^2 = -\lambda_{BB}\left|\tilde{\mathbf{m}}(t)\right|^2. \tag{3.82}$$

This exponential differential equation for the function $\left|\mathbf{m}(t)\right|^2$ has the simple solution,

$$\left|\tilde{\mathbf{m}}(t)\right|^2 = \left|\tilde{\mathbf{m}}_0\right|^2 e^{-2\lambda_{BB}t}, \tag{3.83}$$

where $\tilde{\mathbf{m}}_0$ is an abbreviation for the magnetization vector $\tilde{\mathbf{m}}(0)$ at time $t = 0$. By taking the square root on both sides, one obtains,

$$\left|\tilde{\mathbf{m}}(t)\right| = \left|\tilde{\mathbf{m}}_0\right| e^{-\lambda_{BB}t}. \tag{3.84}$$

The magnitude of the transformed transverse magnetization decays exponentially with decay rate λ_{BB}. Since a compression transformation is a linear transformation, and does not change an exponential decay rate, λ_{BB} is also the decay rate of the x- and of the y-components of the transverse magnetization components $m_x(t)$ and $m_y(t)$.

Step 2: In order to obtain the trajectory in the uncompressed coordinates in polar form, one introduces the dynamic polar angle $\tilde{\varphi}(t)$,

$$\tilde{m}_x(t) = \left|\tilde{\mathbf{m}}(t)\right| \cos\tilde{\varphi}(t) = \tilde{\mathbf{m}}_0 e^{-\lambda_{BB} t} \cos\tilde{\varphi}(t) \tag{3.85}$$

$$\tilde{m}_y(t) = \left|\tilde{\mathbf{m}}(t)\right| \sin\tilde{\varphi}(t) = \tilde{\mathbf{m}}_0 e^{-\lambda_{BB} t} \sin\tilde{\varphi}(t). \tag{3.86}$$

Substitution of the polar coordinate representation into the first equation of motion in Eq. (3.78) yields,

$$-\lambda_{BB} |\mathbf{m}_0| \cos\tilde{\varphi}(t) - \frac{d\tilde{\varphi}(t)}{dt} |\mathbf{m}_0| \sin\tilde{\varphi}(t) = \tag{3.87}$$

$$-\sqrt{\omega_x \omega_y}\, |\mathbf{m}_0| \sin\tilde{\varphi}(t) - \lambda_{BB} |\mathbf{m}_0| \cos\tilde{\varphi}(t)$$

After cancellation of the term $-\lambda_{BB} |\mathbf{m}_0| \cos\tilde{\varphi}(t)$ on both sides and of the factor $|\mathbf{m}_0| \sin\tilde{\varphi}(t)$ in the remaining terms, the equation simplifies to

$$\frac{d\tilde{\varphi}(t)}{dt} = \sqrt{\omega_x \omega_y}\,. \tag{3.88}$$

This means that the angular velocity of the magnetization spiral in $\tilde{m}_x(t)$ and $\tilde{m}_y(t)$ is constant in time. In fact, this angular velocity is equal to the Kittel resonance frequency $\sqrt{\omega_x \omega_y}$. If the polar angle has the initial value $\tilde{\varphi}(0) = \tilde{\varphi}_0$, then Eq. (3.88) implies that

$$\tilde{\varphi}(t) = \tilde{\varphi}_0 + |\gamma| \sqrt{X_H Y_H} \cdot t\,. \tag{3.89}$$

Elimination of the time t from Eq. (3.84) by use of Eq. (3.89) yields the representation of the trajectory in polar coordinates:

$$\left|\widetilde{\mathbf{m}}(t)\right| = \left|\widetilde{\mathbf{m}}_0\right| e^{-\frac{\lambda_{BB}}{|\gamma|^2\sqrt{X_H Y_H}}\left[\tilde{\varphi}(t)-\tilde{\varphi}_0\right]}. \tag{3.90}$$

This polar equation has the form $r = r_0 e^{-\mu(\varphi-\varphi_0)}$ of a standard logarithmic spiral . In this case, $r_0 = |\mathbf{m}_0|$ is the polar radius of the spiral for the polar angle φ_0. The factor $\mu = \lambda_{BB}/\sqrt{\omega_x\omega_y}$ in the exponent is the constant amplitude decay rate of the magnetization trajectory with respect to the polar angle. It has units of $1/rad$, and was shown here to be inversely proportional to the Kittel resonance frequency $\sqrt{\omega_x\omega_y}$ for BB and for MBB damping.

3.4.b Trajectory of the free precession decay with LL damping

The previous section showed that the free precession trajectory for BB damping is a compressed logarithmic spiral. The BB damping terms are unaffected by the uncompression transformation. This section will show that, in contrast, the LL damping terms are changed by the uncompression transformation. As a consequence, the LL free decay trajectory is a compressed logarithmic spiral, rotated by a small angle $\varphi_{LL} = (1/2)\arctan\alpha_{LL}$. Recall that α_{LL} is the dimensionless LL damping parameter $\lambda_{LL}/|\gamma|M_s$. Figure 3-12 shows a sketch of the LL free decay response. The algebra below will develop the equations for this response.

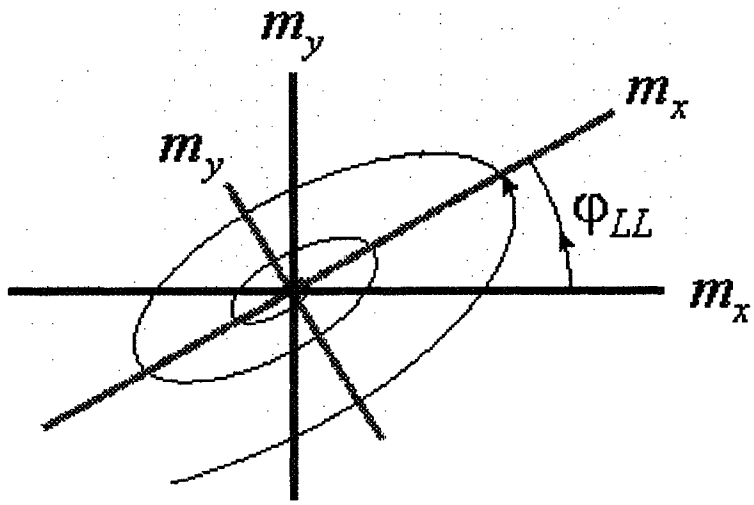

Figure 3-12: The free decay trajectory of the transverse magnetization with LL damping is a compressed logarithmic spiral. It is compressed along axes obtained from the principal axes of the sample ellipsoid (dotted) through counter-clockwise rotation by a small angle $\varphi_{LL} = (1/2)\arctan\alpha_{LL}$.

Recall that the equations of motion for the undriven precession with LL damping in an ellipsoidal sample with stiffness frequencies $\omega_x = |\gamma| X_H$ and $\omega_y = |\gamma| Y_H$ are given in the small signal limit by

$$\frac{dm_x(t)}{dt} = -\omega_y m_y(t) - \alpha_{LL}\omega_x m_x(t) \tag{3.91}$$

and

$$\frac{dm_y(t)}{dt} = +\omega_x m_x(t) - \alpha_{LL}\omega_y m_y(t). \tag{3.92}$$

Notice that in these LL equations the coefficients of $m_x(t)$ and $m_y(t)$ in the damping terms are $-\alpha_{LL}\omega_x$ and $-\alpha_{LL}\omega_y$, respectively. In general, these coefficients are not equal except for the

special cases of rotational symmetry with $N_x = N_y$, $X_H = Y_H$, and $\omega_x = \omega_y$. In all other cases, the damping coefficients in the LL component equations can be made equal by a suitable rotation of the coordinate axes. A rotation of the x-y coordinate system by an angle φ_{LL} results in a transformation of the magnetization components according to

$$\begin{pmatrix} m_x'(t) \\ m_y'(t) \end{pmatrix} = \begin{pmatrix} \cos\varphi_{LL} & \sin\varphi_{LL} \\ -\sin\varphi_{LL} & \cos\varphi_{LL} \end{pmatrix} \begin{pmatrix} m_x(t) \\ m_y(t) \end{pmatrix}. \tag{3.93}$$

In the new coordinates, Eqs. (3.91) and (3.92) become

$$\begin{pmatrix} \frac{dm_x'(t)}{dt} \\ \frac{dm_y'(t)}{dt} \end{pmatrix} = \begin{pmatrix} \cos\varphi_{LL} & \sin\varphi_{LL} \\ -\sin\varphi_{LL} & \cos\varphi_{LL} \end{pmatrix} \begin{pmatrix} -\alpha_{LL}\omega_x & -\omega_y \\ \omega_x & -\alpha_{LL}\omega_y \end{pmatrix} \begin{pmatrix} \cos\varphi_{LL} & -\sin\varphi_{LL} \\ \sin\varphi_{LL} & \cos\varphi_{LL} \end{pmatrix} \begin{pmatrix} m_x'(t) \\ m_y'(t) \end{pmatrix}$$

$$= \begin{pmatrix} -\alpha_{LL}\left(\omega_x\cos^2\varphi_{LL} + \omega_y\sin^2\varphi_{LL}\right) & -\left(\omega_x\sin^2\varphi_{LL} + \omega_y\cos^2\varphi_{LL}\right) \\ +\left(\omega_x - \omega_y\right)\sin\varphi_{LL}\cos\varphi_{LL} & +\alpha_{LL}\left(\omega_x - \omega_y\right)\sin\varphi_{LL}\cos\varphi_{LL} \\ \left(\omega_x\cos^2\varphi_{LL} + \omega_y\sin^2\varphi_{LL}\right) & -\alpha_{LL}\left(\omega_x\sin^2\varphi_{LL} + \omega_y\cos^2\varphi_{LL}\right) \\ +\alpha_{LL}\left(\omega_x - \omega_y\right)\sin\varphi_{LL}\cos\varphi_{LL} & -\left(\omega_x - \omega_y\right)\sin\varphi_{LL}\cos\varphi_{LL} \end{pmatrix} \begin{pmatrix} m_x'(t) \\ m_y'(t) \end{pmatrix}. \tag{3.94}$$

With the trigonometric identities $\sin(2\varphi) = 2\sin\varphi\cos\varphi$ and $\cos(2\varphi) = \cos^2\varphi - \sin^2\varphi$ this equation simplifies to

$$\begin{pmatrix} \frac{dm_x'(t)}{dt} \\ \frac{dm_y'(t)}{dt} \end{pmatrix} =$$

$$= \begin{pmatrix} -\alpha_{LL}\left(\frac{\omega_x+\omega_y}{2}+\frac{\omega_x-\omega_y}{2}\cos 2\varphi_{LL}\right) & -\frac{\omega_x+\omega_y}{2}+\frac{\omega_x-\omega_y}{2}\cos 2\varphi_{LL} \\ +\frac{\omega_x-\omega_y}{2}\sin 2\varphi_{LL} & +\alpha_{LL}\frac{\omega_x-\omega_y}{2}\sin 2\varphi_{LL} \\ \frac{\omega_x+\omega_y}{2}+\frac{\omega_x-\omega_y}{2}\cos 2\varphi_{LL} & -\alpha_{LL}\left(\frac{\omega_x+\omega_y}{2}-\frac{\omega_x-\omega_y}{2}\cos 2\varphi_{LL}\right) \\ +\alpha_{LL}\frac{\omega_x-\omega_y}{2}\sin 2\varphi_{LL} & -\frac{\omega_x-\omega_y}{2}\sin 2\varphi_{LL} \end{pmatrix} \begin{pmatrix} m_x'(t) \\ m_y'(t) \end{pmatrix}. \tag{3.95}$$

The diagonal elements of the 4×4 matrix in this equation are equal if and only if

$$-\alpha_{LL}\frac{\omega_x-\omega_y}{2}\cos 2\varphi_{LL}+\frac{\omega_x-\omega_y}{2}\sin 2\varphi_{LL}=0. \tag{3.96}$$

For $\omega_x=\omega_y$ this equation is always fulfilled. For Eq. (3.96) can be divided by $(\omega_x-\omega_y)/2$, and yields the simple condition,

$$\tan 2\varphi_{LL}=\alpha_{LL}, \tag{3.97}$$

or, solved for the rotation angle φ_{LL},

$$\varphi_{LL}=\frac{1}{2}\arctan\alpha_{LL}. \tag{3.98}$$

With this rotation angle, the system in Eq. (3.95) may be written as

$$\frac{dm_x'(t)}{dt}=-\left[\frac{\omega_x+\omega_y}{2}-\frac{\omega_x-\omega_y}{2}\sqrt{1+\alpha_{LL}^2}\right]m_y'(t)-\alpha_{LL}\frac{\omega_x+\omega_y}{2}m_x'(t) \tag{3.99}$$

and

$$\frac{dm_y'(t)}{dt} = +\left[\frac{\omega_x+\omega_y}{2}+\frac{\omega_x-\omega_y}{2}\sqrt{1+\alpha_{LL}^2}\right]m_x'(t)-\alpha_{LL}\frac{\omega_x+\omega_y}{2}m_y'(t). \tag{3.100}$$

These equations have the same form as the BB/MBB equations in Eqs. (3.78) and (3.79), if in those equations ω_x is replaced by

$$\tilde{\omega}_x = \frac{\omega_x+\omega_y}{2}+\frac{\omega_x-\omega_y}{2}\sqrt{1+\alpha_{LL}^2}\ , \tag{3.101}$$

and ω_y is replaced by

$$\tilde{\omega}_y = \frac{\omega_x+\omega_y}{2}-\frac{\omega_x-\omega_y}{2}\sqrt{1+\alpha_{LL}^2}\ , \tag{3.102}$$

and λ_{LL} is replaced by

$$\tilde{\lambda}_{LL} = \alpha_{LL}\frac{\omega_x+\omega_y}{2}. \tag{3.103}$$

One then has

$$\frac{dm_x'(t)}{dt} = -\tilde{\omega}_y m_y'(t)-\tilde{\lambda}_{LL}m_x'(t), \tag{3.104}$$

and

$$\frac{dm_y'(t)}{dt} = \tilde{\omega}_x m_x'(t)-\tilde{\lambda}_{LL}m_y'(t). \tag{3.105}$$

The transformations as in Eqs. (3.76) and (3.77), now written as

$$\tilde{m}_{x'}(t) = \sqrt{\tilde{\omega}_x}\ m_{x'}(t) \tag{3.106}$$

and

$$\widetilde{m}_{y'}(t)=\sqrt{\widetilde{\omega}_y}\; m_{y'}(t), \tag{3.107}$$

yield transformed LL free decay response equations in the form

$$\frac{d\widetilde{m}_{x'}(t)}{dt}=-\sqrt{\widetilde{\omega}_x\widetilde{\omega}_y}\;\widetilde{m}_{y'}(t)-\tilde{\lambda}_{LL}\widetilde{m}_{x'}(t) \tag{3.108}$$

and

$$\frac{d\widetilde{m}_{y'}(t)}{dt}=\sqrt{\widetilde{\omega}_x\widetilde{\omega}_y}\;\widetilde{m}_{x'}(t)-\tilde{\lambda}_{LL}\widetilde{m}_{y'}(t). \tag{3.109}$$

Based on the above, one can carry over the full logarithmic spiral analysis from Sec. 3.4.a. The Step 1 result goes over to

$$\left|\widetilde{\mathbf{m}}(t)\right|=\left|\widetilde{\mathbf{m}}_0\right|e^{-\tilde{\lambda}_{LL}t} \tag{3.110}$$

The Step 2 result goes over to

$$\tilde{\varphi}_{LL}(t)=\tilde{\varphi}_0+\sqrt{\widetilde{\omega}_x\widetilde{\omega}_y}\;t \tag{3.111}$$

and

$$\left|\widetilde{\mathbf{m}}(t)\right|_{LL}=\left|\widetilde{\mathbf{m}}_0\right|e^{-\frac{\tilde{\lambda}_{LL}}{\sqrt{\widetilde{\omega}_x\widetilde{\omega}_y}}\left[\tilde{\varphi}_{LL}(t)-\tilde{\varphi}_0\right]}. \tag{3.112}$$

In the limit of small damping, $\alpha_{LL}\ll 1$, one may neglect the α_{LL}^2 terms in the above equations. In this limit, $\widetilde{\omega}_x\to\omega_x$ and $\widetilde{\omega}_y\to\omega_y$.

It was shown that the free decay trajectory of the precession with LL damping is a compressed logarithmic spiral whose compression axes form an angle of

$$\varphi_{LL}=\frac{1}{2}\arctan\alpha_{LL} \tag{3.113}$$

with the principal axes of the sample ellipsoid. This situation was depicted in Fig. 3-8. The angle φ_{LL} will be referred to as the tilt angle of the spiral.

3.4.c Trajectory of the free precession decay with G damping

As developed in Sec. 3.3.d, Gilbert damping can be viewed as a Landau-Lifshitz damping with a gyromagnetic ratio proportional to $1/\left(1+\alpha_G^2\right)$. Consequently all results for LL damping are converted into results for G damping, when α_{LL} is replaced by α_G and when $|\gamma|$ is replaced by $|\gamma|/\left(1+\alpha_G^2\right)$ in the LL equation of motion. Therefore, the trajectory of the free precession decay with G damping is a compressed logarithmic spiral whose compression axes form an angle of

$$\varphi_G = \frac{1}{2}\arctan\alpha_G \tag{3.114}$$

with the principal axes of the sample ellipsoid. That means it is impossible to judge from the shape of the trajectory whether G or LL damping is at work. However, there is a clear distinction between G and LL damping as regards the relaxation rate (see Section 3.4.e).

3.4.d Trajectory of the free precession decay with COT damping

As explained in Section 3.3.c, Codrington-Olds-Torrey damping with COT damping time constant T_2 can be viewed as a Landau-Lifshitz damping with the dimensionless LL damping parameter α_{LL} replaced by

$$\alpha_{COT} = \frac{1}{T_2|\gamma|H_{\text{int}}}. \tag{3.115}$$

Therefore, the trajectory of the free precession decay with COT damping is a compressed logarithmic spiral whose compression axes form an angle of

$$\varphi_{COT} = \frac{1}{2}\arctan\alpha_{COT} = \frac{1}{2}\arctan\frac{1}{T_2|\gamma|H_{\text{int}}} \tag{3.116}$$

with the principal axes of the sample ellipsoid.

Eq. (3.116) shows that for COT damping, the tilt angle φ_{COT} of the spiral trajectory depends on the static internal field. This is a unique characteristic of the COT damping model.

3.4.e The relaxation rate of the free precession decay

The amplitude decay for the free precession trajectory with BB/MBB damping was shown to be

$$\left|\tilde{\mathbf{m}}(t)\right| = \left|\tilde{\mathbf{m}}_0\right| e^{-\lambda_{BB}t}, \tag{3.117}$$

with the rate parameter

$$\lambda_{BB} = \frac{1}{T_2}. \tag{3.118}$$

Recall that the tilde over the magnetization signifies that this is the magnetization after the compression transformation to rotational symmetry, which transforms the elliptical precession response into a circular response. The transformation to rotational symmetry linearly rescales the x- and y-axes, but does not change the decay characteristics of the precession such as the exponential decay rate, which is also called relaxation rate. Therefore, the relaxation rate of the magnetization amplitude can be extracted directly from Eq. (3.117). The relaxation rate is the

decay parameter

$$\eta_{BB} = \lambda_{BB} = \frac{1}{T_2}. \tag{3.119}$$

For Landau-Lifshitz damping, on the other hand, the magnetization amplitude decay after transformation to rotational symmetry was shown to be

$$\left|\widetilde{\mathbf{m}}(t)\right| = \left|\widetilde{\mathbf{m}}_0\right| e^{-\tilde{\lambda}_{LL}t} \tag{3.120}$$

with the decay parameter

$$\tilde{\lambda}_{LL} = \alpha_{LL}\frac{\omega_x + \omega_y}{2}. \tag{3.121}$$

By the same reasoning as for the BB damping, the LL relaxation rate is identical to this LL decay parameter:

$$\eta_{LL} = \tilde{\lambda}_{LL} = \alpha_{LL}|\gamma|\frac{X_H + Y_H}{2} = \alpha_{LL}\frac{\omega_x + \omega_y}{2}. \tag{3.122}$$

The G relaxation rate is obtained from the LL relaxation rate in Eq. (3.121), when α_{LL} is replaced by α_G and $|\gamma|$ is replaced by $|\gamma|/\left(1+\alpha_G^2\right)$. The result is

$$\eta_G = \alpha_G\frac{|\gamma|}{1+\alpha_G^2}\frac{X_H + Y_H}{2} = \frac{\alpha_G}{1+\alpha_G^2}\frac{\omega_x + \omega_y}{2}. \tag{3.123}$$

Notice that the G and LL relaxation rates depend very differently on the respective dimensionless damping parameter. Whereas the LL relaxation rate is linear in α_{LL}, the G relaxation rate contains a factor $\alpha_G/\left(1+\alpha_G^2\right)$. Figure 3-13 illustrates this difference. The G relaxation rate attains a maximum at $\alpha_G = 1$ and then tends to zero as $\alpha_G \to \infty$. One calls $\alpha_G = 1$ the critical value of the damping parameter α_G. There is no critical value of the damping parameter for LL damping.

Finally, the COT relaxation rate is obtained from the LL relaxation rate when the

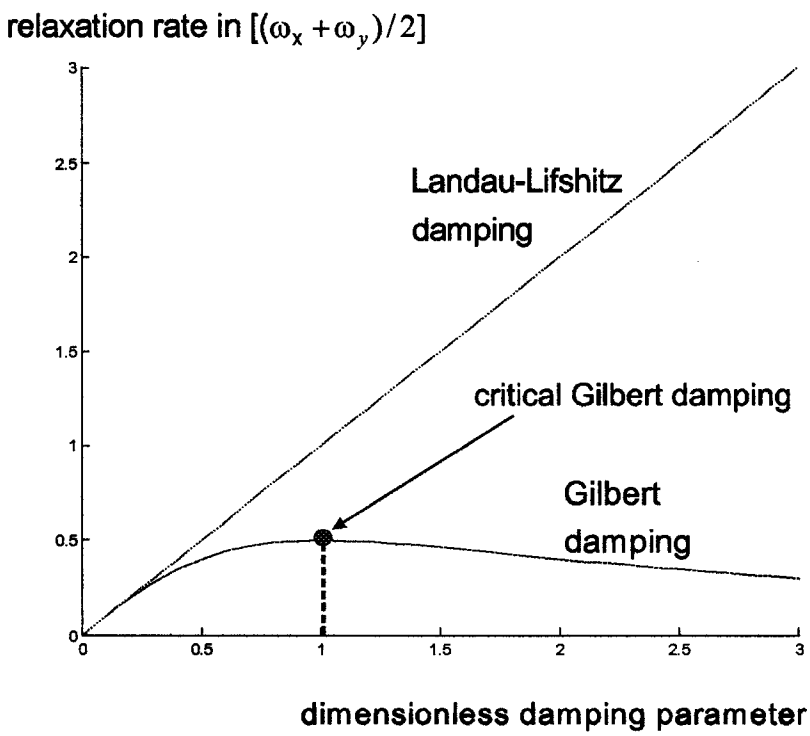

Figure 3-13: Dependence of relaxation rate on damping parameter, contrasted for LL and G damping. The dependence is linear for LL damping. For G damping it is nonlinear, and attains a maximum at the critical value $\alpha_G = 1$. Such critical damping occurs only for the Gilbert damping model, and for none other one of the five damping models considered in this thesis.

dimensionless LL damping parameter α_{LL} is replaced by $\alpha_{COT} = 1/T_2|\gamma|H_{\text{int}}$. Therefore, the COT relaxation rate is given by

$$\eta_{COT} = \alpha_{COT}\frac{\omega_x + \omega_y}{2} = \frac{1}{T_2|\gamma|H_{\text{int}}}. \tag{3.124}$$

3.4.f Comparison of trajectory tilt angles and relaxation rates

For the free precession decay, Table 3-2 compares for the five damping models the relaxation rates and the tilt angle of the spiral trajectory against the transverse principal axes of the sample ellipsoid. For the free decay, the BB and MBB models are identical, and therefore share a common row in the table.

The relaxation rate is independent of both the sample geometry and the static internal field for the BB/MBB models. The relaxation rate scales linearly with a geometry factor for the LL, G, and COT models. This geometry factor is the same for these three models, and is the arithmetic mean of the stiffness frequencies. The COT model is the only model of the five for which the relaxation rate is inversely proportional to the static internal field; the other four models show no field dependence of the relaxation rate. Finally, the Gilbert relaxation rate scales in a nonlinear way with the damping parameter α_G. Maximum relaxation is attained for the critical value $\alpha_G = 1$ (critical damping).

For all five damping models the trajectory is, in general, a compressed logarithmic spiral. For the BB and MBB damping models, the spiral is compressed along one of the transverse principal axes of the sample ellipsoid. In contrast, for the LL, G and COT models, the logarithmic

spirals are tilted away from the principal axes by a small rotation angle. This rotation angle is one half of the arctangent of the respective dimensionless damping parameter. Recall that the dimensionless damping parameter is $\alpha_{LL} = \lambda_{LL}/(|\gamma|M_s)$ for LL damping, α_G for G damping, and $\alpha_{COT} = 1/(T_2|\gamma|H_{\text{int}})$ for COT damping.

Damping Model	Relaxation rate η of magnetization amplitude after transformation to rotational symmetry $\lvert\tilde{\mathbf{m}}(t)\rvert = \lvert\tilde{\mathbf{m}}_0\rvert e^{-\eta t}$	Tilt angle φ of the spiral trajectory against the transverse principal axes of the sample ellipsoid
BB/MBB	$\eta_{BB} = \frac{1}{T_2}$	no tilt
LL	$\eta_{LL} = \alpha_{LL}\frac{\omega_x + \omega_y}{2}$	$\varphi_{LL} = \frac{1}{2}\arctan\alpha_{LL}$
G	$\eta_G = \frac{\alpha_G}{1+\alpha_G^2}\frac{\omega_x + \omega_y}{2}$	$\varphi_G = \frac{1}{2}\arctan\alpha_G$
COT	$\eta_{COT} = \frac{1}{T_2\lvert\gamma\rvert H_{\text{int}}}\frac{\omega_x + \omega_y}{2} = \frac{1}{T_2}\frac{X_H + Y_H}{2H_{\text{int}}}$	$\varphi_{COT} = \frac{1}{2}\arctan\frac{1}{T_2\lvert\gamma\rvert H_{\text{int}}}$

Table 3-2: Comparison of the relaxation rate, and the tilt angle of the logarithmic spiral trajectory for the five damping models.

3.5 Smith matrix formulations of the damped precession response

In Section 3.3, the equations of motion for the five damping models were derived in the small signal limit in a form that was explicitly solved for the time derivatives of the transverse magnetization components. When these equations are solved for the components of the external microwave driving field instead, another form of the equations of motion is obtained which will

prove very useful in developing expressions for the energy loss and for the susceptibility tensors. This representation is very common in engineering mechanics, but has only recently been applied to the damped magnetic precession in Smith [2002]. This form of the equations of motion was already used for the undamped equations of motion in Chapter 2 of this thesis, and will be derived here for Landau-Lifshitz damping. The Smith matrix form of the equations of motion for the other four damping models will be given afterwards in a table. The starting point is the LL equations of motion in the small signal limit,

$$\frac{dm_x(t)}{dt} = -|\gamma|\left[Y_H m_y(t) - M_s h_{ext-y}(t)\right] - \frac{\lambda_{LL}}{M_s}\left[X_H m_x(t) - M_s h_{ext-x}(t)\right], \tag{3.125}$$

and

$$\frac{dm_y(t)}{dt} = +|\gamma|\left[X_H m_x(t) - M_s h_{ext-x}(t)\right] - \frac{\lambda_{LL}}{M_s}\left[Y_H m_y(t) - M_s h_{ext-y}(t)\right]. \tag{3.126}$$

With the dimensionless LL damping parameter $\alpha_{LL} = \lambda_{LL}/(|\gamma|M_s)$ these equations become

$$\frac{dm_x(t)}{dt} = -\left[\omega_y m_y(t) - |\gamma|M_s h_{ext-y}(t)\right] - \alpha_{LL}\left[\omega_x m_x(t) - |\gamma|M_s h_{ext-x}(t)\right] \tag{3.127}$$

and

$$\frac{dm_y(t)}{dt} = +\left[\omega_x m_x(t) - |\gamma|M_s h_{ext-x}(t)\right] - \alpha_{LL}\left[\omega_y m_y(t) - |\gamma|M_s h_{ext-y}(t)\right] \tag{3.128}$$

The equations of motion will now be solved for the components $h_{ext-x}(t)$ and $h_{ext-y}(t)$ of the driving field. Notice first that the system given in Eqs. (3.127) and (3.128) can be written in matrix form as

$$\begin{bmatrix} dm_x(t)/dt \\ dm_y(t)/dt \end{bmatrix} = |\gamma| M_s \begin{pmatrix} \alpha_{LL} & 1 \\ -1 & \alpha_{LL} \end{pmatrix} \begin{bmatrix} h_{ext-x}(t) - (X_H/M_s) m_x(t) \\ h_{ext-y}(t) - (Y_H/M_s) m_y(t) \end{bmatrix}. \tag{3.129}$$

Multiply both sides by the inverse of the matrix on the right side, and obtain

$$\frac{1}{|\gamma| M_s} \frac{1}{1+\alpha_{LL}^2} \begin{pmatrix} \alpha_{LL} & -1 \\ 1 & \alpha_{LL} \end{pmatrix} \begin{bmatrix} \frac{dm_x(t)}{dt} \\ \frac{dm_y(t)}{dt} \end{bmatrix} = \begin{bmatrix} h_{ext-x}(t) - \frac{X_H}{M_s} m_x(t) \\ h_{ext-y}(t) - \frac{Y_H}{M_s} m_y(t) \end{bmatrix}. \tag{3.130}$$

Solved for the driving field vector $\left[h_{ext-x}(t), h_{ext-y}(t)\right]^T$, this equation becomes

$$\frac{1}{|\gamma| M_s} \frac{1}{1+\alpha_{LL}^2} \begin{pmatrix} \alpha_{LL} & -1 \\ 1 & \alpha_{LL} \end{pmatrix} \begin{bmatrix} \frac{dm_x(t)}{dt} \\ \frac{dm_y(t)}{dt} \end{bmatrix} + \begin{pmatrix} \frac{X_H}{M_s} & 0 \\ 0 & \frac{Y_H}{M_s} \end{pmatrix} \begin{bmatrix} m_x(t) \\ m_y(t) \end{bmatrix} = \begin{bmatrix} h_{ext-x}(t) \\ h_{ext-y}(t) \end{bmatrix}. \tag{3.131}$$

This is the Smith matrix form of the LL equations of motion in the small signal limit.

Now compare the damped equation in Eq. (3.131) with the undamped equation,

$$\frac{1}{|\gamma| M_s} \begin{pmatrix} 0 & -1 \\ 1 & 0 \end{pmatrix} \begin{bmatrix} \frac{dm_x(t)}{dt} \\ \frac{dm_y(t)}{dt} \end{bmatrix} + \begin{pmatrix} \frac{X_H}{M_s} & 0 \\ 0 & \frac{Y_H}{M_s} \end{pmatrix} \begin{bmatrix} m_x(t) \\ m_y(t) \end{bmatrix} = \begin{bmatrix} h_{ext-x}(t) \\ h_{ext-y}(t) \end{bmatrix}. \tag{3.132}$$

The matrix multiplying the magnetization vector in the second term is the same for the undamped equation and the equation with LL damping. Recall that this matrix is the stiffness matrix

$$\vec{\vec{\mathbf{K}}}_{LL} = \vec{\vec{\mathbf{K}}}_{undamped} = \begin{pmatrix} \frac{X_H}{M_s} & 0 \\ 0 & \frac{Y_H}{M_s} \end{pmatrix}. \tag{3.133}$$

From Eq. (3.131) it is seen that the matrix multiplying the time derivative of the

magnetization for LL decay is

$$\vec{\mathbf{G}}_{LL} = \frac{1}{|\gamma| M_s} \frac{1}{1+\alpha_{LL}^2} \begin{pmatrix} \alpha_{LL} & -1 \\ 1 & \alpha_{LL} \end{pmatrix}. \tag{3.134}$$

This matrix is no longer anti-symmetric as the one for the undamped equation in Eq. (3.132), which is the gyroscopic matrix

$$\vec{\mathbf{G}}_{undamped} = \frac{1}{|\gamma| M_s} \begin{pmatrix} 0 & -1 \\ 1 & 0 \end{pmatrix}. \tag{3.135}$$

To isolate the effect of damping, the matrix $\vec{\mathbf{G}}_{LL}$ can be written as the sum of the gyroscopic matrix $\vec{\mathbf{G}}_{undamped}$ and a small correction matrix, which is called the LL damping matrix $\vec{\mathbf{D}}_{LL}$. Consequently the LL damping matrix $\vec{\mathbf{D}}_{LL}$ is obtained as the difference of the matrices $\vec{\mathbf{G}}_{LL}$ and $\vec{\mathbf{G}}_{undamped}$ as

$$\begin{aligned} \vec{\mathbf{D}}_{LL} &= \vec{\mathbf{G}}_{LL} - \vec{\mathbf{G}}_{undamped} \\ &= \frac{1}{|\gamma| M_s} \frac{1}{1+\alpha_{LL}^2} \begin{pmatrix} \alpha_{LL} & -1 \\ 1 & \alpha_{LL} \end{pmatrix} - \frac{1}{|\gamma| M_s} \begin{pmatrix} 0 & -1 \\ 1 & 0 \end{pmatrix} \\ &= \frac{1}{|\gamma| M_s} \frac{\alpha_{LL}}{1+\alpha_{LL}^2} \begin{pmatrix} 1 & \alpha_{LL} \\ -\alpha_{LL} & 1 \end{pmatrix}. \end{aligned} \tag{3.136}$$

Notice that the LL damping matrix is not symmetric. Its antisymmetric part,

$$\vec{\mathbf{D}}_{LL}^{antisym} = \frac{1}{|\gamma| M_s} \frac{\alpha_{LL}^2}{1+\alpha_{LL}^2} \begin{pmatrix} 0 & 1 \\ -1 & 0 \end{pmatrix}, \tag{3.137}$$

is not zero, but is of second order in the dimensionless damping parameter α_{LL}. It may be combined with the gyroscopic matrix $\vec{\mathbf{G}}_{undamped}$, which is also antisymmetric. The symmetric part of the damping matrix, on the other hand,

$$\vec{\mathbf{D}}_{LL}^{sym} = \frac{1}{|\gamma| M_s} \frac{\alpha_{LL}}{1+(\alpha_{LL})^2} \begin{pmatrix} 1 & 0 \\ 0 & 1 \end{pmatrix}, \tag{3.138}$$

is of first order in the damping parameter α_{LL}. It determines the energy loss of the driven precession, as will be shown in Chapter 4. With these matrices, the LL equation of motion becomes

$$\left(\vec{\mathbf{G}}_{undamped} + \vec{\mathbf{D}}_{LL}\right) \cdot \frac{d\mathbf{m}(t)}{dt} + \vec{\mathbf{K}}_{LL} \cdot \mathbf{m}(t) = \mathbf{h}_{ext}(t). \tag{3.139}$$

Table 3-3 shows the damping matrix and the stiffness matrix for each of the five damping models. In the LL, COT, G and MBB models the stiffness matrix is the same as in the undamped torque equation. It is a symmetric matrix. For BB damping, however, the stiffness matrix is not symmetric, but has a small anti-symmetric part that is linear in the damping parameter. Chapter 4 shows that this non-symmetric BB stiffness matrix leads to negative loss under certain conditions.

Another anomaly of BB damping is the zero damping matrix. The other four models have a damping matrix whose elements are of the order of the damping parameter. In Chapter 4 it is shown that only the symmetric part $\vec{\mathbf{D}}^{sym}$ of the damping matrix contributes to the energy loss. Notice that $\vec{\mathbf{D}}^{sym}$ is a multiple of the unit matrix for the LL, G, and COT damping models. Chapter 5 demonstrates that this implies an isotropic distribution of the thermal noise fields. For the MBB damping model, the diagonal elements of $\vec{\mathbf{D}}^{sym}$ are, in the general case that $\omega_x \neq \omega_y$, not equal. Hence $\vec{\mathbf{D}}^{sym}$ is *not* a multiple of the unit matrix, and the thermal noise is not distributed isotropically. This special role of the MBB damping model is developed in Chapter 5.

Damping model	Damping matrix $\vec{\vec{\mathbf{D}}}$	Stiffness matrix $\vec{\vec{\mathbf{K}}}$
no damping	none	$\vec{\vec{\mathbf{K}}}_{undamped} = \begin{pmatrix} \frac{X_H}{M_s} & 0 \\ 0 & \frac{Y_H}{M_s} \end{pmatrix}$
LL	$\vec{\vec{\mathbf{D}}}_{LL} = \frac{1}{\lvert\gamma\rvert M_s} \frac{1}{1+(\alpha_{LL})^2} \begin{pmatrix} \alpha_{LL} & (\alpha_{LL})^2 \\ -(\alpha_{LL})^2 & \alpha_{LL} \end{pmatrix}$, $\alpha_{LL} = \frac{\lambda_{LL}}{\lvert\gamma\rvert M_s}$	$\vec{\vec{\mathbf{K}}}_{LL} = \begin{pmatrix} \frac{X_H}{M_s} & 0 \\ 0 & \frac{Y_H}{M_s} \end{pmatrix}$
BB	none	$\vec{\vec{\mathbf{K}}}_{BB} = \begin{pmatrix} X_H/M_s & -\alpha_{BB} \\ \alpha_{BB} & Y_H/M_s \end{pmatrix}$, $\alpha_{BB} = \frac{1}{T_2\lvert\gamma\rvert M_s}$
COT	$\vec{\vec{\mathbf{D}}}_{COT} = \frac{1}{\lvert\gamma\rvert M_s} \frac{\alpha_{COT}}{1+\alpha_{COT}^2} \begin{pmatrix} 1 & \alpha_{COT} \\ -\alpha_{COT} & 1 \end{pmatrix}$, $\alpha_{COT} = \frac{1}{T_2\lvert\gamma\rvert H_{\text{int}}}$	$\vec{\vec{\mathbf{K}}}_{COT} = \begin{pmatrix} \frac{X_H}{M_s} & 0 \\ 0 & \frac{Y_H}{M_s} \end{pmatrix}$
G	$\vec{\vec{\mathbf{D}}}_{G} = \frac{1}{\lvert\gamma\rvert M_s} \begin{pmatrix} \alpha_G & 0 \\ 0 & \alpha_G \end{pmatrix}$	$\vec{\vec{\mathbf{K}}}_{G} = \begin{pmatrix} \frac{X_H}{M_s} & 0 \\ 0 & \frac{Y_H}{M_s} \end{pmatrix}$
MBB	$\vec{\vec{\mathbf{D}}}_{MBB} = \frac{1}{\lvert\gamma\rvert M_s} \frac{\lambda_{MBB}}{\omega_x\omega_y + \lambda_{MBB}^2} \begin{pmatrix} \omega_x & \lambda_{MBB} \\ -\lambda_{MBB} & \omega_y \end{pmatrix}$, $\lambda_{MBB} = \frac{1}{T_2}$	$\vec{\vec{\mathbf{K}}}_{MBB} = \begin{pmatrix} \frac{X_H}{M_s} & 0 \\ 0 & \frac{Y_H}{M_s} \end{pmatrix}$

Table 3-3: Comparison of damping and stiffness matrices for the five damping models.

3.6 External susceptibility tensor

When a system of coupled harmonic oscillators is driven by a sinusoidal driving force, the system response is completely described by a complex-valued susceptibility tensor. In Chapter 2 the susceptibility tensor was derived for the undamped precession response to a small microwave driving field in an ellipsoidal ferromagnetic sample. The microwave field must be perpendicular to a static applied magnetic field, and small in magnitude compared to it. The goal of this section is to extract the susceptibility tensors from the small signal limit x-y equations of motion and a general elliptically polarized applied microwave field $\left[h_{ext-x}(t), h_{ext-y}(t)\right]^T$ for each of the five phenomenological damping models. Traditionally the susceptibility tensor is obtained directly from the equations of motion. This involves a cumbersome calculation with large complex fractions. Smith [2002], however, has shown that the inverse of the susceptibility tensor may be written in a very simple form as a linear combination of various matrices in the Smith matrix form of the equations of motion. The importance of the inverse susceptibility tensor will be recognized in Chapter 4. There the energy loss in the sample is conveniently expressed in terms of the inverse susceptibility tensor and the magnetization components instead of the susceptibility tensor and the applied microwave field components.

Recall from Chapter 2, that the external susceptibility tensor relates the transverse magnetization response to the complex amplitude of the transverse microwave external driving field. The inverse of the external susceptibility tensor was expressed in a simple way in terms of the Smith matrices. In this way the susceptibility tensor could be obtained without solving the coupled differential equations of motion for the magnetization response. This section generalizes

the treatment of susceptibility with Smith matrices to include damping.

As in the undamped case, the transverse microwave driving field $\mathbf{h}_{ext}(t)$ and the corresponding transverse magnetization response $\mathbf{m}(t)$ are expressed in terms of their complex amplitudes $\mathbf{h}_{ext-0}$ and $\mathbf{m}_0$ and the driving frequency ω,

$$\mathbf{h}_{ext}(t) = \mathrm{Re}\left(\mathbf{h}_{ext-0}e^{i\omega t}\right) \tag{3.140}$$

and

$$\mathbf{m}(t) = \mathrm{Re}\left(\mathbf{m}_0 e^{i\omega t}\right). \tag{3.141}$$

The external susceptibility tensor $\overleftrightarrow{\chi}(\omega)$ relates the complex amplitudes of driving field and magnetization response according to

$$\mathbf{m}_0 = \overleftrightarrow{\chi}(\omega)\mathbf{h}_{ext-0}. \tag{3.142}$$

Multiplication from the left by the inverse of the susceptibility tensor yields,

$$\mathbf{h}_{ext-0} = \overleftrightarrow{\chi}^{-1}(\omega)\mathbf{m}_0. \tag{3.143}$$

The inverse susceptibility tensor is easily determined from the general equations of motion for the damped precession in Smith matrix form,

$$\left(\overrightarrow{\mathbf{D}} + \overrightarrow{\mathbf{G}}\right)\frac{d\mathbf{m}(t)}{dt} + \overrightarrow{\mathbf{K}}\mathbf{m}(t) = \mathbf{h}_{ext}(t). \tag{3.144}$$

Elimination of the time dependence in Eq. (3.144) with the help of Eqs. (3.140) and (3.141) yields a linear system for the magnetization complex amplitude $\mathbf{m}_0$ in terms of the applied microwave complex amplitude $\mathbf{h}_{ext-0}$,

$$\left(\vec{\mathbf{D}}+\vec{\mathbf{G}}\right)\cdot i\omega\mathbf{m}_0+\vec{\mathbf{K}}\cdot\mathbf{m}_0=\mathbf{h}_{ext-0}, \tag{3.145}$$

that is,

$$\left[i\omega\left(\vec{\mathbf{D}}+\vec{\mathbf{G}}\right)+\vec{\mathbf{K}}\right]\cdot\mathbf{m}_0=\mathbf{h}_{ext-0}. \tag{3.146}$$

By comparison with Eq. (3.143) the inverse susceptibility tensor is recognized as

$$\vec{\chi}^{-1}(\omega)=i\omega\left(\vec{\mathbf{D}}+\vec{\mathbf{G}}\right)+\vec{\mathbf{K}}. \tag{3.147}$$

The gyroscopic matrix $\vec{\mathbf{G}}$ is always

$$\vec{\mathbf{G}}=\frac{1}{|\gamma|M_s}\begin{pmatrix}0 & -1\\ 1 & 0\end{pmatrix}. \tag{3.148}$$

For the five phenomenological damping models the damping matrix $\vec{\mathbf{D}}$ and the stiffness matrix $\vec{\mathbf{K}}$ were tabulated in Table 3-3. Therefore the inverse susceptibility tensor can easily be calculated for each of the five damping models. By inverting the inverse susceptibility tensor, one obtains the susceptibility tensor itself for each damping model. Both the susceptibility tensor and its inverse are shown in Table 3-4 for the undamped precession and for each of the five damping models.

Notice that by taking the inverse of the inverse susceptibility, for each damping model a frequency-dependent resonance denominator D is introduced. In the undamped case, the resonance denominator is real. It becomes zero exactly at the Kittel frequency, leading to an infinite amplitude of the magnetization response at resonance. In the damped case, the resonance denominator is complex. Its magnitude attains a minimum near the Kittel frequency. In both cases, the inverse susceptibility matrix never has a frequency-dependent resonance denominator.

As a consequence, the inverse susceptibility tensor has a simpler form than the susceptibility tensor. In particular, it contains no quotients of complex numbers. Therefore, in the loss analysis of the next chapter, it proves easier to work with the inverse susceptibility tensor instead of the susceptibility tensor.

A consequence from Eq. (3.147) is the close connection between the damping matrix and the anti-hermitian part of the susceptibility tensor, which will be used in Chapter 5. The anti-hermitian part of the susceptibility tensor is given by

$$\begin{aligned}\frac{\overleftrightarrow{\chi}^{-1}(\omega)-\left[\overleftrightarrow{\chi}^{-1}(\omega)\right]^{\dagger}}{2i} &= \frac{\left[i\omega\left(\overrightarrow{\mathbf{D}}+\overrightarrow{\mathbf{G}}\right)+\overrightarrow{\mathbf{K}}\right]-\left[i\omega\left(\overrightarrow{\mathbf{D}}+\overrightarrow{\mathbf{G}}\right)+\overrightarrow{\mathbf{K}}\right]^{\dagger}}{2i} \\ &= \frac{\left[i\omega\left(\overrightarrow{\mathbf{D}}+\overrightarrow{\mathbf{G}}\right)+\overrightarrow{\mathbf{K}}\right]+i\omega\left(\overrightarrow{\mathbf{D}}^{T}+\overrightarrow{\mathbf{G}}^{T}\right)-\overrightarrow{\mathbf{K}}^{T}}{2i}.\end{aligned} \tag{3.149}$$

Here the dagger superscript denotes the conjugate transpose of a matrix. The right side of Eq. (3.149) simplifies considerably, because the symmetric stiffness matrix $\overrightarrow{\mathbf{K}}$ and the anti-symmetric gyroscopic matrix $\overrightarrow{\mathbf{G}}$ cancel out due to $\overrightarrow{\mathbf{K}}^{T}=\overrightarrow{\mathbf{K}}$ and $\overrightarrow{\mathbf{G}}^{T}=-\overrightarrow{\mathbf{G}}$. Therefore

$$\frac{\overleftrightarrow{\chi}^{-1}(\omega)-\left[\overleftrightarrow{\chi}^{-1}(\omega)\right]^{\dagger}}{2i}=\omega\frac{\overrightarrow{\mathbf{D}}+\overrightarrow{\mathbf{D}}^{T}}{2}=\omega\overrightarrow{\mathbf{D}}^{sym}, \tag{3.150}$$

or

$$\overrightarrow{\mathbf{D}}^{sym}=\frac{\overleftrightarrow{\chi}^{-1}(\omega)-\left[\overleftrightarrow{\chi}^{-1}(\omega)\right]^{\dagger}}{2i\omega}. \tag{3.151}$$

This identity will play an important role in Chapter 5, where the fluctuation-dissipation theorem is applied to magnetic damping.

Table 3-4 (next two pages): Susceptibility tensor and its inverse for the five damping models. In the second column the inverse susceptibility tensor is calculated as a linear combination of Smith matrices. Then in the third column, the susceptibility tensor is given as the inverse matrix of the second column.

Model	Inverse of external susceptibility tensor $\overleftrightarrow{\chi}^{-1}(\omega) = i\omega\left(\overleftrightarrow{\mathbf{D}} + \overleftrightarrow{\mathbf{G}}\right) + \overleftrightarrow{\mathbf{K}}$	External susceptibility tensor $\overleftrightarrow{\chi}(\omega) = \left[i\omega\left(\overleftrightarrow{\mathbf{D}} + \overleftrightarrow{\mathbf{G}}\right) + \overleftrightarrow{\mathbf{K}}\right]^{-1}$
None	$\left(\overleftrightarrow{\chi}_0\right)^{-1} = \frac{1}{\lvert\gamma\rvert M_s}\frac{1}{\lvert\gamma\rvert M_s}\begin{pmatrix}\omega_x & -i\omega\\ i\omega & \omega_y\end{pmatrix}$	$\overleftrightarrow{\chi}_0 = \frac{\lvert\gamma\rvert M_s}{D_0}\begin{pmatrix}\omega_y & i\omega\\ -i\omega & \omega_x\end{pmatrix}$, $D_0 = \omega_x\omega_y - \omega^2$.
LL	$\left(\overleftrightarrow{\chi}_{LL}\right)^{-1} = \frac{1}{\lvert\gamma\rvert M_s}\cdot \begin{pmatrix}\omega_x + i\omega\frac{\alpha_{LL}}{1+\alpha_{LL}^2} & -\frac{i\omega}{1+\alpha_{LL}^2}\\ \frac{i\omega}{1+\alpha_{LL}^2} & \omega_y + i\omega\frac{\alpha_{LL}}{1+\alpha_{LL}^2}\end{pmatrix}$	$\overleftrightarrow{\chi}_{LL} = \frac{\lvert\gamma\rvert M_s}{D_{LL}}\cdot \begin{pmatrix}\omega_y + i\omega\frac{\alpha_{LL}}{1+\alpha_{LL}^2} & \frac{i\omega}{1+\alpha_{LL}^2}\\ -\frac{i\omega}{1+\alpha_{LL}^2} & \omega_x + i\omega\frac{\alpha_{LL}}{1+\alpha_{LL}^2}\end{pmatrix}$, $D_{LL} = \left(\omega_x + i\omega\frac{\alpha_{LL}}{1+\alpha_{LL}^2}\right)\left(\omega_y + i\omega\frac{\alpha_{LL}}{1+\alpha_{LL}^2}\right) - \frac{\omega^2}{\left(1+\alpha_{LL}^2\right)^2}$
BB	$\left(\overleftrightarrow{\chi}_{BB}\right)^{-1} = \frac{1}{\lvert\gamma\rvert M_s}\begin{pmatrix}\omega_x & -i\omega - \frac{1}{T_2}\\ i\omega + \frac{1}{T_2} & \omega_y\end{pmatrix}$	$\overleftrightarrow{\chi}_{BB} = \frac{\lvert\gamma\rvert M_s}{D_{BB}}\begin{pmatrix}\omega_y & i\omega + \frac{1}{T_2}\\ -i\omega - \frac{1}{T_2} & \omega_x\end{pmatrix}$, $D_{BB} = \omega_x\omega_y + \left(i\omega + \frac{1}{T_2}\right)^2$

COT	$\left(\ddot{\chi}_{COT}\right)^{-1}=\frac{1}{\lvert\gamma\rvert M_s}\cdot$ $\begin{pmatrix} \omega_x+i\omega\frac{\alpha_{COT}}{1+\alpha_{COT}^2} & -\frac{i\omega}{1+\alpha_{COT}^2} \\ \frac{i\omega}{1+\alpha_{COT}^2} & \omega_y+i\omega\frac{\alpha_{COT}}{1+\alpha_{COT}^2} \end{pmatrix}$, $\alpha_{COT}=\frac{1}{T_2\lvert\gamma\rvert H_{\text{int}}}\cdot$	$\ddot{\chi}_{COT}=\frac{\lvert\gamma\rvert M_s}{D_{COT}}\cdot$ $\begin{pmatrix} \omega_y+i\omega\frac{\alpha_{COT}}{1+\alpha_{COT}^2} & \frac{i\omega}{1+\alpha_{COT}^2} \\ -\frac{i\omega}{1+\alpha_{COT}^2} & \omega_x+i\omega\frac{\alpha_{COT}}{1+\alpha_{COT}^2} \end{pmatrix}$, $D_{COT}=\omega_x\omega_y+\left(i\omega+\frac{1}{T_2}\right)^2$
G	$\left(\ddot{\chi}_G\right)^{-1}\frac{1}{\lvert\gamma\rvert M_s}\begin{pmatrix} \omega_x+i\omega\alpha_G & -i\omega \\ i\omega & \omega_y+i\omega\alpha_G \end{pmatrix}$	$\ddot{\chi}_G=\frac{\lvert\gamma\rvert M_s}{D_G}\begin{pmatrix} \omega_y+i\omega\alpha_G & i\omega \\ -i\omega & \omega_x+i\omega\alpha_G \end{pmatrix}$, $D_G=\left(\omega_x+i\omega\alpha_G\right)\left(\omega_y+i\omega\alpha_G\right)-\omega^2$
MBB	$\left(\ddot{\chi}_{MBB}\right)^{-1}=\frac{1}{\lvert\gamma\rvert M_s}\cdot$ $\begin{pmatrix} \omega_x+i\omega\frac{\lambda_{MBB}\omega_x}{\omega_x\omega_y+\lambda_{MBB}^2} & -\frac{i\omega\omega_x\omega_y}{\omega_x\omega_y+\lambda_{MBB}^2} \\ \frac{i\omega\omega_x\omega_y}{\omega_x\omega_y+\lambda_{MBB}^2} & \omega_y+i\omega\frac{\lambda_{MBB}\omega_y}{\omega_x\omega_y+\lambda_{MBB}^2} \end{pmatrix}$, $\lambda_{MBB}=\frac{1}{T_2}\cdot$	$\ddot{\chi}_{MBB}=\frac{\lvert\gamma\rvert M_s}{D_{MBB}}\cdot$ $\begin{pmatrix} \omega_y+i\omega\frac{\lambda_{MBB}\omega_y}{\omega_x\omega_y+\lambda_{MBB}^2} & \frac{i\omega\omega_x\omega_y}{\omega_x\omega_y+\lambda_{MBB}^2} \\ -\frac{i\omega\omega_x\omega_y}{\omega_x\omega_y+\lambda_{MBB}^2} & \omega_x+i\omega\frac{\lambda_{MBB}\omega_x}{\omega_x\omega_y+\lambda_{MBB}^2} \end{pmatrix}$, $D_{MBB}=$ $\left(\omega_x+i\omega\frac{\lambda_{MBB}\omega_x}{\omega_x\omega_y+\lambda_{MBB}^2}\right)\left(\omega_y+i\omega\frac{\lambda_{MBB}\omega_y}{\omega_x\omega_y+\lambda_{MBB}^2}\right)$ $-\left(\frac{\omega\omega_x\omega_y}{\omega_x\omega_y+\lambda_{MBB}^2}\right)^2$

3.7 Summary comparison of damping models

All damping models except for BB and MBB damping have a damping matrix that is invariant under arbitrary rotations of the coordinate system in the transverse plane. Therefore in the LL, G and COT models the damping can be called isotropic. In contrast, BB and MBB damping are anisotropic. In practical terms this implies that, for BB and MBB damping in the absence of a microwave driving field, the components of the magnetization noise along the principal axes of an ellipsoidal sample are not equal. The calculation of magnetization noise is performed in Chapter 5 by means of the fluctuation-dissipation theorem and the Wiener-Khinchine theorem.

In the absence of a microwave driving field, BB and MBB damping are identical, but in the presence of a driving field, it is shown in Chapter 4 that BB damping leads to negative loss, for example for an anti-Larmor driving field in an infinite medium. Such negative loss is clearly unphysical. The BB damping model is the only one among the five models analyzed in this chapter that leads to negative loss.

LL and G damping are equivalent in the sense that the same precession dynamics can be described by an LL equation and a G equation with the same dimensionless damping parameter, but with a different gyromagnetic ratio. In the small signal limit, the COT damping model can be considered as a special case of the LL damping, where the dimensionless damping parameter is inversely proportional to the static internal field. This characteristic of MBB damping could be verified experimentally, by determining the relaxation rate at different values of the static internal field.

The G damping is the only one among the five damping models examined in this chapter that reveals critical damping, as the damping parameter is increased. Critical damping appears to be a reasonable requirement for a damping model, because without it the relaxation rate goes to infinity and consequently the switching time for magnetization reversal goes to zero, as the damping parameter goes to infinity. Other damping models, such as the LL, COT and the MBB model, can be "Gilbertized" by letting the gyromagnetic ratio depend on the damping parameter in the form $|\gamma| = |\gamma_0| / \left(1+\alpha^2\right)$, where $|\gamma_0|$ is the value of $|\gamma|$ for zero damping. Such "Gilbertized" models reveal critical damping in the same way as the Gilbert damping model. The "Gilbertized" LL damping is the G damping.

The trajectory of the free precession decay is a compressed logarithmic spiral for each of the five phenomenological damping models. The axes along which the logarithmic spiral is compressed coincide with the transverse principal axes of the sample ellipsoid only for BB and MBB damping. The compressed logarithmic spiral is tilted away from those axes by a small angle for LL, G and COT damping. The tilt angle is proportional to the arctangent of the dimensionless damping parameter. Although this tilt angle is small, it could, in principle, be used to distinguish experimentally between the LL, G and COT damping on one hand and the BB and MBB damping on the other.

Chapter 4

Application of the Smith matrix formulation to loss analysis

Table of contents:

4.1 Introduction

The goal of this chapter is to develop simple expressions for the energy loss due to the various phenomenological damping forms in the small signal limit. As shown in the previous chapters, the Smith matrix form of the equations of motion is a valuable tool for the analysis of precession dynamics. One must distinguish between the instantaneous loss (a *time-dependent* quantity), and the time averaged loss (a *time-independent* quantity). From a simple energy balance calculation, the time-averaged loss can be shown to be equal to the time-averaged microwave input energy absorbed by the sample. For a microwave external driving field, the input energy is easily calculated by the method of complex amplitudes. The instantaneous loss cannot, however, be obtained in this way, because it is not equal to the instantaneous microwave input energy absorbed by the sample. This chapter uses a new approach based on the Smith matrix formalism to obtain expressions for the instantaneous loss.

Both the instantaneous and the time averaged loss are calculated for the five phenomenological damping models that were developed in Chapter 3. Three different methods are used for the loss calculation:

a) Traditionally the time averaged loss is calculated from the imaginary part of a linear combination of external susceptibility components. This method requires the knowledge of the external susceptibility tensor for the given sample geometry. The necessary linear combination of susceptibility tensor components depends on the magnitude and polarization of the driving field. Then the imaginary part must be determined from a quotient of two complex expressions. Of the three loss calculation methods, this one is computationally the most intensive.

b) An alternative method to determine the sign (positive or negative) of the loss is based on the phase angle between the x-components of applied microwave field and magnetization, and the phase angle between the y-components. For every damping model, the two phase angles can always be determined from the components of the susceptibility tensor and the components of the complex amplitude vector of the driving field.

c) The instantaneous loss as well as the time averaged loss can be expressed in terms of the damping matrix and the stiffness matrix that occur in the Smith matrix form of the equations of motion for the magnetization in the small signal limit. The Smith matrix form of the equations of motion was given in detail for the undamped magnetization precession in Chapter 3 and for the damped precession in Chapter 3. The Smith matrix approach is the only one by which one can calculate both instantaneous and time averaged loss. By this approach, the sign of the loss can be easily determined from basic properties of the Smith matrices or components thereof. As already developed in Chapter 3, these matrices are obtained by inspection directly from the equations of motion. For the Smith matrix calculations, therefore, it is not necessary to solve the equations of motion or to determine the susceptibility tensor.

Section 4.2 shows how time averaged loss is traditionally calculated from the imaginary part of a linear combination of external susceptibility components. The loss is specifically calculated in this

way for both Gilbert and Bloch-Bloembergen damping in a spherical sample for two special cases of the microwave driving field: for a linearly polarized field and for a field circularly polarized in the anti-Larmor sense. It is shown that for Bloch-Bloembergen damping, the anti-Larmor drive produces negative loss.

Section 4.3 provides an alternative approach to the calculation of time averaged loss. If the x-component of the magnetization response *lags* the x-component of the driving field, and the y-component of the magnetization response *lags* the y-component of the driving field, then the loss is positive. Conversely, if both magnetization components *lead* their respective driving field components, then the time averaged loss is negative. With this simple rule it is shown that for Bloch-Bloembergen damping, the time averaged loss is negative for an anti-Larmor driving field in an infinite medium.

Section 4.4 reviews the Smith matrix formulation of the equations of motion that was developed in Chapter 2 for the undamped precession and expanded in Chapter 3 to include the damped response.

In Section 4.5 the instantaneous loss is calculated as the difference between the microwave input energy and the instantaneous internal energy. The result expresses the loss in terms of the instantaneous magnetization, its time derivative, and the damping and the stiffness matrices in the Smith matrix form of the equations of motion. For damping models with a *symmetric* stiffness matrix, it is shown that the loss can never be negative. Conversely, for damping models with an *asymmetric* stiffness matrix, the instantaneous loss can be positive or negative, depending on the sample geometry and the external microwave frequency. Negative loss, of course, constitutes a violation of the energy conservation and is unphysical.

Based on the results for the instantaneous loss in Section 4.5, Section 4.6 presents an analysis of the time averaged loss with the method of complex amplitudes. The result confirms the Section 4.2 conclusion that the time averaged loss is negative for Bloch-Bloembergen damping for an anti-Larmor polarized microwave driving field.

Section 4.7 summarizes the results of this chapter.

4.2 Time averaged loss calculation from the susceptibility

Traditionally, time averaged loss is calculated in terms of the components of the susceptibility tensor and the magnitude, polarization and frequency of the applied microwave driving field. Which susceptibility component, or which specific linear combination of susceptibility components is needed, depends on the polarization of the applied microwave field. This section first develops an expression for the time averaged loss for a general elliptically polarized driving field. It then treats two special cases for a spherical sample: a linearly polarized driving field and a driving field circularly polarized in the anti-Larmor sense.

Consider basic energy conservation in a sample that is subjected to an elliptically polarized microwave driving field. One part of the instantaneous microwave input power $P_{in}(t)$ increases the potential magnetic energy $U_{pot}(t)$ in the sample, the other part is dissipated as loss power $P_{loss}(t)$.

$$P_{in}(t)=\frac{dU_{pot}(t)}{dt}+P_{loss}(t). \tag{4.1}$$

For a periodic driving field, the potential energy $U_{pot}(t)$ will vary in a periodic fashion as well. As a consequence, the time averaged change of $U_{pot}(t)$ is zero. Therefore, the time averaged input power and the time averaged loss are always equal for a periodic driving field.

$$\langle P_{in}(t)\rangle_{\substack{time\\average}}=\langle P_{loss}(t)\rangle_{\substack{time\\average}}. \tag{4.2}$$

This cancellation of the change of energy term in Eq. (4.1) as the time average is taken is the reason why the average loss can be calculated simply as the average input power. Recall from Eq. (2.88) in Chapter 2 that the microwave input power is given by

$$P_{in}(t)=\mathbf{h}_{ext}(t)\cdot\frac{d\mathbf{m}(t)}{dt}, \tag{4.3}$$

where $\mathbf{h}_{ext}(t)$ is the transverse applied microwave driving field and $\mathbf{m}(t)$ is the transverse magnetization response. Recall that for a sinusoidal driving field, these time-varying quantities can be expressed in terms of their complex amplitudes $\mathbf{h}_{ext-0}$ and $\mathbf{m}_0$ in the form

$$\mathbf{h}_{ext}(t) = \mathrm{Re}\left(\mathbf{h}_{ext-0}e^{i\omega t}\right) = \frac{1}{2}\left(\mathbf{h}_{ext-0}e^{i\omega t} + \mathbf{h}^*_{ext-0}e^{-i\omega t}\right) \tag{4.4}$$

and

$$\mathbf{m}(t) = \mathrm{Re}\left(\mathbf{m}_0 e^{i\omega t}\right) = \frac{1}{2}\left(\mathbf{m}_0 e^{i\omega t} + \mathbf{m}^*_0 e^{-i\omega t}\right). \tag{4.5}$$

The input power in Eq. (4.3) becomes

$$P_{in}(t) = \frac{i\omega}{4}\left(\mathbf{h}_{ext-0}\cdot\mathbf{m}_0 e^{2i\omega t} - \mathbf{h}^*_{ext-0}\cdot\mathbf{m}^*_0 e^{-2i\omega t} + \mathbf{h}^*_{ext-0}\cdot\mathbf{m}_0 - \mathbf{h}_{ext-0}\cdot\mathbf{m}^*_0\right). \tag{4.6}$$

When the time average is taken, the first two terms in the parentheses on the right side vanish because the time averages of $e^{2i\omega t}$ and of $e^{-2i\omega t}$ are both zero. The time averaged loss is therefore given by

$$\left\langle P_{in}(t)\right\rangle_{\substack{time\\average}} = \frac{i\omega}{4}\left(\mathbf{h}^*_{ext-0}\cdot\mathbf{m}_0 - \mathbf{h}_{ext-0}\cdot\mathbf{m}^*_0\right). \tag{4.7}$$

Since the inner product $\mathbf{h}_{ext-0}\cdot\mathbf{m}^*_0$ is the complex conjugate of $\mathbf{h}^*_{ext-0}\cdot\mathbf{m}_0$, the difference in the parentheses on the right side can be written as

$$\mathbf{h}^*_{ext-0}\cdot\mathbf{m}_0 - \mathbf{h}_{ext-0}\cdot\mathbf{m}^*_0 = 2i\,\mathrm{Im}\left(\mathbf{h}^*_{ext-0}\cdot\mathbf{m}_0\right). \tag{4.8}$$

The time averaged input power in Eq. (4.7) simplifies to

$$\left\langle P_{in}(t)\right\rangle_{\substack{time\\average}} = -\frac{\omega}{2}\mathrm{Im}\left(\mathbf{h}^*_{ext-0}\cdot\mathbf{m}_0\right). \tag{4.9}$$

Notice that the time averaged input power is indeed a real quantity. By Eq. (4.2), the time averages of loss power and input power are equal. Therefore the time averaged loss is given by

$$\left\langle P_{loss}(t)\right\rangle_{\substack{time\\average}} = -\frac{\omega}{2}\mathrm{Im}\left(\mathbf{h}^{*}_{ext-0}\cdot\mathbf{m}_0\right). \tag{4.10}$$

Recall as well from Eq. (2.37) in Chapter 2 that the complex amplitudes of magnetization and driving field are related linearly through the external susceptibility tensor $\ddot{\chi}(\omega)$ according to

$$\mathbf{m}_0 = \ddot{\chi}(\omega)\cdot\mathbf{h}_{ext-0}\,. \tag{4.11}$$

With this relation, the time averaged loss becomes

$$\left\langle P_{loss}(t)\right\rangle_{\substack{time\\average}} = -\frac{\omega}{2}\mathrm{Im}\left[\mathbf{h}^{*}_{ext-0}\cdot\ddot{\chi}\,(\omega)\mathbf{h}_{ext-0}\right]. \tag{4.12}$$

The inner product on the right side can also be written as a matrix product:

$$\left\langle P_{loss}(t)\right\rangle_{\substack{time\\average}} = -\frac{\omega}{2}\mathrm{Im}\left[\left(\mathbf{h}^{*}_{ext-0}\right)^{T}\ddot{\chi}(\omega)\,\mathbf{h}_{ext-0}\right]. \tag{4.13}$$

To demonstrate the calculation of time averaged loss based on the susceptibility, let us consider four special cases of the driving field for both Gilbert and Bloch-Bloembergen damping in an infinite medium:

a) a driving field linearly polarized in the x-direction,

b) a driving field linearly polarized in the y-direction,

c) a driving field circularly polarized in the Larmor sense,

d) a driving field circularly polarized in the anti-Larmor sense.

From Table 3-4 in Chapter 3 it follows that in an infinite medium the external susceptibility tensor for Gilbert damping is given by

$$\ddot{\chi}_G(\omega) = \frac{|\gamma|M_s}{\left(\omega_H + i\alpha_G\omega\right)^2 - \omega^2}\begin{pmatrix}\omega_H + i\alpha_G\omega & i\omega\\ -i\omega & \omega_H + i\alpha_G\omega\end{pmatrix}, \tag{4.14}$$

whereas the susceptibility tensor for Bloch-Bloembergen damping is given by

$$\overleftrightarrow{\chi}_{BB}(\omega)=\frac{|\gamma|M_s}{\omega_H^2+(i\omega+\lambda_{BB})^2}\begin{pmatrix}\omega_H & i\omega+\lambda_{BB}\\ -i\omega-\lambda_{BB} & \omega_H\end{pmatrix}. \tag{4.15}$$

Here α_G is the dimensionless Gilbert damping parameter, and $\lambda_{BB}=1/T_2$ is the BB relaxation rate in units of 1/s. The complex external driving field vector $\mathbf{h}_{ext-0}$ will take different forms, depending on the polarization. Take scalar complex field amplitudes h_{ext-0x} and h_{ext-0y} for the linear case, and h_{ext-0L} and h_{ext-0A} for Larmor and anti-Larmor polarizations, respectively. One may then write $\mathbf{h}_{ext-0x}=(h_{ext-0x},0)^T$ for an x-direction drive, $\mathbf{h}_{ext-0y}=(0,h_{ext-0y})^T$ for a y-direction drive, $\mathbf{h}_{ext-0L}=h_{ext-0L}(1,-i)^T/\sqrt{2}$ for a Larmor drive, and $\mathbf{h}_{ext-0A}=h_{ext-0A}(1,i)^T/\sqrt{2}$ for an anti-Larmor drive. Table 4-1 tabulates the time averaged loss expressions for G and BB damping for these four types of drive. The table shows that the time-averaged loss is always positive except for the BB damping in a sample subjected to an anti-Larmor polarized driving field. In that case, the time-averaged loss is negative. This violates energy conservation, and is clearly unphysical. The Bloch-Bloembergen damping model therefore leads to an unphysical negative loss for an anti-Larmor oriented driving field in an infinite medium. This is a consequence of the magnetization relaxing to the static internal field rather than to the total internal field.

The disadvantages of the susceptibility approach to loss calculation are the following:

a) The susceptibility tensor must be known first, and is often tedious to calculate from the equations of motion.

b) For every special case of the elliptically polarized driving field, the matrix product in Eq. (4.13) must be calculated anew, in order to determine the sign of its imaginary part. This method does not provide a general condition on the external susceptibility matrix that guarantees positive loss for all possible driving fields.

Polarization of driving field	Time averaged loss for Gilbert damping	Time averaged loss for Bloch-Bloembergen damping
linearly polarized in x-direction $\mathbf{h}_{ext} = (h_{0x}, 0)^T$ $P_{aver.loss,x} = -\frac{\omega}{2}\lvert h_{0x}\rvert^2 \operatorname{Im}(\chi_{xx})$	$P_{aver.loss,x,G} = \frac{1}{2}\alpha\omega^2 \lvert\gamma\rvert M_s \lvert h_{0x}\rvert^2 \cdot \frac{\omega_0^2 + (1+\alpha^2)\omega^2}{\left[\omega_0^2 - (1+\alpha^2)\omega^2\right]^2 + (2\alpha\omega\omega_0)^2}$	$P_{aver.loss,x,BB} = \frac{1}{2}\frac{1}{\omega_0 T_2}\omega^2 \lvert\gamma\rvert M_s \lvert h_{0x}\rvert^2 \cdot \frac{2\omega_0^2}{\left(\omega_0^2 - \omega^2 + 1/T_2^2\right)^2 + (2\omega/T_2)^2}$
linearly polarized in y direction $\mathbf{h}_{ext} = (0, h_{0y})^T$ $P_{aver.loss,y} = -\frac{\omega}{2}\lvert h_{0y}\rvert^2 \operatorname{Im}(\chi_{yy})$	$P_{aver.loss,y,G} = \frac{1}{2}\alpha_G\omega^2 \lvert\gamma\rvert M_s \lvert h_{0y}\rvert^2 \cdot \frac{\omega_0^2 + (1+\alpha_G^2)\omega^2}{\left[\omega_0^2 - (1+\alpha_G^2)\omega^2\right]^2 + (2\alpha_G\omega_0\omega)^2}$	$P_{aver.loss,y,BB} = \frac{1}{2}\frac{1}{T_2\omega_0}\omega^2 \lvert\gamma\rvert M_s \lvert h_{0y}\rvert^2 \cdot \frac{2\omega_0^2}{\left(\omega_0^2 - \omega^2 + 1/T_2^2\right)^2 + (2\omega/T_2)^2}$
circularly polarized, Larmor $\mathbf{h}_{ext} = \frac{h_{0,L}}{\sqrt{2}}(1, -i)^T$ $P_{aver.loss,L} = -\frac{\omega}{2}\lvert h_{0,L}\rvert^2 \cdot \operatorname{Im}\left(\frac{\chi_{xx}+\chi_{yy}}{2} - i\frac{\chi_{xy}-\chi_{yx}}{2}\right)$	$P_{aver.loss,L,G} = \frac{1}{2}\alpha_G\omega^2 \lvert\gamma\rvert M_s \lvert h_{0,L}\rvert^2 \cdot \frac{1}{(\omega_0-\omega)^2 + \alpha^2\omega^2}$	$P_{aver.loss,L,BB} = \frac{1}{2T_2}\omega \lvert\gamma\rvert M_s \lvert h_{0,L}\rvert^2 \cdot \frac{1}{(\omega_0-\omega)^2 + (1/T_2)^2}$
Circularly polarized, anti-Larmor $\mathbf{h}_{ext} = \frac{h_{0,AL}}{\sqrt{2}}(1, i)^T$ $P_{aver.loss,AL} = -\frac{\omega}{2}\lvert h_{0,AL}\rvert^2 \cdot \operatorname{Im}\left(\frac{\chi_{xx}+\chi_{yy}}{2} + i\frac{\chi_{xy}-\chi_{yx}}{2}\right)$	$P_{aver.loss,AL,G} = \frac{1}{2}\alpha_G\omega^2 \lvert\gamma\rvert M_s \lvert h_{0,AL}\rvert^2 \cdot \frac{1}{(\omega_0+\omega)^2 + \alpha_G^2\omega^2}$	$P_{aver.loss,AL,BB} = -\frac{1}{2T_2}\omega \lvert\gamma\rvert M_s \lvert h_{0,AL}\rvert^2 \cdot \frac{1}{(\omega_0+\omega)^2 + (1/T_2)^2}$

Table 4-1: Time averaged loss in an infinite medium for four different polarizations of the driving field. For brevity the subscript "ext" is omitted in the driving field components.

c) No information is obtained about the instantaneous loss. Note that the instantaneous loss could be negative at a certain instant of time, in violation of energy conservation, even though the time averaged loss is still positive. The next section will present a simple formulation in terms of phase that can also give conditions for positive or negative loss. After that, Section 4.4 shows how the Smith matrix form can be used to obtain the instantaneous loss in general form.

4.3 Time averaged loss calculation from phase angles

In the previous section the susceptibility method was used to determine the time averaged loss for the magnetization response to an arbitrary elliptically polarized driving field. In this section the time averaged loss is related to the phase angles by which the magnetization components lag (or lead) the respective driving field components. It will be shown that when both magnetization components *lag* the respective driving field components, then the time averaged loss is positive. Conversely, when the magnetization components *lead* the respective driving field components, then the time averaged loss is negative. This simple rule will be proven and then applied to the loss calculation for an anti-Larmor driving field in the case of Bloch-Bloembergen damping for an infinite medium. The method is, however, valid for any damping model, any polarization of the driving field, and any aspect ratios in an ellipsoidal sample.

To begin, notice that when $m_x(t)$ *lags* $h_{ext-x}(t)$ by a phase angle δ, then δ is the angle from m_{0x} to h_{ext-0x} in the complex plane, measured *counter-clockwise*. Consider the following example where the lag angle is $\delta = 90^0$.

$$h_{ext-x}(t) = A\cos(\omega t), \tag{4.16}$$

and

$$m_x(t) = B\sin(\omega t), \tag{4.17}$$

where A and B are positive amplitudes. Indeed, a sine function lags a cosine function by 90^0. The corresponding complex amplitudes are

$$h_{0x} = A \tag{4.18}$$

and

$$m_{0x} = -iB. \tag{4.19}$$

Indeed, the angle from m_{0x} to h_{ext-0x}, measured counter-clockwise in the complex plane, is equal to the phase lag, $\delta = 90^0$. Now recall from Eq. (4.9) above that

$$\begin{aligned} \left\langle P_{loss}(t)\right\rangle_{\substack{time\\average}} &= -\frac{\omega}{2}\mathrm{Im}\left(\mathbf{h}^*_{ext-0}\cdot\mathbf{m}_0\right) \\ &= -\frac{\omega}{2}\mathrm{Im}\left(h^*_{ext-0x}\cdot m_{0x} + h^*_{ext-0y}\cdot m_{0y}\right) \end{aligned} \tag{4.20}$$

If $m_x(t)$ lags $h_{ext-x}(t)$ by a positive phase angle $\delta_x < 180^0$ and $m_y(t)$ lags $h_{ext-y}(t)$ by a positive phase angle $\delta_y < 180^0$, then

$$\frac{m_{0x}}{|m_{0x}|} = \frac{h_{ext-0x}}{|h_{ext-0x}|}e^{-i\delta_x} \tag{4.21}$$

and

$$\frac{m_{0y}}{|m_{0y}|} = \frac{h_{ext-0y}}{|h_{ext-0y}|}e^{-i\delta_y}. \tag{4.22}$$

Substitution into the expression for the time-averaged loss in Eq. (4.20) yields

$$\left\langle P_{loss}(t)\right\rangle_{\substack{time\\average}} = -\frac{\omega}{2}\mathrm{Im}\left(h^{*}_{ext-0x}\cdot m_{0x} + h^{*}_{ext-0y}\cdot m_{0y}\right)$$

$$= -\frac{\omega}{2}\mathrm{Im}\left[\left|m_{0x}\right|\left|h_{ext-0x}\right|e^{-i\delta_x} + \left|m_{0y}\right|\left|h_{ext-0y}\right|e^{-i\delta_y}\right] \tag{4.23}$$

$$= +\frac{\omega}{2}\left[\left|m_{0x}\right|\left|h_{ext-0x}\right|\sin(\delta_x) + \left|m_{0y}\right|\left|h_{ext-0y}\right|\sin(\delta_y)\right].$$

One sees that, as claimed above, the time averaged loss is positive when both δ_x and δ_y are positive, which implies that both magnetization components *lag* the respective driving field components. In contrast, the time averaged loss is negative when both δ_x and δ_y are negative, which implies that both magnetization components lead the respective driving field components.

As an application, consider Bloch-Bloembergen damping for an infinite medium and for an anti-Larmor oriented driving field given by

$$h_{ext-x}(t) = h_0\cos(\omega t), \tag{4.24}$$

and

$$h_{ext-y}(t) = -h_0\sin(\omega t). \tag{4.25}$$

The corresponding complex amplitude vector has the components

$$h_{ext-0x} = \frac{h_0}{\sqrt{2}} \tag{4.26}$$

and

$$h_{ext-0y} = i\frac{h_0}{\sqrt{2}}. \tag{4.27}$$

Recall the Bloch-Bloembergen susceptibility tensor in an infinite medium, which was given by,

$$\overleftrightarrow{\chi}_{inf}^{(BB)} = \frac{|\gamma| M_s}{\omega_H^2 + (i\omega + \lambda_{BB})^2} \begin{pmatrix} \omega_H & i\omega + \lambda_{BB} \\ -i\omega - \lambda_{BB} & \omega_H \end{pmatrix}, \tag{4.28}$$

where $\lambda_{BB} = 1/T_2$.

The complex amplitude of the magnetization response is calculated by multiplying the susceptibility tensor by the complex amplitude vector of the driving field.

$$\begin{pmatrix} m_{0x} \\ m_{0y} \end{pmatrix} = \frac{|\gamma| M_s}{\omega_H^2 + (i\omega + \lambda_{BB})^2} \begin{pmatrix} \omega_H & i\omega + \lambda_{BB} \\ -i\omega - \lambda_{BB} & \omega_H \end{pmatrix} \begin{pmatrix} h_{ext-0x} \\ h_{ext-0y} \end{pmatrix}$$

$$= \frac{|\gamma| M_s}{\omega_H^2 + (i\omega + \lambda_{BB})^2} \begin{pmatrix} \omega_H & i\omega + \lambda_{BB} \\ -i\omega - \lambda_{BB} & \omega_H \end{pmatrix} \frac{h_0}{\sqrt{2}} \begin{pmatrix} 1 \\ i \end{pmatrix}$$

$$= \frac{|\gamma| M_s}{\omega_H^2 + (i\omega + \lambda_{BB})^2} \frac{h_0}{\sqrt{2}} \begin{pmatrix} \omega_H - \omega + i\lambda_{BB} \\ -i\omega - \lambda_{BB} + i\omega_H \end{pmatrix}$$

$$= \frac{|\gamma| M_s}{\omega_H^2 + (i\omega + \lambda_{BB})^2} \frac{h_0}{\sqrt{2}} (\omega_H - \omega + i\lambda_{BB}) \begin{pmatrix} 1 \\ i \end{pmatrix}$$

$$= \frac{|\gamma| M_s}{\omega_H + \omega - i\lambda_{BB}} \frac{h_0}{\sqrt{2}} \begin{pmatrix} 1 \\ i \end{pmatrix}$$

$$= \frac{|\gamma| M_s}{\omega_H + \omega - i\lambda_{BB}} \begin{pmatrix} h_{ext-0x} \\ h_{ext-0y} \end{pmatrix} \tag{4.29}$$

$$= |\gamma| M_s \frac{\omega_H + \omega + i\lambda_{BB}}{(\omega_H + \omega)^2 + \lambda_{BB}^2} \begin{pmatrix} h_{ext-0x} \\ h_{ext-0y} \end{pmatrix}.$$

Since in this special case, the ratios m_{0x}/h_{ext-0x} and m_{0y}/h_{ext-0y} are equal, the lag angle δ_x between

m_{0x} and h_{ext-0x} is the same as the lag angle δ_y between m_{0y} and h_{ext-0y}. It is given by

$$\delta_x = \delta_y = -\arctan\frac{\lambda_{BB}}{\omega_H + \omega}. \tag{4.30}$$

The lag angle is negative. Therefore both magnetization components *lead* the corresponding driving field components by the absolute value of the lag angle, that is by $\arctan\left[\lambda_{BB}/(\omega_H + \omega)\right]$. By the general rule derived above, this implies that the time averaged loss is negative for the special case considered here, which is Bloch-Bloembergen damping for an infinite medium for an anti-Larmor polarized driving field. This confirms the result that was found in the previous section with the susceptibility method.

4.4 The damped magnetic torque equation of motion in the small signal limit – recap of the Smith matrix form

The Smith matrix form of the magnetic torque equation of motion was introduced for the undamped magnetization precession in Chapter 2 and for damped precession in Chapter 3. It consists of a system of two linear differential equations for the transverse magnetization response. For the damped precession, these response equations were written in compact form as

$$\left(\vec{\mathbf{G}} + \vec{\mathbf{D}}\right)\cdot\frac{d\mathbf{m}(t)}{dt} + \vec{\mathbf{K}}^{(damped)}\cdot\mathbf{m}(t) = \mathbf{h}_{ext}(t). \tag{4.31}$$

Recall that $\mathbf{h}_{ext}(t) = \left[h_{ext-x}(t), h_{ext-y}(t)\right]^T$ is the time-dependent transverse external microwave driving field and $\mathbf{m}(t) = \left[m_x(t), m_y(t)\right]^T$ is the transverse magnetization response. Recall also that the gyroscopic matrix $\vec{\mathbf{G}}$ is given by the anti-symmetric matrix,

$$\vec{\mathbf{G}} = \frac{1}{|\gamma| M_s} \begin{pmatrix} 0 & -1 \\ 1 & 0 \end{pmatrix}. \tag{4.32}$$

The gyroscopic matrix $\vec{\mathbf{G}}$ is responsible for the precessional motion of the magnetization. The damping matrix $\vec{\mathbf{D}}$ acts as a small correction to the gyroscopic matrix. It may be decomposed into a symmetric part and an anti-symmetric part. As will be seen in Section 4.5, the symmetric part represents energy dissipation. The anti-symmetric part, on the other hand, influences the precessional motion, but does not dissipate energy. It may be combined with the anti-symmetric gyroscopic matrix $\vec{\mathbf{G}}$. For the undamped precession, the damping matrix $\vec{\mathbf{D}}$ is zero.

The positive definite matrix $\vec{\mathbf{K}}$ is called the stiffness matrix. Recall that the stiffness matrix is symmetric for the undamped precession, and is the matrix of second partial derivatives of the internal magnetic energy. For the damped precession, however, the stiffness matrix need not be symmetric, and the matrix of second partial derivatives of the potential magnetic energy coincides with the *symmetric part* of the stiffness matrix.

$$U_{pot}(t) = \frac{1}{2}\left[\mathbf{m}(t)\right]^T \vec{\mathbf{K}}^{(sym)} \mathbf{m}(t). \tag{4.33}$$

The anti-symmetric part of the stiffness matrix does not contribute to the potential energy, but, as will be shown in the next two sections, to the energy loss. There the relationship between the symmetric part of the stiffness matrix and the potential magnetic energy is used to derive simple expressions for the instantaneous loss and the time averaged loss.

4.5 Instantaneous loss calculation with Smith matrices

Sections 4.2 and 4.3 took advantage of the fact that, for a given microwave drive field and a steady state magnetization response, the time average of the internal energy will be constant.

Consequently, by the rule "power in = power out", the time averaged loss is equal to the time averaged microwave input power. The time averaged loss is then obtained as the time average of the input power. This method cannot give the instantaneous, time-dependent loss power, because the internal energy does vary with time and has a nonzero time derivative.

From the equations of motion in the Smith matrix form, however, the instantaneous loss can derived in a straightforward way. This is the goal of this section. As an application, the loss is then calculated for the five damping models developed in Chapter 3.

The fundamental equation to calculate the instantaneous loss is based on the same energy balance argument that has been used several times before in this chapter. Microwave power is fed into the sample by an applied microwave field transverse to a static applied field. One part of the input power $P_{in}(t)$ increases the internal magnetic energy $U_{\text{int}}(t)$ in the sample, the other part is dissipated and turned into heat as loss power $P_{loss}(t)$. The instantaneous energy balance may be written as

$$P_{in}(t) = \frac{dU_{pot}(t)}{dt} + P_{loss}(t). \tag{4.34}$$

From this equation, the loss is obtained as

$$P_{loss}(t) = P_{in}(t) - \frac{dU_{pot}(t)}{dt}. \tag{4.35}$$

The instantaneous input power is given by the formula developed in Chapters 2 and 3,

$$P_{in}(t) = \mathbf{h}_{ext}(t) \cdot \frac{d\mathbf{m}(t)}{dt}. \tag{4.36}$$

The applied microwave field $\mathbf{h}_{ext}(t)$ is eliminated from this equation by means of the equation of motion in Smith matrix form,

$$\left(\vec{\mathbf{G}} + \vec{\mathbf{D}}\right) \cdot \frac{d\mathbf{m}(t)}{dt} + \vec{\mathbf{K}} \cdot \mathbf{m}(t) = \mathbf{h}_{ext}(t). \tag{4.37}$$

Substitution of $\mathbf{h}_{ext}(t)$ into Eq. (4.36) gives the input power

$$P_{in}(t)=\left[\left(\vec{\mathbf{D}}+\vec{\mathbf{G}}\right)\frac{d\mathbf{m}(t)}{dt}+\vec{\mathbf{K}}\mathbf{m}(t)\right]\cdot\frac{d\mathbf{m}(t)}{dt}$$

$$= \left[\frac{d\mathbf{m}(t)}{dt}\right]^T\vec{\mathbf{D}}\frac{d\mathbf{m}(t)}{dt}+\left[\frac{d\mathbf{m}(t)}{dt}\right]^T\vec{\mathbf{G}}\frac{d\mathbf{m}(t)}{dt} \tag{4.38}$$

$$+\left[\frac{d\mathbf{m}(t)}{dt}\right]^T\vec{\mathbf{K}}\mathbf{m}(t).$$

Recall from Chapter 2 the matrix identity, $\mathbf{x}^T\vec{\mathbf{A}}^{antisym}\mathbf{x}=0$. This identity is true for any anti-symmetric matrix $\vec{\mathbf{A}}^{antisym}$ and any compatible column vector $\mathbf{x}$. Since the gyroscopic matrix $\vec{\mathbf{G}}$ is anti-symmetric, Eq. (4.38) for the input power simplifies to

$$P_{in}(t)=\left[\frac{d\mathbf{m}(t)}{dt}\right]^T\vec{\mathbf{D}}^{sym}\frac{d\mathbf{m}(t)}{dt}+\left[\frac{d\mathbf{m}(t)}{dt}\right]^T\vec{\mathbf{K}}\mathbf{m}(t), \tag{4.39}$$

where $\vec{\mathbf{D}}^{sym}=\vec{\mathbf{D}}-\vec{\mathbf{D}}^{antisym}$ separates out the symmetric part of the damping matrix $\vec{\mathbf{D}}$.

Recall from the review in Section 4.4 that the potential energy can be written as a quadratic form according to

$$U_{pot}(t)=\frac{1}{2}\left[\mathbf{m}(t)\right]^T\vec{\mathbf{K}}^{sym}\left[\mathbf{m}(t)\right]. \tag{4.40}$$

The time rate of change of the internal energy, by a generalization of the product rule for derivatives, is then given as

$$\frac{dU_{pot}(t)}{dt}=\left[\frac{d\mathbf{m}(t)}{dt}\right]^T\vec{\mathbf{K}}^{sym}\left[\mathbf{m}(t)\right]. \tag{4.41}$$

The instantaneous loss is now calculated by the energy balance equation (4.35), as the difference

between the input power from Eq. (4.39) and the rate of change of the internal energy in Eq. (4.41). The result is,

$$P_{loss}(t) = P_{in}(t) - \frac{dU_{pot}(t)}{dt}$$

$$= \left[\frac{d\mathbf{m}(t)}{dt}\right]^T \vec{\vec{\mathbf{D}}}^{sym} \frac{d\mathbf{m}(t)}{dt} + \left[\frac{d\mathbf{m}(t)}{dt}\right]^T \vec{\vec{\mathbf{K}}}^{antisym} \mathbf{m}(t). \tag{4.42}$$

This is an important result. The instantaneous power loss $P_{loss}(t)$ has two terms: one term for the symmetric part of the damping matrix and the other term for the anti-symmetric part of the stiffness matrix. Table 4-2 gives the matrices $\vec{\vec{\mathbf{D}}}^{sym}$ and $\vec{\vec{\mathbf{K}}}^{antisym}$ for the five phenomenological damping models that are described in Chapter 3. This table is derived from Table 3-3 in Chapter 3, which shows the full $\vec{\vec{\mathbf{D}}}$ and $\vec{\vec{\mathbf{K}}}$ matrices for the five phenomenological damping models. Note that four of the models, LL, COT, G, and MBB, have $\vec{\vec{\mathbf{K}}}^{antisym} = \mathbf{0}$, and all of the loss derives from $\vec{\vec{\mathbf{D}}}^{sym}$. In contrast, for the BB model, one has $\vec{\vec{\mathbf{D}}}^{sym} = \mathbf{0}$ and nonzero $\vec{\vec{\mathbf{K}}}^{antisym}$. In Section 4.6, this will be shown to yield negative time-averaged loss for the BB model. As a consequence of the above, for the LL, COT, G, and MBB models the instantaneous loss contains only the $\vec{\vec{\mathbf{D}}}^{sym}$ term from Eq. (4.42),

$$P_{loss}(t) = \left[\frac{d\mathbf{m}(t)}{dt}\right]^T \vec{\vec{\mathbf{D}}}^{sym} \frac{d\mathbf{m}(t)}{dt} \tag{4.43}$$

Notice further that for these four damping models the $\vec{\vec{\mathbf{D}}}^{sym}$ matrix has the form of a purely diagonal matrix

$$\vec{\vec{\mathbf{D}}}^{sym} = \begin{pmatrix} d_x & 0 \\ 0 & d_y \end{pmatrix}. \tag{4.44}$$

Moreover, it is evident from Table 4-2 that the diagonal elements d_x and d_y are always positive.

Damping model	$\overleftrightarrow{\mathbf{D}}^{sym}$, **the symmetric part of the damping matrix**	$\overleftrightarrow{\mathbf{K}}^{antisym}$, **the anti-symmetric part of the stiffness matrix**
Landau-Lifshitz (L)	$\overleftrightarrow{\mathbf{D}}_{LL}^{sym} = \frac{1}{\lvert\gamma\rvert M_s}\begin{pmatrix} \frac{\alpha_{LL}}{1+\alpha_{LL}^2} & 0 \\ 0 & \frac{\alpha_{LL}}{1+\alpha_{LL}^2} \end{pmatrix}$	$\overleftrightarrow{\mathbf{K}}_{LL}^{antisym} = \overleftrightarrow{\mathbf{0}}$
Codrington-Olds-Torrey (COT)	$\overleftrightarrow{\mathbf{D}}_{COT}^{sym} = \frac{1}{\lvert\gamma\rvert M_s}\begin{pmatrix} \frac{\alpha_{COT}}{1+\alpha_{COT}^2} & 0 \\ 0 & \frac{\alpha_{COT}}{1+\alpha_{COT}^2} \end{pmatrix}$	$\overleftrightarrow{\mathbf{K}}_{COT}^{antisym} = \overleftrightarrow{\mathbf{0}}$
Gilbert (G)	$\overleftrightarrow{\mathbf{D}}_{G}^{sym} = \frac{1}{\lvert\gamma\rvert M_s}\begin{pmatrix} \alpha_G & 0 \\ 0 & \alpha_G \end{pmatrix}$	$\overleftrightarrow{\mathbf{K}}_{G}^{antisym} = \overleftrightarrow{\mathbf{0}}$
Bloch-Bloembergen (BB)	$\overleftrightarrow{\mathbf{D}}_{BB}^{sym} = \overleftrightarrow{\mathbf{0}}$	$\overleftrightarrow{\mathbf{K}}_{BB}^{antisym} = \frac{1}{\lvert\gamma\rvert M_s}\begin{pmatrix} 0 & -1/T_2 \\ 1/T_2 & 0 \end{pmatrix}$
Modified Bloch-Bloembergen (MBB)	$\overleftrightarrow{\mathbf{D}}_{MBB}^{sym} = \frac{1}{\lvert\gamma\rvert M_s}\frac{\lambda_{MBB}}{\omega_x\omega_y + \lambda_{MBB}^2}\begin{pmatrix} \omega_x & 0 \\ 0 & \omega_y \end{pmatrix}$	$\overleftrightarrow{\mathbf{K}}_{MBB}^{antisym} = \overleftrightarrow{\mathbf{0}}$

Table 4-2: Symmetric part of damping matrix and anti-symmetric part of stiffness matrix for five phenomenological damping models in the small signal limit.

The instantaneous loss for these models is

$$P_{loss}(t) = d_x\left[\frac{dm_x(t)}{dt}\right]^2 + d_y\left[\frac{dm_y(t)}{dt}\right]^2. \tag{4.45}$$

One can see, therefore, that the instantaneous loss is always positive for the LL, G, COT and MBB damping models. For the BB damping model, on the other hand, one has an instantaneous loss of the

form

$$P_{loss,BB}(t)=\left[\frac{d\mathbf{m}(t)}{dt}\right]^{T}\overline{\overline{\mathbf{K}}}_{BB}^{antisym}\left[\mathbf{m}(t)\right]=\frac{1}{|\gamma|M_s T_2}\left[m_x(t)\frac{dm_y}{dt}-m_y(t)\frac{dm_x}{dt}\right]. \tag{4.46}$$

This BB calculation gives an instantaneous loss that is not a quadratic form. This means that one cannot make any general statement about the sign of $P_{loss,BB}(t)$. The result for the instantaneous loss in Eq. (4.46), however, serves as a starting point for the calculation of time averaged loss. In the next section, it will be shown that the time averaged loss can be negative for BB damping under certain circumstances.

4.6 Time averaged loss calculation with Smith matrices

In the last section, the instantaneous loss was calculated from a basic energy balance approach, based on the equations of motion in Smith matrix form. The instantaneous loss was shown always to be positive for the LL, G, COT and MBB damping models. For the BB damping model the sign of the instantaneous loss could not be determined in a simple way. In this section, the time averaged loss is derived from the instantaneous loss formulae developed above with the method of complex amplitudes. For BB damping, the time averaged loss proves to be negative for an anti-Larmor polarized magnetization response. Recall that this negative loss result for BB damping was obtained in Sec. 4.2 from a susceptibility tensor analysis, and in Sec. 4.3 by showing that the magnetization response leads the applied anti-Larmor field instead of lagging it. This negative loss result for BB damping is shown here in a more general way with much less computational effort by use of simple matrix algebra.

The time averaged loss is easily obtained from the instantaneous loss in Eq. (4.46) from a complex amplitude representation of the magnetization response.

$$\mathbf{m}(t) = \mathrm{Re}\left(\mathbf{m}_0 e^{i\omega t}\right) = \frac{1}{2}\left(\mathbf{m}_0 e^{i\omega t} + \mathbf{m}_0^* e^{-i\omega t}\right). \tag{4.47}$$

This yields the time derivative of the magnetization as

$$\frac{d\mathbf{m}(t)}{dt} = \frac{i\omega}{2}\left(\mathbf{m}_0 e^{i\omega t} - \mathbf{m}_0^* e^{-i\omega t}\right). \tag{4.48}$$

From the general form for $P_{loss}(t)$ developed above in Eq. (4.42), one then has

$$\begin{aligned}
P_{loss}(t) = &-\frac{\omega^2}{4}\left(\mathbf{m}_0 e^{i\omega t} - \mathbf{m}_0^* e^{-i\omega t}\right)^T \overleftrightarrow{\mathbf{D}}^{sym}\left(\mathbf{m}_0 e^{i\omega t} - \mathbf{m}_0^* e^{-i\omega t}\right) \\
&+ i\frac{\omega}{2}\left(\mathbf{m}_0 e^{i\omega t} - \mathbf{m}_0^* e^{-i\omega t}\right)^T \overleftrightarrow{\mathbf{K}}^{antisym}\left(\mathbf{m}_0 e^{i\omega t} + \mathbf{m}_0^* e^{-i\omega t}\right) \\
= &-\frac{\omega^2}{4}\left[-\left(\mathbf{m}_0\right)^T \overleftrightarrow{\mathbf{D}}^{sym}\mathbf{m}_0^* - \left(\mathbf{m}_0^*\right)^T \overleftrightarrow{\mathbf{D}}^{sym}\mathbf{m}_0\right] \\
&-\frac{\omega^2}{4}\left[\left(\mathbf{m}_0\right)^T \overleftrightarrow{\mathbf{D}}^{sym}\mathbf{m}_0 e^{2i\omega t} + \left(\mathbf{m}_0^*\right)^T \overleftrightarrow{\mathbf{D}}^{sym}\mathbf{m}_0^* e^{-2i\omega t}\right] \\
&+ i\frac{\omega}{2}\left[\left(\mathbf{m}_0\right)^T \overleftrightarrow{\mathbf{K}}^{antisym}\mathbf{m}_0^* - \left(\mathbf{m}_0^*\right)^T \overleftrightarrow{\mathbf{K}}^{antisym}\mathbf{m}_0\right] \\
&+ i\frac{\omega}{2}\left[\left(\mathbf{m}_0\right)^T \overleftrightarrow{\mathbf{K}}^{antisym}\mathbf{m}_0 e^{2i\omega t} - \left(\mathbf{m}_0^*\right)^T \overleftrightarrow{\mathbf{K}}^{antisym}\mathbf{m}_0^* e^{-2i\omega t}\right]
\end{aligned} \tag{4.49}$$

While this expression looks tedious, the fact that the time average of any surviving harmonic term is zero leads to

$$\left\langle P_{loss}(t)\right\rangle_{\substack{time\\average}} = -\frac{\omega^2}{4}\left[-(\mathbf{m}_0)^T\,\vec{\vec{\mathbf{D}}}^{sym}\,\mathbf{m}_0^* - (\mathbf{m}_0^*)^T\,\vec{\vec{\mathbf{D}}}^{sym}\,\mathbf{m}_0\right] + i\frac{\omega}{2}\left[(\mathbf{m}_0)^T\,\vec{\vec{\mathbf{K}}}^{antisym}\,\mathbf{m}_0^* - (\mathbf{m}_0^*)^T\,\vec{\vec{\mathbf{K}}}^{antisym}\,\mathbf{m}_0\right]. \tag{4.50}$$

Even this expression simplifies greatly. Recall that the transpose of a 1×1 matrix is the matrix itself. This allows one to write

$$\begin{aligned} -(\mathbf{m}_0^*)^T\,\vec{\vec{\mathbf{D}}}^{sym}(\mathbf{m}_0) &= -\left[(\mathbf{m}_0^*)^T\,\vec{\vec{\mathbf{D}}}^{sym}(\mathbf{m}_0)\right]^T \\ &= -(\mathbf{m}_0)^T\left(\vec{\vec{\mathbf{D}}}^{sym}\right)^T(\mathbf{m}_0^*) \\ &= -(\mathbf{m}_0)^T\,\vec{\vec{\mathbf{D}}}^{sym}(\mathbf{m}_0^*). \end{aligned} \tag{4.51}$$

In the last step, the symmetry of the matrix $\vec{\vec{\mathbf{D}}}^{sym}$ was used. A symmetric matrix is also its own transpose. It follows that the two terms in the first bracket in Eq. (4.50) are equal. By a similar argument, the two terms in the second bracket are equal as well.

$$\begin{aligned} -(\mathbf{m}_0^*)^T\,\vec{\vec{\mathbf{K}}}^{antisym}\,\mathbf{m}_0 &= -\left[(\mathbf{m}_0^*)^T\,\vec{\vec{\mathbf{K}}}^{antisym}\,\mathbf{m}_0\right]^T \\ &= -(\mathbf{m}_0)^T\left(\vec{\vec{\mathbf{K}}}^{antisym}\right)^T\mathbf{m}_0^* \\ &= (\mathbf{m}_0)^T\,\vec{\vec{\mathbf{K}}}^{antisym}\,\mathbf{m}_0^*. \end{aligned} \tag{4.52}$$

In the last step the anti-symmetry of the matrix $\vec{\vec{\mathbf{K}}}^{antisym}$ was used. The time averaged loss in Eq. (4.50) now simplifies to

$$\begin{aligned} \left\langle P_{loss}(t)\right\rangle_{\substack{time\\average}} &= \frac{\omega^2}{2}[\mathbf{m}_0]^T\,\vec{\vec{\mathbf{D}}}^{sym}\left[\mathbf{m}_0^*\right] + i\omega[\mathbf{m}_0]^T\,\vec{\vec{\mathbf{K}}}^{antisym}\left[\mathbf{m}_0^*\right] \\ &= \omega[\mathbf{m}_0]^T\left[\frac{\omega}{2}\vec{\vec{\mathbf{D}}}^{sym} + i\vec{\vec{\mathbf{K}}}^{antisym}\right]\left[\mathbf{m}_0^*\right]. \end{aligned} \tag{4.53}$$

In this formula, the time averaged loss has been expressed in terms of the matrices $\vec{\vec{\mathbf{D}}}^{sym}$, $\vec{\vec{\mathbf{K}}}^{antisym}$ and

the complex magnetization response amplitude vector $\mathbf{m}_0$. This result allows for the easy examination of positive or negative loss. First, for the loss to be positive for small driving frequencies in the limit $\omega \to 0$, it is required that

$$(\mathbf{m}_0)^T \left(i\overleftrightarrow{\mathbf{K}}^{antisym}\right)\mathbf{m}_0^* \geq 0, \tag{4.54}$$

for all possible magnetization responses. That means that both eigenvalues of the matrix $i\overleftrightarrow{\mathbf{K}}^{antisym}$ must be nonnegative real numbers. In mathematical terms, such a matrix is called positive semidefinite. As an anti-symmetric 2×2 matrix, $\overleftrightarrow{\mathbf{K}}^{antisym}$ has the form

$$\overleftrightarrow{\mathbf{K}}^{antisym} = \begin{pmatrix} 0 & a \\ -a & 0 \end{pmatrix}, \tag{4.55}$$

where a is some suitable real number, not necessarily positive. The eigenvalues of the matrix

$$i\overleftrightarrow{\mathbf{K}}^{antisym} = \begin{pmatrix} 0 & ia \\ -ia & 0 \end{pmatrix} \tag{4.56}$$

are $+a$ and $-a$. For both of these eigenvalues to be nonnegative, the real number a must be zero. That means for a positive time averaged loss it is necessary that the matrix $\overleftrightarrow{\mathbf{K}}^{antisym}$ vanishes. Indeed, this is the case for the LL, COT, G, and MBB models, but is not the case for BB damping. For LL, COT, G, and MBB damping, one then has

$$\left\langle P_{loss}(t)\right\rangle_{\substack{time \\ average}} = \frac{\omega^2}{2}(\mathbf{m}_0)^T \overleftrightarrow{\mathbf{D}}^{sym}\mathbf{m}_0^*. \tag{4.57}$$

For a positive time averaged loss, one can see from this form that the matrix $\overleftrightarrow{\mathbf{D}}^{sym}$ must be positive definite. It is clear, therefore, that the combination of two conditions is sufficient and necessary for positive time averaged loss: (1) $\overleftrightarrow{\mathbf{K}}$ must be symmetric, and (2) $\overleftrightarrow{\mathbf{D}}^{sym}$ must be positive definite.

4.7 Summary

In this chapter both instantaneous loss and time averaged loss were given in terms of the Smith matrices, which are easily extracted from the equations of motion in the small signal limit. Required for a physically reasonable damping model, that yields positive loss for all driving fields, are a positive definite symmetric part of the damping matrix and a symmetric and positive definite stiffness matrix. These conditions are sufficient and necessary for positive time averaged loss and also for positive instantaneous loss. While the instantaneous loss is given by

$$P_{loss}(t) = \left[\frac{d\mathbf{m}(t)}{dt}\right]^T \vec{\mathbf{D}}^{sym} \frac{d\mathbf{m}(t)}{dt}, \tag{4.58}$$

the time averaged loss is given by

$$\left\langle P_{loss}(t)\right\rangle_{\substack{time\\average}} = \frac{\omega^2}{2}(\mathbf{m}_0)^T \vec{\mathbf{D}}^{sym} \mathbf{m}_0^*. \tag{4.59}$$

Here is the complex amplitude vector of the steady state magnetization response to an elliptically polarized driving field. In these matrix equations the loss is expressed in terms of the magnetization response, and not in terms of the driving field. In this way both instantaneous and time averaged loss are determined solely by the symmetric part of the damping matrix. In the next chapter it will become clear that the symmetric part of the damping matrix plays an important role also in the analysis of thermal magnetic noise with the help of the fluctuation-dissipation theorem.

Chapter 5

The fluctuation-dissipation theorem, applied to magnetic damping

Table of contents:

5.1 Introduction

Consider a closed, macroscopic system in equilibrium, described by certain macroscopic, time-dependent, physical quantities, which will be termed the state variables. For a closed system equilibrium, the time average of each system variable remains constant in time at the equilibrium value. Due to thermal motion, however, the state variables perform small fluctuations about these equilibrium points. The time averages are taken over a period of time that is large compared with the time scale of the fluctuations.

The microscopic fluctuations of the state variables can be viewed as the response of the system to thermally generated and microscopic random driving forces. Since the system is closed, there is no macroscopic, externally applied driving force. Chapters 2 and 3 presented the equations of motion that model the macroscopic response of a system to a macroscopic, externally applied driving force. The same equations can be used to describe the microscopic response to the microscopic and thermally generated random driving force.

This chapter is concerned with both the statistical and dynamical analysis of the random driving force and the corresponding response for a system in equilibrium. In statistical terms, this response is described in terms of the means, variances, covariances, and correlations of the system variables. Using these concepts, this chapter focuses on five questions:

a) How are the components of the random driving force correlated?

b) How are the components of the system response correlated?

c) What are the spectral densities of the driving force and the system response components?

d) How can the results of a) to c) be applied to the damped magnetic precession?

e) What are the predictions of the fluctuation-dissipation theorem for the phenomenological damping models introduced in chapter 3, and are these predictions reasonable or unreasonable?

Here is the roadmap for the chapter:

In Section 5.2, a statistical approach is used to characterize the state variables and their mutual

relationships. To this end, the state variables are considered not as known functions of time, but as random variables. The mean of a state variable is defined as its ensemble average, that is the average of a large number of measurements of the variable in identically prepared systems. The probability distributions of the state variables and their relationships can be described in terms of three sets of quantities:

a) the mean of each variable, that is, the ensemble averages of these quantities,

b) the variance of each variable, that is the "width of the spread" in these quantities about their mean values,

c) the mutual covariance of each pair of variables, that is, their correlation.

The means, variances, and covariances of a set of random variables can be calculated explicitly when their joint probability distribution is known. The distribution is approximated by a multivariate Gaussian. The parameter matrix of the Gaussian distribution is obtained by a Taylor expansion of the internal energy of the system to second order about the equilibrium. This section features a proof of the well-known theorem that the covariance matrix of a multivariate Gaussian distribution is the inverse of its parameter matrix. This fact plays a central role in the proof of the classical version of the fluctuation-dissipation theorem developed in Section 5.3.

In contrast to the statistical treatment in Section 5.2, Section 5.3 describes the system as a dynamical system, modeled by a system of ordinary differential equations for time-dependent state variables. In the equations of motion, the fluctuations of the state variables are modeled as the response to a microscopic random driving force. In the small signal limit, the equations of motion are linear differential equations that can be solved explicitly for the time-dependent system response in terms of the random driving forces. From this solution, the correlations of the random driving force components are calculated. The result is a special case of the fluctuation-dissipation theorem. It is shown that the correlation matrix of the random driving force components is a multiple of the symmetric part of the damping matrix.

In Section 5.4, the spectral resolution of the noise power is calculated by taking the Fourier

transform of the correlations of the random force components. The primary tool for this procedure is the Wiener-Khinchine theorem. By a linear transformation, the power spectral densities are obtained also for the components of the system response. As an application, the power spectral densities of the random driving field components and of the magnetization components are given for each of the five damping models from Chapter 3.

Section 5.5 summarizes the results of the chapter.

5.2 Statistical description of equilibrium systems

5.2.a System variables and their means, variances and covariances

Consider a closed system in macroscopic equilibrium, described by n time-dependent physical quantities denoted as $x_1(t),...,x_n(t)$. These quantities are called state variables. Since the system is in equilibrium and no external forces are applied, the time averages $x_1^*,...,x_n^*$ of the state variables remain constant in time. These time averages are taken over a time period that is large compared with the time scale of the fluctuations of the state variables about their equilibrium values.

For the statistical treatment in this section, however, the state variables will be considered not as functions of time $x_1(t),...,x_n(t)$, but as time-independent random variables $X_1,...,X_n$. In equilibrium, the mean $\langle X_i \rangle$ of the random variable X_i coincides with the time average x_i^* of the corresponding system variable $x_i(t)$. Recall from basic thermodynamics that the mean of a quantity is defined as its ensemble average over a large number of identically prepared systems.

The joint probability distribution of the n system variables can be described in terms of means, variances and covariances. The mean $\langle X_i \rangle$ of a random variable X_i is the ensemble average, as already explained. The variance of X_i is the mean of the squared deviation from the mean,

$$Var(X_i) = \left\langle \left[X_i - \langle X_i \rangle \right]^2 \right\rangle . \tag{5.1}$$

Because of the linearity of the mean the variance can be written as

$$\begin{aligned} Var(X_i) &= \left\langle \left[X_i - \langle X_i \rangle \right]^2 \right\rangle \\ &= \left\langle X_i^2 - 2X_i \langle X_i \rangle + \langle X_i \rangle^2 \right\rangle \\ &= \left\langle X_i^2 \right\rangle - 2\langle X_i \rangle^2 + \langle X_i \rangle^2 \\ &= \left\langle X_i^2 \right\rangle - \langle X_i \rangle^2 . \end{aligned} \tag{5.2}$$

This definition may be expanded to include two random variables, which leads to the concept of covariance. The covariance of two random variables is defined as the mean of the product of their deviations from the mean,

$$Cov(X_i, X_j) = \left\langle \left(X_i - \langle X_i \rangle \right) \cdot \left(X_j - \langle X_j \rangle \right) \right\rangle . \tag{5.3}$$

The covariance is a statistical measure of the correlation between two random variables. If the two random variables are completely independent, their covariance will be zero. When each covariance $Cov(X_i, X_j)$ is entered into the i-th row and j-th column of a matrix, one obtains the covariance matrix $\overleftrightarrow{\mathbf{Cov}}(\mathbf{X})$. This matrix is symmetric, by definition. The diagonal elements of the covariance matrix are the variances. That is,

$$Cov(X_i, X_i) = \left\langle \left(X_i - \langle X_i \rangle \right)^2 \right\rangle = Var(X_i) . \tag{5.4}$$

The variances and covariances of a set of random variables can be calculated explicitly, if their probability distribution is known. The next section will approximate the distribution of the system variables in a closed equilibrium system by a Gaussian distribution.

5.2.b Gaussian distribution of system variables

The probability distribution of n system variables can be expressed in terms of a joint distribution function $w(\mathbf{x})$. Then the probability, that the system is found in a state in the intervals $a_1 \le x_1 \le b_1$, $a_2 \le x_2 \le b_2$, ..., $a_n \le x_n \le b_n$, is given by the n-dimensional integral

$$P = \int_{a_1}^{b_1}\int_{a_2}^{b_2}\ldots\int_{a_n}^{b_n} w(\mathbf{x})dx_1dx_2\ldots dx_n . \tag{5.5}$$

Here $\mathbf{x} = (x_1,\ldots,x_n)^T$ is a vector of values $x_1,\ldots,x_n$ of the state variables $X_1,\ldots,X_n$. Of course, the probability that the system is found in any state must be 1, which leads to the normalization condition

$$\int_{-\infty}^{\infty}\int_{-\infty}^{\infty}\ldots\int_{-\infty}^{\infty} w(\mathbf{x})dx_1dx_2\ldots dx_n = 1. \tag{5.6}$$

For many physical applications, the distribution of system variables obeys a Boltzmann distribution, of the form

$$w(\mathbf{x}) = A\exp\left[-\frac{U_{pot}(\mathbf{x})}{k_BT}\right]. \tag{5.7}$$

Here $U_{pot}(x_1,\ldots,x_n)$ is the internal energy of the system, k_B is Boltzmann's constant, T is the temperature, and A is a positive factor to fulfill the normalization condition in Eq. (5.6). Note that the potential energy is minimized if the system variables take their respective mean values, that is for $\mathbf{x} = \mathbf{x}^*$. It follows that $\nabla U_{pot}(\mathbf{x}^*) = 0$, and, by Taylor expansion up to second order, that

$$
\begin{aligned}
& w(\mathbf{x}) \\
& \approx A\exp\left[\frac{-U_{pot}(\mathbf{x}^*)-\nabla U_{pot}(\mathbf{x}^*)\cdot(\mathbf{x}-\mathbf{x}^*)-\frac{1}{2}\sum_{i=1}^{n}\sum_{k=1}^{n}\left(\frac{\partial^2 U_{pot}}{\partial x_i \partial x_k}\right)\Big|_{\mathbf{x}=\mathbf{x}^*}(x_i-x_i^*)(x_k-x_k^*)}{k_B T}\right] \\
& = A\exp\left[-\frac{U_{pot}(\mathbf{x}^*)}{k_B T}\right]\cdot\exp\left[-\frac{\sum_{i=1}^{n}\sum_{k=1}^{n}\left(\frac{\partial^2 U_{pot}}{\partial x_i \partial x_k}\right)\Big|_{\mathbf{x}=\mathbf{x}^*}(x_i-x_i^*)(x_k-x_k^*)}{2k_B T}\right].
\end{aligned}
\tag{5.8}
$$

With the abbreviation,

$$
\beta_{ik}=\frac{\left(\frac{\partial^2 U_{pot}}{\partial x_i \partial x_k}\right)\Big|_{\mathbf{x}=\mathbf{x}^*}}{k_B T},
\tag{5.9}
$$

the distribution function becomes,

$$
w(\mathbf{x})=A\exp\left[-\frac{U_{pot}(\mathbf{x}^*)}{k_B T}\right]\cdot\exp\left[-\frac{1}{2}\sum_{i=1}^{n}\sum_{k=1}^{n}\beta_{ik}(x_i-x_i^*)(x_k-x_k^*)\right].
\tag{5.10}
$$

The coefficients β_{ik} form a symmetric $n\times n$ matrix $\ddot{\boldsymbol{\beta}}$. In matrix notation, the distribution function takes the compact form,

$$
\begin{aligned}
w(\mathbf{x}) &= A\exp\left[-\frac{U_{pot}(\mathbf{x}^*)}{k_B T}\right]\cdot\exp\left[-\frac{1}{2}(\mathbf{x}-\mathbf{x}^*)^T\ddot{\boldsymbol{\beta}}(\mathbf{x}-\mathbf{x}^*)\right] \\
&= A'\exp\left[-\frac{1}{2}(\mathbf{x}-\mathbf{x}^*)^T\ddot{\boldsymbol{\beta}}(\mathbf{x}-\mathbf{x}^*)\right].
\end{aligned}
\tag{5.11}
$$

To determine the value of the normalization factor A', one uses the definite integral result (e.g. in Gradshtein/Ryshik [1984]),

$$
\int_{-\infty}^{\infty}\cdots\int_{-\infty}^{\infty}\exp\left[-\frac{1}{2}(\mathbf{x}-\mathbf{x}^*)^T\ddot{\boldsymbol{\beta}}(\mathbf{x}-\mathbf{x}^*)\right]dx_1\ldots dx_n=\frac{(2\pi)^{n/2}}{\sqrt{\det\ddot{\boldsymbol{\beta}}}},
\tag{5.12}
$$

For this formula the positive definiteness of the matrix $\ddot{\boldsymbol{\beta}}$ is a prerequisite. Since the potential energy $U_{pot}(\mathbf{x})$ has a minimum at the equilibrium $\mathbf{x}=\mathbf{x}^*$, the matrix of second partial derivatives of $U_{pot}(\mathbf{x})$ at $\mathbf{x}=\mathbf{x}^*$ is positive definite, and with Eq. (5.9) the matrix $\ddot{\boldsymbol{\beta}}$ is positive definite as well. From Eqs. (5.6), (5.11) and (5.12), the probability distribution is found to be

$$w(\mathbf{x})=\frac{\sqrt{\det\ddot{\boldsymbol{\beta}}}}{(2\pi)^{n/2}}\cdot\exp\left[-\frac{1}{2}(\mathbf{x}-\mathbf{x}^*)^T\ddot{\boldsymbol{\beta}}(\mathbf{x}-\mathbf{x}^*)\right]. \tag{5.13}$$

This is a multivariate Gaussian distribution with parameter matrix $\ddot{\boldsymbol{\beta}}$. Remember that this distribution is an approximation, obtained by Taylor expansion of the potential energy, for a system performing small fluctuations about the equilibrium.

In the magnetic precession system with two degrees of freedom, as presented in the first four chapters of this thesis, the volume density of the potential energy, u_{pot}, was expressed in terms of a stiffness matrix $\ddot{\mathbf{K}}$ in the form,

$$u_{pot}(\mathbf{m})=\frac{1}{2}\mathbf{m}^T\ddot{\mathbf{K}}\mathbf{m}. \tag{5.14}$$

In the lossless case, and for all damping models except BB, the stiffness matrix was shown to be the same as the matrix of second partial derivatives of u_{pot},

$$\left(\ddot{\mathbf{K}}\right)_{ik}=\left.\frac{\partial^2 u_{pot}}{\partial m_i\partial m_k}\right|_{\mathbf{m}=\mathbf{0}}=\left.\frac{1}{V}\frac{\partial^2 U_{pot}}{\partial m_i\partial m_k}\right|_{\mathbf{m}=\mathbf{0}}, \tag{5.15}$$

where V is the sample volume. By comparison of Eqs. (5.9)and (5.15), one sees that the Gaussian parameter matrix for a magnetic system in the small signal limit is related to the stiffness matrix by the linear relation

$$\left(\ddot{\boldsymbol{\beta}}\right)_{ik} = \frac{\left(\dfrac{\partial^2 U_{pot}}{\partial x_i \partial x_k}\right)\Big|_{\mathbf{x}=\mathbf{x}^*}}{k_B T} = \frac{V}{k_B T}\left(\frac{\partial^2 u_{pot}}{\partial x_i \partial x_k}\right)\Big|_{\mathbf{x}=\mathbf{x}^*} = \frac{V}{k_B T}\left(\vec{\mathbf{K}}\right)_{ik}. \tag{5.16}$$

This relation will be used in Section 5.4, when the fluctuation-dissipation result of this chapter is applied to the various phenomenological models of magnetic damping.

The Gaussian joint distribution function $w(\mathbf{x})$ can be used to calculate explicitly the two quantities from Section 5.2.a that describe the statistical relationship of the system variables in a closed equilibrium system. Recall that these descriptive quantities are the variances and covariances. Arranged in matrix form, they form the covariance matrix. The goal of this section is to show that the covariance matrix is the inverse of the Gaussian parameter matrix $\ddot{\boldsymbol{\beta}}$. Following the outline in Landau-Lifshitz [1958], recall that the statistical mean of any function $f(\mathbf{X})$ of the n state variables is given by

$$\left\langle f(\mathbf{X})\right\rangle = \int_{-\infty}^{\infty}\cdots\int_{-\infty}^{\infty} f(\mathbf{x})w(\mathbf{x})dx_1\ldots dx_n. \tag{5.17}$$

In particular, the mean of the i-th random variable can be expressed in the form

$$x_i^* = \langle X_i\rangle = \int_{-\infty}^{\infty}\cdots\int_{-\infty}^{\infty} x_i w(\mathbf{x})dx_1\ldots dx_n. \tag{5.18}$$

With the Gaussian distribution function from the last section, this equation becomes,

$$x_i^* = \frac{\sqrt{\det\ddot{\boldsymbol{\beta}}}}{(2\pi)^{n/2}}\int_{-\infty}^{\infty}\cdots\int_{-\infty}^{\infty} x_i \exp\left[-\frac{1}{2}\left(\mathbf{x}-\mathbf{x}^*\right)^T\ddot{\boldsymbol{\beta}}\left(\mathbf{x}-\mathbf{x}^*\right)\right]dx_1\ldots dx_n \tag{5.19}$$

Now on both sides of this equation, take the partial derivative with respect to the mean x_k^* of the k-th system variable, for any $k = 1,\ldots,n$. On the left hand side one obtains the Kronecker delta δ_{ik}. On the right hand side the partial differentiation is carried out under the integral. In generalization of the

product rule of differentiation, one has the formula $\nabla\left(\mathbf{x}^T \vec{\vec{\mathbf{A}}}\mathbf{x}\right) = 2\vec{\vec{\mathbf{A}}}\mathbf{x}$ for any *symmetric* square matrix $\vec{\vec{\mathbf{A}}}$ and any compatible column vector $\mathbf{x}$. Since the matrix $\vec{\vec{\boldsymbol{\beta}}}$ is symmetric, the differentiation of Eq. (5.19) with respect to x_k^* yields,

$$\begin{aligned}\delta_{ik} &= \frac{\sqrt{\det\vec{\vec{\boldsymbol{\beta}}}}}{(2\pi)^{n/2}}\int_{-\infty}^{\infty}\cdots\int_{-\infty}^{\infty} x_i\sum_{j=1}^{n}\beta_{jk}\left(x_j - x_j^*\right)\exp\left[-\frac{1}{2}\left(\mathbf{x}-\mathbf{x}^*\right)^T\vec{\vec{\boldsymbol{\beta}}}\left(\mathbf{x}-\mathbf{x}^*\right)\right]dx_1\ldots dx_n \\ &= \int_{-\infty}^{\infty}\cdots\int_{-\infty}^{\infty} x_i\sum_{j=1}^{n}\beta_{jk}\left(x_j - x_j^*\right)w(x_1,\ldots,x_n)dx_1\ldots dx_n \\ &= \left\langle X_i\sum_{j=1}^{n}\beta_{jk}\left[X_j - x_j^*\right]\right\rangle = \sum_{j=1}^{n}\beta_{jk}\left\langle X_i\left[X_j - x_j^*\right]\right\rangle\end{aligned} \tag{5.20}$$

The last step is justified by the linearity of the mean. Also by the linearity of the mean, one has,

$$\begin{aligned}\left\langle\left[X_i - x_i^*\right]\left[X_j - x_j^*\right]\right\rangle &= \left\langle X_i\left[X_j - x_j^*\right]\right\rangle - x_i^*\left\langle X_j - x_j^*\right\rangle \\ &= \left\langle X_i\left[X_j - x_j^*\right]\right\rangle - x_i^*\left(x_j^* - x_j^*\right) \\ &= \left\langle X_i\left[X_j - x_j^*\right]\right\rangle.\end{aligned} \tag{5.21}$$

With this identity, Eq. (5.20) can be written as

$$\delta_{ik} = \sum_{j=1}^{n}\beta_{jk}\left\langle\left[X_i - x_i^*\right]\left[X_j - x_j^*\right]\right\rangle = \sum_{j=1}^{n}\beta_{jk}Cov\left(X_i, X_j\right). \tag{5.22}$$

The right side is the matrix element in the i-th row and the k-th column of the product of the covariance matrix $Cov(\mathbf{X})$ and the Gaussian parameter matrix $\vec{\vec{\boldsymbol{\beta}}}$. In matrix notation, Eq. (5.22) becomes,

$$\vec{\vec{\mathbf{I}}}_n = \overrightarrow{\mathbf{Cov}}(\mathbf{X})\cdot\vec{\vec{\boldsymbol{\beta}}}. \tag{5.23}$$

Here $\vec{\vec{\mathbf{I}}}_n$ is the nxn unit matrix. It follows that the covariance matrix is indeed the inverse of the Gaussian parameter matrix.

$$\overleftrightarrow{\mathbf{Cov}}(\mathbf{X}) = \ddot{\boldsymbol{\beta}}^{-1}. \tag{5.24}$$

This basic theorem result provides an important piece in the proof of a special case of the fluctuation-dissipation theorem in the next section. For n=1, Eq. (5.24) takes the simple form,

$$Var(X) = \frac{1}{\beta}. \tag{5.25}$$

In this case X is a single random variable with Gaussian distribution

$$w(x) = \sqrt{\frac{\beta}{2\pi}} \exp\left[-\frac{1}{2}\beta\left(x - x^*\right)^2 \right]. \tag{5.26}$$

When the parameter β is expressed as reciprocal of the variance according to Eq. (5.25), then the Gaussian distribution takes the familiar form,

$$\begin{aligned} w(x) &= \sqrt{\frac{1}{2\pi Var(X)}} \exp\left[-\frac{1}{2}\frac{\left(x - x^*\right)^2}{Var(X)} \right] \\ &= \sqrt{\frac{1}{2\pi\sigma^2}} \exp\left[-\frac{1}{2}\frac{\left(x - x^*\right)^2}{\sigma^2} \right], \end{aligned} \tag{5.27}$$

where $\sigma = \sqrt{Var(X)}$ is the standard deviation of X. In this way the result in Eq. (5.24) is the generalization of the familiar result in Eq. (5.25) to n dimensions.

5.3 Dynamics of thermal fluctuations in an equilibrium system

5.3.a Equations of motion with noise as random driving force

Section 5.2 explained that in a stable equilibrium, a closed system is in a state of minimum internal energy. This state is stationary in the sense that the mean values of the system variables

remain constant in time. Recall, however, that the system variables perform thermally generated, random motions about their equilibrium values. These random motions are called fluctuations, or noise. This section introduces the equations of motion for a closed system which undergoes small fluctuations about its equilibrium. This is done by adding a random force term in the equations of motion without noise.

Recall from Chapter 3 that the equations of motion of coupled harmonic oscillators near a stable equilibrium can be written in the Smith matrix form,

$$\left(\vec{\mathbf{G}}+\vec{\mathbf{D}}\right)\frac{d\mathbf{m}(t)}{dt}+\vec{\mathbf{K}}\mathbf{m}(t)=\mathbf{h}_{ext}(t). \tag{5.28}$$

Here $\mathbf{m}(t)$ is the system response to an external driving field $\mathbf{h}_{ext}(t)$. The stiffness of the system, or inverse static susceptibility, is given by the stiffness matrix $\vec{\mathbf{K}}$. The kinetic qualities of the system, such as its precession frequency and its decay rate, are determined by the stiffness matrix $\vec{\mathbf{K}}$, the gyroscopic matrix $\vec{\mathbf{G}}$ and the damping matrix $\vec{\mathbf{D}}$. The goal of this section is to prove that the correlation matrix of the random driving force components is a multiple of the damping matrix. This is a special case of the fluctuation-dissipation theorem.

In an undriven system without thermal noise, the driving field $\mathbf{h}_{ext}(t)$ is zero. In a system without externally applied driving force, but with thermal noise, the thermal noise can be modeled as a small random driving field $\mathbf{h}_{ext}^{(th)}(t)$. The superscript (th) stands for "thermal". In this way the equation of motion is a linear differential equation with a random driving field as inhomogeneity. Note that the Smith matrix form of the equations of motion is solved for the driving field. In contrast, when solving the equation of motion for the time derivative of the response, one obtains,

$$\frac{d\mathbf{m}(t)}{dt}=-\left(\vec{\mathbf{G}}+\vec{\mathbf{D}}\right)^{-1}\vec{\mathbf{K}}\mathbf{m}(t)+\left(\vec{\mathbf{G}}+\vec{\mathbf{D}}\right)^{-1}\mathbf{h}_{ext}^{(th)}(t). \tag{5.29}$$

In this equation, it is assumed that the matrix $\left(\vec{\mathbf{G}}+\vec{\mathbf{D}}\right)$ has an inverse. Since the damping matrix $\vec{\mathbf{D}}$ is

a small perturbation of the gyroscopic matrix $\vec{\vec{\mathbf{G}}}$, and the matrix $\vec{\vec{\mathbf{G}}}$ has an inverse, this assumption is fulfilled for all damping models. Following the notation in Landau-Lifshitz [1958], one defines a decay matrix

$$\vec{\vec{\lambda}} = \left(\vec{\vec{\mathbf{G}}} + \vec{\vec{\mathbf{D}}}\right)^{-1} \vec{\vec{\mathbf{K}}}, \tag{5.30}$$

and a driving term

$$\mathbf{y}(t) = \left(\vec{\vec{\mathbf{G}}} + \vec{\vec{\mathbf{D}}}\right)^{-1} \mathbf{h}_{ext}^{(th)}(t). \tag{5.31}$$

Then the equation of motion takes the form,

$$\frac{d\mathbf{m}(t)}{dt} = -\vec{\vec{\lambda}}\mathbf{m}(t) + \mathbf{y}(t). \tag{5.32}$$

Notice that with the relationship in Eq. (5.16), $\vec{\vec{\mathbf{K}}} = (k_B T / V)\vec{\vec{\boldsymbol{\beta}}}$, the linear transformation in Eq. (5.31) becomes,

$$\begin{aligned}
\mathbf{y}(t) &= \left(\vec{\vec{\mathbf{G}}} + \vec{\vec{\mathbf{D}}}\right)^{-1} \mathbf{h}_{ext}^{(th)}(t) \\
&= \vec{\vec{\lambda}}\vec{\vec{\mathbf{K}}}^{-1}\mathbf{h}_{ext}^{(th)}(t) \\
&= \vec{\vec{\lambda}}\left(\frac{V}{k_B T}\vec{\vec{\boldsymbol{\beta}}}^{-1}\right)\mathbf{h}_{ext}^{(th)}(t) \\
&= \frac{V}{k_B T}\vec{\vec{\lambda}}\vec{\vec{\boldsymbol{\beta}}}^{-1}\mathbf{h}_{ext}^{(th)}(t).
\end{aligned} \tag{5.33}$$

Instead of the original problem in Smith matrix form, now the transformed problem in Eq. (5.32) will be explicitly solved for the system response $\mathbf{m}(t)$ in terms of the driving term $\mathbf{y}(t)$. The transformed problem is a linear differential equation of first order with constant coefficients. Its general solution is the sum of the general solution of the homogeneous problem *without* the noise term, and any particular solution of the problem *with* the noise term. The homogeneous solution is given by

$$\mathbf{m}_{\text{hom}}(t) = \left[\exp\left(-\vec{\lambda}t\right)\right]\mathbf{u}. \tag{5.34}$$

Here $\mathbf{u}$ is an arbitrary column vector of length n. The expression $\exp\left(-\vec{\lambda}t\right)$ is actually an $n \times n$ matrix, given by the exponential series

$$\exp\left(-\vec{\lambda}t\right) = \sum_{n=0}^{\infty}\left(-\vec{\lambda}t\right)^n. \tag{5.35}$$

When the noise term $\mathbf{y}(t)$ is included, a particular solution $\mathbf{m}_p(t)$ of Eq. (5.32) can be found by the method of variation of constants. This is done with the approach

$$\mathbf{m}_p(t) = \left[\exp\left(-\vec{\lambda}t\right)\right]\mathbf{u}(t) \tag{5.36}$$

Now the $n \times 1$ column vector $\mathbf{u}(t)$ is an unknown function of time t. This function is found by inserting $\mathbf{m}_p(t)$ into the differential equation in Eq. (5.32). One obtains

$$-\vec{\lambda}\exp\left(-\vec{\lambda}t\right)\mathbf{u}(t) + \exp\left(-\vec{\lambda}t\right)\frac{d\mathbf{u}(t)}{dt} = -\vec{\lambda}\exp\left(-\vec{\lambda}t\right)\mathbf{u}(t) + \mathbf{y}(t). \tag{5.37}$$

The first terms on both sides of the equation are equal and cancel, and one obtains

$$\frac{d\mathbf{u}(t)}{dt} = \exp\left(\vec{\lambda}t\right)\mathbf{y}(t). \tag{5.38}$$

One solution for the unknown $\mathbf{u}(t)$ is,

$$\mathbf{u}(t) = \int_{-\infty}^{t}\exp\left(\vec{\lambda}\tau\right)\mathbf{y}(\tau)d\tau. \tag{5.39}$$

Insertion into Eq. (5.36). yields the particular solution for the system response,

$$\begin{aligned}\mathbf{m}_p(t) &= \exp\left(-\vec{\lambda}t\right)\mathbf{u}(t) \\ &= \exp\left(-\vec{\lambda}t\right)\int_{-\infty}^{t}\exp\left(\vec{\lambda}\tau\right)\mathbf{y}(\tau)d\tau \\ &= \int_{-\infty}^{t} e^{-\vec{\lambda}(t-\tau)}\mathbf{y}(\tau)d\tau\end{aligned} \tag{5.40}$$

The general solution is the sum of the homogeneous solution in Eq. (5.34) and the particular solution just found. Therefore,

$$\begin{aligned}\mathbf{m}(t) &= \mathbf{m}_{\text{hom}}(t)+\mathbf{m}_p(t) \\ &= \exp\left(-\vec{\lambda}t\right)\mathbf{u}+\int_{-\infty}^{t} e^{-\vec{\lambda}(t-\tau)}\mathbf{y}(\tau)d\tau.\end{aligned} \tag{5.41}$$

The first term decays exponentially to zero. Therefore, after a long time, the system response to the driving term $\mathbf{y}(t)$ is independent of its initial state at $t=0$, and is given by,

$$\mathbf{m}(t) = \int_{-\infty}^{t} e^{-\vec{\lambda}(t-\tau)}\mathbf{y}(\tau)d\tau\,. \tag{5.42}$$

This equation makes intuitive sense: The value of the response function at a certain time is the time integral over the driving force up to this time, where the driving force is weighted with an exponential decay factor.

5.3.b Correlations of field noise: a case of the fluctuation-dissipation theorem

The correlation between two time dependent quantities $m_i(t')$ and $m_k(t)$ for different times t and t' is defined as the mean value $\langle m_i(t')m_k(t)\rangle$ of their product. Notice that since the system is in equilibrium, the correlation $\langle m_i(t')m_k(t)\rangle$ depends only on the time difference $\tau = t'-t$ and can be written in terms of a correlation matrix,

$$\Phi_{ik}(t'-t) = \langle m_i(t')m_k(t)\rangle = \langle m_i(t'-t)m_k(0)\rangle. \tag{5.43}$$

The correlation matrix can be written in this way because the means $\langle m_k(t)\rangle$ are zero. Equivalently, the correlation matrix can be expressed in terms of the time difference $\tau = t'-t$,

$$\Phi_{ik}(\tau) = \langle m_i(\tau)m_k(0)\rangle. \tag{5.44}$$

When the time difference is set to zero, the correlation matrix $\langle m_i(\tau)m_k(0)\rangle$ goes over into the covariance matrix $\langle m_i(0)m_k(0)\rangle$. As explained in the previous section, the covariance matrix in an equilibrium system is constant in time, and is equal to the inverse of the Gaussian parameter matrix. In the following, correlation matrices of the form $\langle m_i(\tau_1)m_k(\tau_2)\rangle$ are written in dyadic product notation as $\langle \mathbf{m}(\tau_1)\mathbf{m}^T(\tau_2)\rangle$.

The first goal of this section is the calculation of the correlation matrix for the driving term $\mathbf{y}(t)$ in the equation of motion with noise. Recall that this equation was given in the last section as

$$\frac{d\mathbf{m}(t)}{dt} = -\ddot{\boldsymbol{\lambda}}\mathbf{m}(t) + \mathbf{y}(t), \tag{5.45}$$

and has the solution

$$\mathbf{m}(t) = \int_{-\infty}^{t} e^{-\ddot{\lambda}(t-\tau)}\mathbf{y}(\tau)d\tau. \tag{5.46}$$

The second goal is to use the result from the first goal to establish the correlation matrix for the physical random driving field $\mathbf{h}_{ext}^{(th)}(t)$, which is a linear transformation of the driving term $\mathbf{y}(t)$.

To start, insert the solution from Eq. (5.46) into the covariance matrix for the system response $\mathbf{m}(t)$. From the previous section it is known that this covariance matrix is constant in time, and is equal to the inverse $\boldsymbol{\beta}^{-1}$ of the Gaussian parameter matrix. In this way one has,

$$\boldsymbol{\beta}^{-1} = \left\langle \mathbf{m}(0)\mathbf{m}^T(0) \right\rangle = \left\langle \left(\int_{-\infty}^{0} e^{\tilde{\lambda}\tau} \mathbf{y}(\tau) d\tau \right) \left(\int_{-\infty}^{0} e^{\tilde{\lambda}\tau} \mathbf{y}(\tau) d\tau \right)^T \right\rangle. \tag{5.47}$$

The transpose commutes with the integral and also with the exponential function, so that

$$\boldsymbol{\beta}^{-1} = \left\langle \left(\int_{-\infty}^{0} e^{\tilde{\lambda}\tau} \mathbf{y}(\tau) d\tau \right) \left(\int_{-\infty}^{0} \mathbf{y}(\tau)^T e^{\tilde{\lambda}^T \tau} d\tau \right) \right\rangle. \tag{5.48}$$

Now write the integral as a double integral,

$$\boldsymbol{\beta}^{-1} = \left\langle \int_{-\infty}^{0} \int_{-\infty}^{0} e^{\tilde{\lambda}\tau_1} \mathbf{y}(\tau_1) \mathbf{y}(\tau_2)^T e^{\tilde{\lambda}^T \tau_2} d\tau_1 d\tau_2 \right\rangle. \tag{5.49}$$

Because of the linearity of the mean, this implies,

$$\boldsymbol{\beta}^{-1} = \int_{-\infty}^{0} \int_{-\infty}^{0} e^{\tilde{\lambda}\tau_1} \left\langle \mathbf{y}(\tau_1) \mathbf{y}(\tau_2)^T \right\rangle e^{\tilde{\lambda}^T \tau_2} d\tau_1 d\tau_2 . \tag{5.50}$$

This is an inverse problem for the unknown correlation $\langle y(\tau_1) y(\tau_2) \rangle$. To solve it, Landau and Lifshitz [1958] simplify the integral by setting up the correlation as a multiple of a delta function. The physical significance is that the random driving force components should be uncorrelated over a time scale that is big compared to the characteristic time scale of the fluctuations. Therefore one uses the approach,

$$\left\langle \mathbf{y}(\tau_1) \mathbf{y}^T(\tau_2) \right\rangle = \vec{\mathbf{A}} \delta(\tau_1 - \tau_2), \tag{5.51}$$

where $\mathbf{A}$ is a constant matrix. To determine the matrix $\mathbf{A}$, insert the correlation matrix from Eq. (5.50) into Eq. (5.49). The delta function collapses the double integral to a single integral, and one obtains,

$$\boldsymbol{\beta}^{-1} = \int_{-\infty}^{0} e^{\tilde{\lambda}\tau} \ \vec{\mathbf{A}} \ e^{\tilde{\lambda}^T \tau} \, d\tau . \tag{5.52}$$

Note that the integrand contains the product of three matrices which *do not commute*. The unknown

matrix $\mathbf{A}$ is caught in the middle and can, therefore, not be extracted out of the integral. Nevertheless Eq. (5.52) can be solved for the unknown matrix $\mathbf{A}$ by integration by parts. The formula for integration by parts is in our case,

$$\int_{-\infty}^{0} \frac{d\vec{\vec{\mathbf{U}}}(\tau)}{d\tau}\vec{\vec{\mathbf{V}}}(\tau)d\tau = \vec{\vec{\mathbf{U}}}(\tau)\vec{\vec{\mathbf{V}}}(\tau)\Big|_{-\infty}^{0} - \int_{-\infty}^{0} \vec{\vec{\mathbf{U}}}(\tau)\frac{d\vec{\vec{\mathbf{V}}}}{d\tau}(\tau)d\tau. \tag{5.53}$$

Here $\vec{\vec{\mathbf{U}}}(\tau)$ and $\vec{\vec{\mathbf{V}}}(\tau)$ are matrices given by $\vec{\vec{\mathbf{U}}}(\tau) = \vec{\vec{\lambda}}^{-1} e^{\vec{\vec{\lambda}}\tau}$ and $\vec{\vec{\mathbf{V}}}(\tau) = \vec{\vec{\mathbf{A}}} e^{\vec{\vec{\lambda}}^T \tau}$. The derivative of a matrix exponential function $e^{\vec{\vec{\lambda}}\tau}$ is $\vec{\vec{\lambda}} e^{\vec{\vec{\lambda}}\tau}$, in analogy to the derivative of a scalar exponential function $e^{\lambda\tau}$ being $\lambda e^{\lambda\tau}$. Therefore,

$$\begin{aligned}
\frac{d\vec{\vec{\mathbf{U}}}(\tau)}{d\tau} &= \frac{d}{d\tau}\left(\vec{\vec{\lambda}}^{-1} e^{\vec{\vec{\lambda}}\tau}\right) \\
&= \vec{\vec{\lambda}}^{-1} \frac{d}{d\tau}\left(e^{\vec{\vec{\lambda}}\tau}\right) \\
&= \vec{\vec{\lambda}}^{-1}\left(\vec{\vec{\lambda}} e^{\vec{\vec{\lambda}}\tau}\right) \\
&= \left(\vec{\vec{\lambda}}^{-1}\vec{\vec{\lambda}}\right) e^{\vec{\vec{\lambda}}\tau} \\
&= e^{\vec{\vec{\lambda}}\tau}.
\end{aligned} \tag{5.54}$$

Similarly,

$$\begin{aligned}
\frac{d\vec{\vec{\mathbf{V}}}(\tau)}{d\tau} &= \frac{d}{d\tau}\left(\vec{\vec{\mathbf{A}}} e^{\vec{\vec{\lambda}}^T \tau}\right) \\
&= \vec{\vec{\mathbf{A}}} \frac{d}{d\tau}\left(e^{\vec{\vec{\lambda}}^T \tau}\right) \\
&= \vec{\vec{\mathbf{A}}}\left(\vec{\vec{\lambda}}^T e^{\vec{\vec{\lambda}}^T \tau}\right).
\end{aligned} \tag{5.55}$$

Since the matrix exponential $e^{\vec{\vec{\lambda}}^T \tau}$ is a series in the matrix $\vec{\vec{\lambda}}^T$, it commutes with this matrix, that is $e^{\vec{\vec{\lambda}}^T \tau}\vec{\vec{\lambda}}^T = \vec{\vec{\lambda}}^T e^{\vec{\vec{\lambda}}^T \tau}$. Therefore from Eq. (5.55) it follows that

$$\frac{d\vec{\vec{V}}(\tau)}{d\tau} = \vec{\vec{A}}\left(\vec{\vec{\lambda}}^T e^{\vec{\vec{\lambda}}^T\tau}\right)$$
$$= \vec{\vec{A}}\left(e^{\vec{\vec{\lambda}}^T\tau}\vec{\vec{\lambda}}^T\right) \qquad (5.56)$$
$$= \left(\vec{\vec{A}}e^{\vec{\vec{\lambda}}^T\tau}\right)\vec{\vec{\lambda}}^T.$$

The result of the integration by parts of Eq. (5.52) is, therefore,

$$\begin{aligned}
\vec{\vec{\beta}}^{-1} &= \int_{-\infty}^{0} e^{\vec{\vec{\lambda}}\tau}\left(\vec{\vec{A}}\, e^{\vec{\vec{\lambda}}^T\tau}\right)d\tau \\
&= \int_{-\infty}^{0}\left[\frac{d}{d\tau}\left(\vec{\vec{\lambda}}^{-1}e^{\vec{\vec{\lambda}}\tau}\right)\right]\left(\vec{\vec{A}}\, e^{\vec{\vec{\lambda}}^T\tau}\right)d\tau \\
&= \left(\vec{\vec{\lambda}}^{-1}e^{\vec{\vec{\lambda}}\tau}\right)\left(\vec{\vec{A}}\, e^{\vec{\vec{\lambda}}^T\tau}\right)\Big|_{\tau=-\infty}^{0} - \int_{-\infty}^{0}\left(\vec{\vec{\lambda}}^{-1}e^{\vec{\vec{\lambda}}\tau}\right)\left[\frac{d}{d\tau}\left(\vec{\vec{A}}\, e^{\vec{\vec{\lambda}}^T\tau}\right)\right]d\tau \\
&= \left(\vec{\vec{\lambda}}^{-1}e^{\vec{\vec{\lambda}}\tau}\right)\left(\vec{\vec{A}}\, e^{\vec{\vec{\lambda}}^T\tau}\right)\Big|_{\tau=-\infty}^{0} - \int_{-\infty}^{0}\left(\vec{\vec{\lambda}}^{-1}e^{\vec{\vec{\lambda}}\tau}\right)\left(\vec{\vec{A}}\, e^{\vec{\vec{\lambda}}^T\tau}\vec{\vec{\lambda}}^T\right)d\tau.
\end{aligned} \qquad (5.57)$$

Because of the positive definiteness of the matrices $\vec{\vec{\lambda}}$ and $\vec{\vec{\lambda}}^T$ the first term on the right side vanishes at the lower limit of integration, that is for $\tau \to -\infty$. At the upper limit of integration, $\tau = 0$, the matrix exponentials are unit matrices. Therefore,

$$\left(\vec{\vec{\lambda}}^{-1}e^{\vec{\vec{\lambda}}\tau}\right)\left(\vec{\vec{A}}\, e^{\vec{\vec{\lambda}}^T\tau}\right)\Big|_{\tau=-\infty}^{0} = \vec{\vec{\lambda}}^{-1}\,\vec{\vec{A}}\,. \qquad (5.58)$$

The second term on the right hand side of Eq. (5.57) is an integral with a product of five matrices in the integrand. These matrices do, in general, *not commute*. However one is allowed by the law of associativity to group the matrices within the product in an arbitrary way. It follows that

$$\vec{\vec{\beta}}^{-1} = \vec{\vec{\lambda}}^{-1}\vec{\vec{A}} - \int_{-\infty}^{0}\vec{\vec{\lambda}}^{-1}\left(e^{\vec{\vec{\lambda}}\tau}\vec{\vec{A}}e^{\vec{\vec{\lambda}}^T\tau}\right)\vec{\vec{\lambda}}^T\, d\tau. \qquad (5.59)$$

Next, in the integral on the right side, the constant matrix $\vec{\vec{\lambda}}^{-1}$ on the left and the constant matrix $\vec{\vec{\lambda}}^T$ on the right may be taken outside the integral. One obtains,

$$\vec{\vec{\beta}}^{-1} = \vec{\vec{\lambda}}^{-1}\vec{\vec{A}} - \vec{\vec{\lambda}}^{-1} \cdot \int_{-\infty}^{0} e^{\vec{\vec{\lambda}}\tau} \vec{\vec{A}} e^{\vec{\vec{\lambda}}^T \tau} d\tau \cdot \vec{\vec{\lambda}}^T . \tag{5.60}$$

Notice that the integral on the right side is equal to $\vec{\vec{\beta}}^{-1}$ because of the original equation in Eq. (5.52) that was the starting point. This observation results in a linear equation for the unknown matrix $\vec{\vec{A}}$,

$$\vec{\vec{\beta}}^{-1} = \vec{\vec{\lambda}}^{-1}\vec{\vec{A}} - \vec{\vec{\lambda}}^{-1} \cdot \vec{\vec{\beta}}^{-1} \cdot \vec{\vec{\lambda}}^T . \tag{5.61}$$

Multiplication of each term by $\vec{\vec{\lambda}}$ from the left yields,

$$\vec{\vec{\lambda}}\vec{\vec{\beta}}^{-1} = \vec{\vec{A}} - \vec{\vec{\beta}}^{-1} \cdot \vec{\vec{\lambda}}^T . \tag{5.62}$$

It follows that

$$\vec{\vec{A}} = \vec{\vec{\lambda}}\vec{\vec{\beta}}^{-1} + \vec{\vec{\beta}}^{-1} \cdot \vec{\vec{\lambda}}^T . \tag{5.63}$$

Since $\vec{\vec{\beta}}$ is symmetric, so is $\vec{\vec{\beta}}^{-1}$. Therefore the second term in Eq. (5.63) is the transpose of the first term, and the result can be written as

$$\vec{\vec{A}} = 2\left(\vec{\vec{\lambda}}\vec{\vec{\beta}}^{-1}\right)^{sym} . \tag{5.64}$$

The unknown correlation of the transformed random forces is, therefore,

$$\left\langle \mathbf{y}(\tau_1)\mathbf{y}(\tau_2)^T \right\rangle = \vec{\vec{A}}\delta(\tau_1 - \tau_2) = 2\left(\vec{\vec{\lambda}}\vec{\vec{\beta}}^{-1}\right)^{sym} \delta(\tau_1 - \tau_2). \tag{5.65}$$

This result expresses the correlation matrix of the transformed random forces $\mathbf{y}(\tau)$ in terms of the decay matrix $\vec{\vec{\lambda}}$ and the stiffness matrix $\vec{\vec{\beta}}$. Observe that for $\tau_1 \neq \tau_2$, the correlation matrix is zero. Physically this means that the components of the random forces are uncorrelated over time spans much larger than the characteristic time scale of their fluctuations. Eq. (5.65) is a special case of the fluctuation-dissipation theorem.

From this result one immediately obtains the correlation matrices of both the magnetization

response and the random driving fields. For with Eq. (5.65) it follows that

$$\begin{aligned}\left\langle \mathbf{m}(t)\mathbf{m}^T(0)\right\rangle &= \left\langle \left(\int_{-\infty}^{t} e^{-\vec{\vec{\lambda}}(t-\tau)}\mathbf{y}(\tau)d\tau\right)\left(\int_{-\infty}^{0} e^{\vec{\vec{\lambda}}\tau}\mathbf{y}(\tau)d\tau\right)^T\right\rangle \\ &= \left\langle \left(\int_{-\infty}^{0} e^{\vec{\vec{\lambda}}\sigma}\mathbf{y}(t+\sigma)d\sigma\right)\left(\int_{-\infty}^{0} e^{\vec{\vec{\lambda}}\tau}\mathbf{y}(\tau)d\tau\right)^T\right\rangle \\ &= \int_{-\infty}^{0}\int_{-\infty}^{0} e^{\vec{\vec{\lambda}}\sigma}\left\langle \mathbf{y}(t+\sigma)\left[\mathbf{y}(\tau)\right]^T\right\rangle e^{\vec{\vec{\lambda}}^T\tau}d\sigma d\tau \\ &= \int_{-\infty}^{0}\int_{-\infty}^{0} e^{\vec{\vec{\lambda}}\sigma}\left(\vec{\vec{\lambda}}\vec{\vec{\beta}}^{-1}+\vec{\vec{\beta}}^{-1}\vec{\vec{\lambda}}^T\right)e^{\vec{\vec{\lambda}}^T\tau}\delta(t+\sigma-\tau)d\sigma d\tau.\end{aligned} \tag{5.66}$$

For $t>0$, this equation simplifies to

$$\begin{aligned}\left\langle \mathbf{m}(t)\mathbf{m}^T(0)\right\rangle &= \left\{\int_{-\infty}^{-t} e^{\vec{\vec{\lambda}}\sigma}\left(\vec{\vec{\lambda}}\vec{\vec{\beta}}^{-1}+\vec{\vec{\beta}}^{-1}\vec{\vec{\lambda}}^T\right)e^{\vec{\vec{\lambda}}^T\sigma}d\sigma\right\}e^{\vec{\vec{\lambda}}^T t} \\ &= e^{\vec{\vec{\lambda}}\sigma}\left(\vec{\vec{\lambda}}\vec{\vec{\beta}}^{-1}+\vec{\vec{\beta}}^{-1}\vec{\vec{\lambda}}^T\right)e^{\vec{\vec{\lambda}}^T\sigma}\left(\vec{\vec{\lambda}}^T\right)^{-1}\Big|_{\sigma=-\infty}^{-t} e^{\vec{\vec{\lambda}}^T t} \\ &\quad -\vec{\vec{\lambda}}\int_{-\infty}^{-t} e^{\vec{\vec{\lambda}}\sigma}\left(\vec{\vec{\lambda}}\vec{\vec{\beta}}^{-1}+\vec{\vec{\beta}}^{-1}\vec{\vec{\lambda}}^T\right)e^{\vec{\vec{\lambda}}^T\sigma}d\sigma\ \left(\vec{\vec{\lambda}}^T\right)^{-1}e^{\vec{\vec{\lambda}}^T t} \\ &= e^{-\vec{\vec{\lambda}}t}\left[\vec{\vec{\lambda}}\vec{\vec{\beta}}^{-1}\left(\vec{\vec{\lambda}}^T\right)^{-1}+\vec{\vec{\beta}}^{-1}\right]-\vec{\vec{\lambda}}\left\langle \mathbf{m}(t)\mathbf{m}^T(0)\right\rangle\left(\vec{\vec{\lambda}}^T\right)^{-1}.\end{aligned} \tag{5.67}$$

When this equation is multiplied from the right by $\vec{\vec{\lambda}}^T$, and the second term on the right side is brought to the left side, on obtains,

$$\begin{aligned}\left\langle \mathbf{m}(t)\mathbf{m}^T(0)\right\rangle\vec{\vec{\lambda}}^T+\vec{\vec{\lambda}}\left\langle \mathbf{m}(t)\mathbf{m}^T(0)\right\rangle &= e^{-\vec{\vec{\lambda}}t}\left[\vec{\vec{\lambda}}\vec{\vec{\beta}}^{-1}+\vec{\vec{\beta}}^{-1}\vec{\vec{\lambda}}^T\right] \\ &= e^{-\vec{\vec{\lambda}}t}\left[\vec{\vec{\beta}}^{-1}\vec{\vec{\lambda}}^T+\vec{\vec{\lambda}}\vec{\vec{\beta}}^{-1}\right] \\ &= \left(e^{-\vec{\vec{\lambda}}t}\vec{\vec{\beta}}^{-1}\right)\vec{\vec{\lambda}}^T+\vec{\vec{\lambda}}\left(e^{-\vec{\vec{\lambda}}t}\vec{\vec{\beta}}^{-1}\right)\end{aligned} \tag{5.68}$$

Comparison of the left side with the right side yields the desired correlation matrix for the magnetization response:

$$\left\langle \mathbf{m}(t)\mathbf{m}^T(0)\right\rangle = e^{-\vec{\lambda}t}\vec{\beta}^{-1}. \tag{5.69}$$

Recall that this result was derived for the case that $t > 0$. If, on the other hand, $t < 0$, then Eq. (5.66) simplifies to

$$\begin{aligned}\left\langle \mathbf{m}(t)\mathbf{m}^T(0)\right\rangle &= \left\{ \int_{-\infty}^{0} e^{\vec{\lambda}\sigma}\left(\vec{\lambda}\vec{\beta}^{-1} + \vec{\beta}^{-1}\vec{\lambda}^T\right)e^{\vec{\lambda}^T\sigma}d\sigma \right\} e^{\vec{\lambda}^T t} \\ &= e^{\vec{\lambda}\sigma}\left(\vec{\lambda}\vec{\beta}^{-1} + \vec{\beta}^{-1}\vec{\lambda}^T\right)e^{\vec{\lambda}^T\sigma}\left(\vec{\lambda}^T\right)^{-1}\Big|_{\sigma=-\infty}^{0} e^{\vec{\lambda}^T t} \\ &\quad - \vec{\lambda}\int_{-\infty}^{0} e^{\vec{\lambda}\sigma}\left(\vec{\lambda}\vec{\beta}^{-1} + \vec{\beta}^{-1}\vec{\lambda}^T\right)e^{\vec{\lambda}^T\sigma}d\sigma \ \left(\vec{\lambda}^T\right)^{-1} e^{\vec{\lambda}^T t} \\ &= \left[\vec{\lambda}\vec{\beta}^{-1}\left(\vec{\lambda}^T\right)^{-1} + \vec{\beta}^{-1}\right]e^{\vec{\lambda}^T t} - \vec{\lambda}\left\langle \mathbf{m}(t)\mathbf{m}^T(0)\right\rangle\left(\vec{\lambda}^T\right)^{-1}.\end{aligned} \tag{5.70}$$

This equation is equivalent to

$$\begin{aligned}\left\langle \mathbf{m}(t)\mathbf{m}^T(0)\right\rangle\vec{\lambda}^T + \vec{\lambda}\left\langle \mathbf{m}(t)\mathbf{m}^T(0)\right\rangle &= \left[\vec{\lambda}\vec{\beta}^{-1} + \vec{\beta}^{-1}\vec{\lambda}^T\right]e^{\vec{\lambda}^T t} \\ &= \left[\vec{\beta}^{-1}\vec{\lambda}^T + \vec{\lambda}\vec{\beta}^{-1}\right]e^{\vec{\lambda}^T t} \\ &= \left(\vec{\beta}^{-1}e^{\vec{\lambda}^T t}\right)\vec{\lambda}^T + \vec{\lambda}\left(\vec{\beta}^{-1}e^{\vec{\lambda}^T t}\right).\end{aligned} \tag{5.71}$$

This implies that for $t < 0$, the correlation is

$$\left\langle \mathbf{m}(t)\mathbf{m}^T(0)\right\rangle = \vec{\beta}^{-1}e^{\vec{\lambda}^T t}. \tag{5.72}$$

Notice that both the limit $t \to 0$ from the right in Eq. (5.69) and the limit $t \to 0$ from the left in Eq. (5.72) yield the covariance matrix $\left\langle \mathbf{m}(0)\mathbf{m}^T(0)\right\rangle = \vec{\beta}^{-1}$. This means that the correlation function is continuous at $t = 0$, though in general not differentiable.

Next, determine the correlation matrix of the physical noise field $\mathbf{h}_{ext}^{(m)}(t)$. Recall from Eq. (5.33) that the noise field is related to the driving term $\mathbf{y}(t)$ by the linear relationship

$$\mathbf{y}(t)=\frac{V}{k_BT}\ddot{\boldsymbol{\lambda}}\ddot{\boldsymbol{\beta}}^{-1}\mathbf{h}_{ext}^{(th)}(t). \tag{5.73}$$

Substitution into the result in Eq. (5.65) yields,

$$\left(\frac{V}{k_BT}\right)^2\left\langle\left[\ddot{\boldsymbol{\lambda}}\ddot{\boldsymbol{\beta}}^{-1}\mathbf{h}_{ext}^{(th)}(\tau_1)\right]\left[\ddot{\boldsymbol{\lambda}}\ddot{\boldsymbol{\beta}}^{-1}\mathbf{h}_{ext}^{(th)}(\tau_2)\right]^T\right\rangle=2\left(\ddot{\boldsymbol{\lambda}}\ddot{\boldsymbol{\beta}}^{-1}\right)^{sym}\delta(\tau_1-\tau_2). \tag{5.74}$$

Resolving the matrix transpose on the right side, and extracting constant matrices out of the mean yields,

$$\left(\frac{V}{k_BT}\right)^2\ddot{\boldsymbol{\lambda}}\ddot{\boldsymbol{\beta}}^{-1}\left\langle\mathbf{h}_{ext}^{(th)}(\tau_1)\left[\mathbf{h}_{ext}^{(th)}(\tau_2)\right]^T\right\rangle\left(\ddot{\boldsymbol{\lambda}}\ddot{\boldsymbol{\beta}}^{-1}\right)^T=2\left(\ddot{\boldsymbol{\lambda}}\ddot{\boldsymbol{\beta}}^{-1}\right)^{sym}\delta(\tau_1-\tau_2). \tag{5.75}$$

With the abbreviation $\ddot{\boldsymbol{\gamma}}=\ddot{\boldsymbol{\lambda}}\ddot{\boldsymbol{\beta}}^{-1}$, this equation becomes,

$$\left(\frac{V}{k_BT}\right)^2\ddot{\boldsymbol{\gamma}}\left\langle\mathbf{h}_{ext}^{(th)}(\tau_1)\left[\mathbf{h}_{ext}^{(th)}(\tau_2)\right]^T\right\rangle\ddot{\boldsymbol{\gamma}}^T=2\ddot{\boldsymbol{\gamma}}^{sym}\delta(\tau_1-\tau_2). \tag{5.76}$$

Multiplication by $\left(\frac{k_BT}{V}\right)^2\ddot{\boldsymbol{\gamma}}^{-1}$ from the left and by $\left(\ddot{\boldsymbol{\gamma}}^T\right)^{-1}$ from the right leads to the correlation matrix for the random driving field,

$$\begin{aligned}\left\langle\mathbf{h}_{ext}^{(th)}(\tau_1)\left[\mathbf{h}_{ext}^{(th)}(\tau_2)\right]^T\right\rangle&=2\left(\frac{k_BT}{V}\right)^2\ddot{\boldsymbol{\gamma}}^{-1}\left[\frac{\ddot{\boldsymbol{\gamma}}+\ddot{\boldsymbol{\gamma}}^T}{2}\right]\left(\ddot{\boldsymbol{\gamma}}^T\right)^{-1}\delta(\tau_1-\tau_2)\\&=2\left(\frac{k_BT}{V}\right)^2\left[\frac{\left(\ddot{\boldsymbol{\gamma}}^T\right)^{-1}+\ddot{\boldsymbol{\gamma}}^{-1}}{2}\right]\delta(\tau_1-\tau_2).\end{aligned} \tag{5.77}$$

Since the transpose and the inverse of a nonsingular square matrix commute, the matrix in the brackets on the right side is the symmetric part of $\ddot{\boldsymbol{\gamma}}^{-1}$. It follows that

$$\left\langle \mathbf{h}_{ext}^{(th)}(\tau_1)\left[\mathbf{h}_{ext}^{(th)}(\tau_2)\right]^T\right\rangle = 2\left(\frac{k_BT}{V}\right)^2\left(\overleftrightarrow{\boldsymbol{\gamma}}^{-1}\right)^{sym}\delta(\tau_1-\tau_2)$$
$$= 2\left(\frac{k_BT}{V}\right)^2\left(\overleftrightarrow{\boldsymbol{\beta}}\overleftrightarrow{\boldsymbol{\lambda}}^{-1}\right)^{sym}\delta(\tau_1-\tau_2). \tag{5.78}$$

To get a better understanding of the right side of this equation, one can express $\left(\overleftrightarrow{\boldsymbol{\gamma}}^{-1}\right)^{sym}$ in terms of the Smith matrices,

$$\left(\overleftrightarrow{\boldsymbol{\gamma}}^{-1}\right)^{sym} = \left[\left(\overleftrightarrow{\boldsymbol{\lambda}}\overleftrightarrow{\boldsymbol{\beta}}^{-1}\right)^{-1}\right]^{sym} = \left[\overleftrightarrow{\boldsymbol{\beta}}\left(\overleftrightarrow{\boldsymbol{\lambda}}^{-1}\right)\right]^{sym} = \left[\frac{V}{k_BT}\overleftrightarrow{\mathbf{K}}\overleftrightarrow{\mathbf{K}}^{-1}(\mathbf{D}+\mathbf{G})\right]^{sym} = \frac{V}{k_BT}\mathbf{D}^{sym}. \tag{5.79}$$

Substitution into Eq. (5.78) yields,

$$\left\langle \mathbf{h}_{ext}^{(th)}(\tau_1)\left[\mathbf{h}_{ext}^{(th)}(\tau_2)\right]^T\right\rangle = 2\frac{k_BT}{V}\left(\overleftrightarrow{\mathbf{D}}^{sym}\right)\delta(\tau_1-\tau_2). \tag{5.80}$$

The correlation matrix of the random force components is seen to be a multiple of the symmetric part of the damping matrix. Recall that in Chapter 4, the symmetric part of the damping matrix was shown to be responsible for the loss in a uniformly magnetized sample. Therefore the right side of Eq. (5.80) describes dissipation, whereas the left side is the correlation of fluctuations in the random driving force components. This important result is a special case of the fluctuation-dissipation theorem. In the literature it is often found expressed in terms of the inverse susceptibility matrix $\chi^{-1}(\omega)$, in the form

$$\left\langle\left[\mathbf{h}_{ext}^{(th)}(\tau_1)\right]\left[\mathbf{h}_{ext}^{(th)}(\tau_2)\right]^T\right\rangle = 2\frac{k_BT}{V}\left\{\frac{\chi^{-1}(\omega)-\left[\chi^{-1}(\omega)\right]^\dagger}{2i\omega}\right\}\delta(\tau_1-\tau_2). \tag{5.81}$$

That the two forms of the fluctuation-dissipation theorem in Eq. (5.80) and Eq. (5.81) are equivalent follows from the identity,

$$\overleftrightarrow{\mathbf{D}}^{sym} = \frac{\overleftrightarrow{\chi}^{-1}(\omega)-\left[\overleftrightarrow{\chi}^{-1}(\omega)\right]^\dagger}{2i\omega}, \tag{5.82}$$

which was given at the end of Chapter 3. (Recall that the superscript dagger denotes the complex conjugate transpose of a matrix.) The result in Eqs. (5.80) and (5.81) will now be used to obtain the spectral power density of both the noise field and the magnetization response with the help of the Wiener-Khinchine theorem.

5.4 Spectral resolution of field noise and magnetization response for the damped magnetic precession

5.4.a Connection between auto-correlation and spectral power density: the Wiener-Khinchine theorem

The Fourier transform of the autocorrelation of a fluctuating quantity is proportional to the spectral density of its mean square. This powerful fact, also known as the Wiener-Khinchine theorem in signal processing, can be illustrated in a non-rigorous way. Let

$$\left(x^2\right)_\omega = \int_{-\infty}^{\infty} \left\langle x(t)x(0)\right\rangle e^{i\omega t}dt \tag{5.83}$$

denote the Fourier transform of the autocorrelation function $\left\langle x(t)x(0)\right\rangle$ of a fluctuating physical quantity $x(t)$. This Fourier transform has units of $[x]^2[t]$, that is units of $[x]^2/[\omega]$. These are indeed units of the spectral (or frequency) density of $x^2(t)$. Besides this dimensional argument, consider now the inverse Fourier transform of Eq. (5.83), given by

$$\left\langle x(t)x(0)\right\rangle = \frac{1}{2\pi}\int_{-\infty}^{\infty}\left(x^2\right)_\omega e^{-i\omega t}d\omega\,. \tag{5.84}$$

Setting $t=0$ yields

$$\left\langle x^2(0)\right\rangle = \frac{1}{2\pi}\int_{-\infty}^{\infty}\left(x^2\right)_\omega d\omega \,. \tag{5.85}$$

Recall that for a system in equilibrium, the mean of the quantity $x(t)$ as well as the mean of $x^2(t)$ do not change in time. Therefore

$$\left\langle x^2(t)\right\rangle = \frac{1}{2\pi}\int_{-\infty}^{\infty}\left(x^2\right)_\omega d\omega = const. \tag{5.86}$$

This equation suggests that the quantity $\left(x^2\right)_\omega / 2\pi$ is the spectral density of the mean square, $\left\langle x^2(t)\right\rangle$. A rigorous mathematical proof can be found in any signal processing engineering textbook, and will not be presented here.

Signal processing engineers call the mean square, $\left\langle x^2(t)\right\rangle$, the "power" of the "signal" $x(t)$. In general, this "signal power" is not the physical power, measured in watts, that is dissipated in the material. In the study of the noise power of magnetic precession, great care must be exerted to distinguish between the *signal power of the internal magnetic field*, the *signal power of the magnetization*, and the *loss power*, measured in watts, that is dissipated in the material. In the absence of an applied driving field, the loss power dissipated in the material is, of course, zero, in the same way that no heat is dissipated in an electrical resistor without an applied voltage.

In the next section the Wiener-Khinchine theorem is applied to derive the spectral power density of the magnetic noise components from their correlation matrix, which was determined in Section 5.3. The spectral power densities are different for the signal power of the random magnetic noise fields and the signal power of the corresponding magnetization response.

5.4.b Spectral distribution of thermal field noise and magnetization response noise

With the Wiener-Khinchine theorem introduced in the last section, one can determine the spectral power density of the random noise field from its correlation matrix. Recall from Eq. (5.80) that this correlation matrix is given by

$$\left\langle \mathbf{h}_{ext}^{(th)}(\tau)\left[\mathbf{h}_{ext}^{(th)}(0)\right]^{T}\right\rangle = 2\frac{k_B T}{V}\left(\vec{\mathbf{D}}^{sym}\right)\delta(\tau). \tag{5.87}$$

From this matrix equation, the auto-correlation for the x-component $h_{ext-x}^{(th)}(t)$ of the random field is obtained as

$$\left\langle h_{ext-x}^{(th)}(\tau)h_{ext-x}^{(th)}(0)\right\rangle = 2\frac{k_B T}{V}D_{xx}^{sym}\delta(\tau). \tag{5.88}$$

By the Wiener-Khinchine theorem, this implies that

$$\begin{aligned}\left[\left(h_{ext-x}^{(th)}\right)^2\right]_{\omega} &= \int_{-\infty}^{\infty}\left\langle h_{ext-x}^{(th)}(u)h_{ext-x}^{(th)}(0)\right\rangle e^{i\omega u}\,du \\ &= \int_{-\infty}^{\infty}2\frac{k_B T}{V}D_{xx}\delta(u)\,e^{i\omega u}\,du \\ &= 2\frac{k_B T}{V}D_{xx}\end{aligned} \tag{5.89}$$

and

$$\begin{aligned}\left[\left(h_{ext-y}^{(th)}\right)^2\right]_{\omega} &= \int_{-\infty}^{\infty}\left\langle h_{ext-y}^{(th)}(u)h_{ext-y}^{(th)}(0)\right\rangle e^{i\omega u}\,du \\ &= \int_{-\infty}^{\infty}2\frac{k_B T}{V}D_{yy}\delta(u)\,e^{i\omega u}\,du \\ &= 2\frac{k_B T}{V}D_{yy}.\end{aligned} \tag{5.90}$$

The following observations can be made about this power density of the random magnetic noise

fields:

a) The power density is independent of frequency for both components of the noise field. That means that the noise is *white noise*.

b) The noise power is proportional to the absolute temperature.

c) The noise power spectral density of the x- and y-components of the random fields are proportional to the respective diagonal elements of the damping matrix. Consequently, the power densities are the same for x- and y-component if and only if the diagonal elements of the damping matrix are the same.

d) The noise power spectral density is isotropic, if the symmetry property in c) is invariant under rotations of the coordinate system. This is the case if the symmetric part of the damping matrix is a multiple of the unit matrix. The reason for that is explained now.

If the damping matrix has the form

$$\vec{\mathbf{D}} = \begin{pmatrix} a & b \\ c & a \end{pmatrix}, \tag{5.91}$$

then the transformed matrix under a rotation with an arbitrary angle φ is

$$\begin{aligned} &\begin{pmatrix} \cos\varphi & -\sin\varphi \\ \sin\varphi & \cos\varphi \end{pmatrix}\begin{pmatrix} a & b \\ c & a \end{pmatrix}\begin{pmatrix} \cos\varphi & \sin\varphi \\ -\sin\varphi & \cos\varphi \end{pmatrix} \\ &= \begin{pmatrix} \cos\varphi & -\sin\varphi \\ \sin\varphi & \cos\varphi \end{pmatrix}\begin{pmatrix} a\cos\varphi - b\sin\varphi & a\sin\varphi + b\cos\varphi \\ c\cos\varphi - a\sin\varphi & c\sin\varphi + a\cos\varphi \end{pmatrix} \\ &= \begin{pmatrix} a - (b+c)\sin\varphi\cos\varphi & b\cos^2\varphi - c\sin^2\varphi \\ -b\sin^2\varphi + c\cos^2\varphi & a + (b+c)\sin\varphi\cos\varphi \end{pmatrix} \end{aligned} \tag{5.92}$$

One sees that the diagonal elements of the rotated matrix are equal for every rotation angle φ if and only if $c = -b$. In this case, the damping matrix has the form,

$$\vec{\mathbf{D}} = \begin{pmatrix} a & b \\ -b & a \end{pmatrix}. \tag{5.93}$$

This matrix is indeed invariant under arbitrary rotations, because

$$\begin{pmatrix} \cos\varphi & -\sin\varphi \\ \sin\varphi & \cos\varphi \end{pmatrix}\begin{pmatrix} a & b \\ -b & a \end{pmatrix}\begin{pmatrix} \cos\varphi & \sin\varphi \\ -\sin\varphi & \cos\varphi \end{pmatrix} = \begin{pmatrix} a & b \\ -b & a \end{pmatrix}. \tag{5.94}$$

That means that the symmetric part of the damping matrix must be a multiple of the unit matrix:

$$\overleftrightarrow{\mathbf{D}}^{sym} = \begin{pmatrix} D & 0 \\ 0 & D \end{pmatrix} = D\begin{pmatrix} 1 & 0 \\ 0 & 1 \end{pmatrix} \tag{5.95}$$

with a scalar damping parameter D. Therefore the noise field is isotropic if and only if the symmetric part of the damping matrix is a multiple of the unit matrix. In this case the power density of the noise is the same in every direction, and is given by

$$\left(h^2\right)_\omega = \frac{2k_B T}{V} D. \tag{5.96}$$

In Table 5-1 the damping matrix and its symmetric part are given for each of the five phenomenological damping models in Chapter 3. As discussed there, the BB model has a zero damping matrix, and the theory developed in Chapter 5 will not be applied to the BB model. For the LL, G and COT models, the damping matrix is a multiple of the unit matrix, which implies isotropic noise. For the MBB model, on the other hand, the diagonal elements in the damping matrix are in general different, and the noise is not isotropic, but depends on the sample geometry. In this way the MBB damping model is fundamentally different from the LL, G and COT models.

In this section, the interest was focused on the Fourier transform of the diagonal elements of the correlation matrix. These Fourier transforms have a physical significance as spectral power densities of the noise components. In a more general sense, the Fourier transform of the entire correlation matrix is called the *spectral density matrix*. The spectral density matrix of the random noise field components is given by,

$$\left[\left(\mathbf{h}_{ext}^{(th)}\right)\left(\mathbf{h}_{ext}^{(th)}\right)^{\dagger}\right]_{\omega} = \int_{-\infty}^{\infty}\left\langle \mathbf{h}_{ext}^{(th)}(t)\left[\mathbf{h}_{ext}^{(th)}(0)\right]^{T}\right\rangle e^{i\omega t}\, dt$$

$$= \int_{-\infty}^{\infty} 2\frac{k_B T}{V}\mathbf{D}^{sym}\delta(t)\, e^{i\omega t}\, dt \qquad (5.97)$$

$$= 2\frac{k_B T}{V}\mathbf{D}^{sym}.$$

The spectral power density of the magnetization response components, on the other hand, is obtained as the Fourier transform of the correlation matrix from Eqs. (5.69) and (5.72) for positive and negative times, respectively.

$$\left[\mathbf{m}\mathbf{m}^{\dagger}\right]_{\omega} = \int_{-\infty}^{\infty}\left\langle \mathbf{m}(t)\mathbf{m}(0)^{T}\right\rangle e^{i\omega t}\, dt$$

$$= \int_{-\infty}^{0} \vec{\vec{\beta}}^{-1} e^{\vec{\vec{\lambda}}^{T} t}\, e^{i\omega t}\, dt + \int_{0}^{\infty} e^{-\vec{\vec{\lambda}} t}\, \vec{\vec{\beta}}^{-1} e^{i\omega t}\, dt \qquad (5.98)$$

$$= \vec{\vec{\beta}}^{-1}\left(\vec{\vec{\lambda}}^{T} + i\omega\vec{\vec{\mathbf{I}}}\right)^{-1} - \left(-\vec{\vec{\lambda}} + i\omega\vec{\vec{\mathbf{I}}}\right)^{-1}\vec{\vec{\beta}}^{-1}$$

$$= \vec{\vec{\beta}}^{-1}\left(\vec{\vec{\lambda}}^{T} + i\omega\vec{\vec{\mathbf{I}}}\right)^{-1} + \left[\vec{\vec{\beta}}^{-1}\left(\vec{\vec{\lambda}}^{T} + i\omega\vec{\vec{\mathbf{I}}}\right)^{-1}\right]^{\dagger}.$$

Model	Damping matrix, $\vec{\mathbf{D}}$	$\vec{\mathbf{D}}^{sym}$
LL	$\vec{\mathbf{D}}_{LL} = \frac{1}{\lvert\gamma\rvert M_s}\frac{1}{1+(\alpha_{LL})^2}\begin{pmatrix} \alpha_{LL} & (\alpha_{LL})^2 \\ -(\alpha_{LL})^2 & \alpha_{LL} \end{pmatrix}$, $\alpha_{LL} = \frac{\lambda_{LL}}{\lvert\gamma\rvert M_s}$	$\vec{\mathbf{D}}_{LL}^{sym} = \frac{1}{\lvert\gamma\rvert M_s}\frac{1}{1+\alpha_{LL}^2}\begin{pmatrix} \alpha_{LL} & 0 \\ 0 & \alpha_{LL} \end{pmatrix}$
COT	$\vec{\mathbf{D}}_{COT} = \frac{1}{\lvert\gamma\rvert M_s}\frac{\alpha_{COT}}{1+\alpha_{COT}^2}\begin{pmatrix} 1 & \alpha_{COT} \\ -\alpha_{COT} & 1 \end{pmatrix}$, $\alpha_{COT} = \frac{1}{T_2\lvert\gamma\rvert H_{\text{int}}}$	$\vec{\mathbf{D}}_{COT}^{sym} = \frac{1}{\lvert\gamma\rvert M_s}\frac{\alpha_{COT}}{1+\alpha_{COT}^2}\begin{pmatrix} 1 & 0 \\ 0 & 1 \end{pmatrix}$
G	$\vec{\mathbf{D}}_G = \frac{1}{\lvert\gamma\rvert M_s}\begin{pmatrix} \alpha_G & 0 \\ 0 & \alpha_G \end{pmatrix}$	$\vec{\mathbf{D}}_G^{sym} = \frac{1}{\lvert\gamma\rvert M_s}\begin{pmatrix} \alpha_G & 0 \\ 0 & \alpha_G \end{pmatrix}$
MBB	$\vec{\mathbf{D}}_{MBB} = \frac{1}{\lvert\gamma\rvert M_s}\frac{1}{\omega_x\omega_y+\lambda_{MBB}^2}\begin{pmatrix} \lambda_{MBB}\omega_x & \lambda_{MBB}^2 \\ -\lambda_{MBB}^2 & \lambda_{MBB}\omega_y \end{pmatrix}$, $\lambda_{MBB} = \frac{1}{T_2}$	$\vec{\mathbf{D}}_{MBB}^{sym} = \frac{1}{\lvert\gamma\rvert M_s}\frac{\lambda_{MBB}}{\omega_x\omega_y+\lambda_{MBB}^2}\begin{pmatrix} \omega_x & 0 \\ 0 & \omega_y \end{pmatrix}$

Table 5-1: Damping matrix and its symmetric part for the LL, COT, G and MBB models.

The spectral power densities of the magnetization components m_x and m_y are given by the diagonal elements of the spectral density matrix in Eq.(5.98). Table 5-2 shows the power spectrum of the x-component of the magnetization for the LL, G, COT, and MBB damping models. In each model, the power density of the noise shows a characteristic maximum at the Kittel resonance

frequency $\sqrt{\omega_x \omega_y}$. The third column of Table 5-2 shows the approximation for small damping, where the terms quadratic in the damping parameter can be omitted in comparison with unity. Also in this approximation the sample is assumed to have rotational symmetry, that is $\omega_x = \omega_y = \omega_0$. One observes:

a) The noise power density in the zero frequency limit goes as $1/\omega_0^2$ for the LL, G and COT models, but as $1/\omega_0^3$ for the MBB model.

b) The noise power density in the infinite frequency limit goes as $1/\omega_0^2$ for the LL, G, COT and MBB models.

Model	Power spectral density for x-component of the Magnetization response	Approximation for small damping and rotational symmetry $(\omega_x = \omega_y = \omega_0)$.
LL	$\left\|(m_x)_\omega\right\|^2_{LL} = 2\frac{k_B T}{V}\lvert\gamma\rvert M_s \cdot \frac{\frac{\alpha_{LL}}{1+\alpha_{LL}^2}\left(\omega_y^2 + \frac{\omega^2}{1+\alpha_{LL}^2}\right)}{\left(\omega_x\omega_y - \frac{\omega^2}{1+\alpha_{LL}^2}\right)^2 + \left(\frac{\alpha_{LL}}{1+\alpha_{LL}^2}\right)^2 \omega^2(\omega_x+\omega_y)^2}$	$\left\|(m_x)_\omega\right\|^2_{LL} = 2\frac{k_B T}{V}\lvert\gamma\rvert M_s \cdot \frac{\alpha_{LL}(\omega_0^2+\omega^2)}{(\omega_0^2-\omega^2)^2 + 4\alpha_{LL}{}^2\omega_0^2\omega^2}$
COT	$\left\|(m_x)_\omega\right\|^2_{COT} = 2\frac{k_B T}{V}\lvert\gamma\rvert M_s \cdot \frac{\frac{\alpha_{COT}}{1+\alpha_{COT}^2}\left(\omega_y^2 + \frac{\omega^2}{1+\alpha_{COT}^2}\right)}{\left(\omega_x\omega_y - \frac{\omega^2}{1+\alpha_{COT}^2}\right)^2 + \left(\frac{\alpha_{COT}}{1+\alpha_{COT}^2}\right)^2 \omega^2(\omega_x+\omega_y)^2}$	$\left\|(m_x)_\omega\right\|^2_{COT} = 2\frac{k_B T}{V}\lvert\gamma\rvert M_s \cdot \frac{\alpha_{COT}(\omega_0^2+\omega^2)}{(\omega_0^2-\omega^2)^2 + 4\alpha_{COT}^2\omega_0^2\omega^2}$
G	$\left\|(m_x)_\omega\right\|^2_{G} = 2\frac{k_B T}{V}\lvert\gamma\rvert M_s \cdot \frac{\alpha_G\left[\omega_y^2 + (1+\alpha_G^2)\omega^2\right]}{\left[\omega_x\omega_y - (1+\alpha_G^2)\omega^2\right]^2 + \left[\alpha_G\omega(\omega_x+\omega_y)\right]^2}$	$\left\|(m_x)_\omega\right\|^2_{G} = 2\frac{k_B T}{V}\lvert\gamma\rvert M_s \cdot \frac{\alpha_G(\omega_0^2+\omega^2)}{(\omega_0^2-\omega^2)^2 + 4\alpha_G^2\omega^2\omega_0^2}$
MBB	$\left\|(m_x)_\omega\right\|^2_{MBB} = 2\frac{k_B T}{V}\lvert\gamma\rvert M_s \cdot \frac{\lambda_{MBB}(\lambda_{MBB}^2 + \omega_x\omega_y + \omega^2)}{\omega_x\left[(\lambda_{MBB}^2 + \omega_x\omega_y - \omega^2)^2 + (2\lambda_{MBB}\omega)^2\right]}$	$\left\|(m_x)_\omega\right\|^2_{MBB} = 2\frac{k_B T}{V}\lvert\gamma\rvert M_s \cdot \frac{\lambda_{MBB}\left(\omega_0 + \frac{\omega^2}{\omega_0}\right)}{(\omega_0^2-\omega^2)^2 + 4\lambda_{MBB}^2\omega^2}$

Table 5-2: Spectral density of magnetization noise power for damping models.

5.5 Remarks on the quantum-mechanical version of the fluctuation-dissipation theorem

The derivation of the fluctuation-dissipation theorem in this chapter and all conclusions from it are classical. All quantum effects are neglected. Under which conditions are the quantum effects negligible, and how can the fluctuation-dissipation theorem be modified if they are not negligible? Following the treatment in Landau-Lifshitz [1958], one starts with the quantum-mechanical energy uncertainty relation for a time-dependent physical quantity $x(t)$,

$$\Delta U_{pot}\Delta x \sim \hbar\frac{dx}{dt}. \tag{5.99}$$

If τ is a characteristic time constant for the rate of change of the quantity $x(t)$, then

$$\frac{dx}{dt} \sim \frac{x}{\tau}. \tag{5.100}$$

Consequently, the uncertainty relation in Eq. (5.99) becomes,

$$\Delta U_{pot}\Delta x \sim \hbar\frac{x}{\tau}. \tag{5.101}$$

Assuming that the quantity $x(t)$ is a macroscopic quantity with a definite value, its uncertainty is small, that means

$$\Delta x \ll x. \tag{5.102}$$

Therefore Eq (5.101) implies that

$$\Delta U_{pot} \gg \frac{\hbar}{\tau}. \tag{5.103}$$

The potential energy of an equilibrium system can be written as the product of temperature and entropy, if no mechanical work is done on the system,

$$U_{pot} = TS. \tag{5.104}$$

At a fixed temperature T, it follows that

$$\Delta U_{pot} = T\,\Delta S. \tag{5.105}$$

Substitution into Eq. (5.103) yields,

$$T\,\Delta S \gg \frac{\hbar}{\tau}. \tag{5.106}$$

Also assuming the entropy uncertainty ΔS of the system to be small compared with the Boltzmann constant k_B, one obtains

$$k_B T \gg \Delta S\; T \gg \frac{\hbar}{\tau}, \tag{5.107}$$

and, therefore,

$$T\tau \gg \frac{\hbar}{k_B}. \tag{5.108}$$

This is the condition under which the fluctuations can be treated classically. When the temperature is too low, or when the fluctuating quantity varies too rapidly, then inequality (5.108) is violated, and the classical treatment is no longer valid. Instead, the fluctuation-dissipation theorem takes the form, developed in Callen and Welton [1951],

$$\left\langle \mathbf{h}_{ext}^{(th)}(\tau_1)\left[\mathbf{h}_{ext}^{(th)}(\tau_2)\right]^T \right\rangle = \frac{1}{2\pi}\int_{-\infty}^{\infty} \frac{\hbar\omega}{V}\coth\frac{\hbar\omega}{2k_B T}\,\vec{\vec{\mathbf{D}}}^{sym} e^{i\omega(\tau_1-\tau_2)} d\omega\,. \tag{5.109}$$

In the Fourier integrals, ω is the frequency of a Fourier component of the fluctuations, and so is of the order $1/\tau$, where τ is the characteristic time constant from the uncertainty analysis $k_B T$ above. Therefore the classical limit from Eq. (5.107) is equivalent to $k_B T \gg \hbar\omega$, that is

$\hbar\omega / k_B T \to 0.$

In this limit, the expression $\frac{\hbar\omega}{2k_BT}\coth\frac{\hbar\omega}{2k_BT}$ tends to unity, as one sees by application of l'Hôpital's rule-, and the integration in Eq. (5.109) yields the classical version of the fluctuation-dissipation theorem,

$$\begin{aligned}\left\langle \mathbf{h}_{ext}^{(th)}(\tau_1)\left[\mathbf{h}_{ext}^{(th)}(\tau_2)\right]^T\right\rangle &= \frac{1}{2\pi}\int_{-\infty}^{\infty}\frac{\hbar\omega}{V}\coth\frac{\hbar\omega}{2k_BT}\vec{\vec{\mathbf{D}}}^{sym}e^{i\omega(\tau_1-\tau_2)}d\omega \\ &= \frac{1}{2\pi}\frac{2k_BT}{V}\int_{-\infty}^{\infty}\frac{\hbar\omega}{2k_BT}\coth\frac{\hbar\omega}{2k_BT}\vec{\vec{\mathbf{D}}}^{sym}e^{i\omega(\tau_1-\tau_2)}d\omega \\ &\to \frac{1}{2\pi}\frac{2k_BT}{V}\int_{-\infty}^{\infty}\vec{\vec{\mathbf{D}}}^{sym}e^{i\omega(\tau_1-\tau_2)}d\omega \\ &= 2\frac{k_BT}{V}\vec{\vec{\mathbf{D}}}^{sym}\frac{1}{2\pi}\int_{-\infty}^{\infty}e^{i\omega(\tau_1-\tau_2)}d\omega \\ &= 2\frac{k_BT}{V}\vec{\vec{\mathbf{D}}}^{sym}\delta(\tau_1-\tau_2).\end{aligned} \tag{5.110}$$

In this way the quantum-mechanical version of the fluctuation-dissipation theorem according to Callen and Welton goes over into the classical result derived in this thesis, when the classical limit is taken.

5.6 Summary

In this chapter the fluctuation-dissipation theorem was proven from basic statistical considerations, using an equation of motion for coupled harmonic oscillators with a random driving force. The proof did not require any integrations in the complex plane and did not involve the susceptibility concept. As a result, the correlation matrix of the thermally generated, random driving force, was shown to be a multiple of the symmetric part of the damping matrix. Recall from Chapter 4 that the symmetric part of the damping matrix is also proportional to the energy loss. The spectral density of the field noise was shown to be independent of frequency. Such noise is called white noise.

In contrast, the spectral density of the magnetization response shows a resonance peak near the Kittel resonance frequency.

Of the phenomenological damping models analyzed in Chapter 3, three models have a multiple of the unit matrix as symmetric part of the damping matrix. These are the Landau-Lifshitz, Gilbert and Codrington-Olds-Torrey damping models. As a consequence of the fluctuation-dissipation theorem, the field noise is isotropic for the models in this category. In contrast, for the MBB damping model, the field noise is not isotropic, but depends on the sample geometry. In this way, the MBB damping model is fundamentally different from the other three damping models, and may be applied only to physical situations where a mechanism for nonlocal, nonisotropic thermal generation of random fields is present.

Chapter 6

Conclusion

In this work five phenomenological damping models were compared: Landau-Lifshitz (LL) damping, Bloch-Bloembergen (BB) damping, Codrington-Olds-Torrey (COT) damping, Gilbert (G) damping and Modified Bloch-Bloembergen (MBB) damping. It was shown that the LL, G, and COT damping models are mathematically equivalent in the sense that their equations of motion coincide when a suitable transformation is made for the damping parameter and the gyromagnetic ratio. Compared to the LL model, the G damping has a gyromagnetic ratio that decreases with the damping parameter; that means that G damping slows the precession. And relative to the LL model, the COT model has a damping parameter that is inversely proportional to the magnitude of the static internal field; that means that COT damping decreases with the static internal field. The explanation of the mathematical equivalence of these three damping models reveals that with regards to their physics they are very different. This difference in physics becomes apparent when one proceeds to extract from the equations of motion "what drives the damping". In the case of the LL model, the damping is field-driven. The damping is driven by the component of the total internal field that is perpendicular to the magnetization. In the case of the COT model, the situation is reversed. COT damping is magnetization-driven, driven by the magnetization component perpendicular to the instantaneous total internal field. The G damping, on the other hand, is viscous damping in the sense that the damping is proportional in magnitude to the time rate of change of the magnetization.

The BB and MBB damping models are fundamentally different from the other three models. The BB damping model relaxes the instantaneous magnetization to the static internal field, and not to the instantaneous total internal field as the other four models. As a consequence of this unphysical assumption, the BB damping model yields negative loss for certain driving fields and

sample geometries. The MBB model, developed as a correction to the BB model, does not have this problem concerning energy conservation. It relaxes the magnetization to the equilibrium magnetization as defined by the total instantaneous applied field. However, the application of the fluctuation-dissipation theorem to the damping models reveals a deep difference between the MBB model on one hand and the LL, G and COT models on the other hand. The difference is that while these three models imply isotropic field noise, the MBB model implies field noise whose power spectral density depends on the direction in the sample and the sample geometry. The four models have in common, however, that the field noise is white, that means its power spectral density is independent of the frequency.

Some other, less spectacular differences between the damping models are the following: The BB and MBB models predict precession orbits of the free magnetization decay that are, for an ellipsoidal sample, logarithmic spirals, compressed along the transverse principal axes of the sample ellipsoid. For the LL, G and COT models, the orbits are also compressed logarithmic spirals. However, their compression axis are tilted away from the transverse principal axes of the sample ellipsoid by a small angle of the same order of magnitude as the dimensionless damping parameter of the model.

The analyses in this work take advantage of the Smith matrix form of the equations of motion for the magnetization precession in the small-signal limit. The Smith matrix form is the general form of a linearized system of coupled harmonic oscillators, solved for the external driving force. Both time-averaged and instantaneous loss are closely related to $\vec{\mathbf{D}}^{sym}$, the symmetric part of the damping matrix, which multiplies the time derivative of the magnetization in the equation of motion. The spectral density matrix of field noise is a multiple of the same matrix, $\vec{\mathbf{D}}^{sym}$. In the formulas in the literature we find, instead of this matrix, the skew-hermitian part of the inverse susceptibility tensor, divided by the frequency. The latter is indeed equal to $\vec{\mathbf{D}}^{sym}$, but the traditional susceptibility-based formulation of the loss theory veils the simplicity of the linearized

approach and makes the results appear unnecessarily complicated.

The treatment of instantaneous loss, while absent in the textbooks, is very simple, when one starts with the Smith matrix form of the equations of motion. Much in the same way as for the simple harmonic oscillator with viscous damping, the difference of input power and change of internal energy gives the instantaneous loss. Surprisingly, for an ellipsoidal sample, the condition for positive loss is the same for the instantaneous and for the time-averaged loss. This condition is the positive definiteness of the matrix $\overline{\overline{\mathbf{D}}}^{sym}$.

As a by-product, this work contains a classical proof of the fluctuation-dissipation theorem. This proof combines ideas from Landau's and Lifshitz' book "Statistical mechanics" (Landau and Lifshitz, [1958]) with the Smith matrix formalism for a system of coupled harmonic oscillators. The proof is valid for an arbitrary such system, not only for the two-dimensional magnetic precession in a uniformly magnetized ellipsoidal ferromagnetic sample. The proof of the fluctuation-dissipation theorem starts with the equations of motion with a random driving force term, the noise term. This system of ordinary differential equations can be solved explicitly for the system response in terms of the random driving force. From this solution, the correlation matrix of the random driving forces is shown to be a multiple of the matrix $\overline{\overline{\mathbf{D}}}^{sym}$ from above. By a linear transformation, one obtains the correlation matrix and power spectral density of the system response from the result for the noise force. This approach uses only elementary theory of ordinary differential equations and of Boltzmann statistics, and does not use any Hamiltonian theory as many textbooks do. With the Smith matrices, the results for noise power spectra are given in a very simple form.

The representation of damping models in the Smith matrix form can be used to develop new damping models, different from the five models presented in this thesis. In the small-signal limit, a damping model is completely characterized by its corresponding damping matrix, which is a 2x2-matrix. As such, the damping matrix has four matrix elements. The most general damping

model, which includes all others as special cases, has, therefore, not one, but four independent parameters, the elements of the damping matrix. The only requirement on such a general damping model is that the damping matrix is positive definite, so that energy conservation is always satisfied. The next step of the work is then to perform the same investigations for this general damping model that were done in this thesis for five particular damping models.

References

A.A. Andronov, A.A Vitt, and S.E. Khaikin, "Theory of Oscillators", Pergamon Press, Oxford (1966).

R. Arias and D.L. Mills, "Extrinsic contributions to the ferromagnetic resonance response of ultrathin films", Phys. Rev. B **60**, 7395 (1999).

F. Bloch, "Nuclear Induction", Phys. Rev. **70**, 460 (1946).

N. Bloembergen, "On the Ferromagnetic Resonance in Nickel and Supermalloy", Phys. Rev. **78**, 572 (1950).

N. Bloembergen, "Magnetic Resonance in Ferrites", Proc. IRE **44**, 1259 (1956).

H. B. Callen, "A Ferromagnetic Dynamical Equation", J. Phys. Chem. Solids **4**, 256 (1958).

H.B. Callen, "Thermodynamics and an introduction to thermostatistics", 2nd ed., Wiley (1985).

R. S. Codrington, J. D. Olds, and H. C. Torrey, "Paramagnetic Resonance in Organic Free Radicals at Low Fields", Phys. Rev. **95**, 607 (1954).

R. C. Fletcher, R. C. LeCraw, and E. G. Spencer, "Electron Spin Relaxation in Ferromagnetic Insulators", Phys. Rev. **117**, 955 (1960).

H.L. Friedman, "A course in statistical mechanics", Prentice-Hall, Englewood Cliffs, NJ (1985).

T. L. Gilbert, Armour Research Foundation Report (May 1956).

I.S. Gradshteyn and I.M. Ryzhik, "Table of integrals, series, and products", Academic Press, Boston (1994).

A.G. Gurevich and G.A. Melkov, "Magnetization Oscillations and Waves", CRC Press, Boca Raton, Florida (1996).

C.W. Haas and H.B. Callen, "10. Ferromagnetic relaxation, and resonance line widths" in "Magnetism I", ed. by G.T. Rado and H. Suhl, Academic Press, New York (1963).

M.J. Hurben and C.E. Patton, "Theory of two magnon scattering microwave relaxation and ferromagnetic resonance linewidth in magnetic thin films", J. Appl. Phys. **83**, 4344 (1998).

L. D. Landau and E. M. Lifshitz, "On the Theory of the Dispersion of Magnetic Permeability in Ferromagnetic Bodies", Physik. Z. Sowjetunion **8**, 153 (1935).

L. D. Landau and E. M. Lifshitz, "Quantum mechanics: non-relativistic theory", third edition, Pergamon Press, Oxford (1977).

L. D. Landau and E. M. Lifshitz, "Statistical Physics", third edition, Pergamon Press, Oxford (1980).

B. Lax and K. J. Button, "Microwave Ferrites and Ferrimagnetics", McGraw-Hill, New York (1962).

J. Lindner, K. Lenz, E. Kosubek, K. Baberschke, D. Spoddig, R. Meckenstock, J. Pelzl, Z. Frait, D.L. Mills, "Non-Gilbert-type damping of the magnetic relaxation in ultrathin ferromagnets: Importance of magnon-magnon scattering", Phys. Rev. B **68**, 060102 (2003).

J. C. Mallinson, "On Damped Gyromagnetic Precession", IEEE Trans. Mag. **23**, 2003 (1981).

C. E. Patton, "Chapter 10: Microwave resonance and relaxation" in "Magnetic Oxides", ed. by D.J. Craik, Wiley, London (1975).

J. Rantschler, Y. Ding, S.-C. Byeon, and C. Alexander, Jr., "Microstructure and damping in FeTiN and CoFe films", J. Appl. Phys. **93**, 6671 (2003).

F. Reif, "Fundamentals of statistical and thermal physics", McGraw-Hill, New York (1965).

S.M. Rytov, Yu. A. Kravtsov, and V.I. Tatarskii, "Principles of statistical radiophysics", Springer-Verlag, Berlin (1988).

V. L. Safonov, "Tensor Form of Magnetization Damping", J. Appl. Phys. **91**, 8653 (2002).

N. Smith, "Fluctuation-Dissipation Considerations for Phenomenological Damping Models for Ferromagnetic Thin Films", J. Appl. Phys. **92**, 3877 (2002).

M. Sparks, "Ferromagnetic relaxation theorey", McGraw-Hill (1964).

N. Stutzke, S.L. Burkett, S.E. Russek, "Temperature and field dependence of high-frequency magnetic noise in spin valve devices", Appl. Phys. L. **82**, 91 (2003).

R. K. Wangsness, "Magnetic Resonance for Arbitrary Field Strengths", Phys. Rev. **98**, 927 (1955).